7-3-2013

Optimization of Properties of Injectable Bone Cement for Vertebral Augmentation Procedures: Application of Response Surface Methodology

Daniel Mamushet Werdofa

OPTIMIZATION OF PROPERTIES OF INJECTABLE BONE CEMENT FOR VERTEBRAL AUGMENTATION PROCEDURES: APPLICATION OF RESPONSE SURFACE METHODOLOGY

by

Daniel Mamushet Werdofa

A Thesis

Submitted in Partial Fulfillment of the

Requirements for the Degree of

Master of Science

Major: Mechanical Engineering

The University of Memphis

August 2013

Acknowledgements

First, I thank God, the Almighty, for everything. Truly, all blessings come from Him. Thank God for the wisdom and perseverance that he bestowed upon me during my thesis work, and, indeed, throughout my life: "I can do everything through him who gives me strength" (Philippians 4: 13). I express my profound gratitude to my major advisor, Dr. Gladius Lewis, for his support, dedication, and commitment during my thesis work, from conception of the project through to writing of the thesis. I also thank Dr. Lewis for providing the experimental data. I thank Dr. Hsiang-Hsi Lin and Dr. Teong Tan, for their service on my thesis committee. It would not have been possible to complete my thesis work without the love and support of my wife, Fana Ezra, and my children, Ruth and George. Fana has been my best friend and great companion, who has encouraged, entertained, and helped me get through this period. I thank my mother, Abeba, for her unconditional support and unfailing encouragement; and my sister, Samrawit, for her advice and encouragement.

ABSTRACT

Werdofa, Daniel Mamushet. M.S. The University of Memphis. August/2013. Optimization of Properties of Injectable Bone Cement for Vertebral Augmentation Procedures: Application of Response Surface Methodology. Major Professor: Gladius Lewis, Ph.D.

The literature on the interaction effects of explanatory variables on properties of injectable bone cements used in the vertebral augmentation procedures of vertebroplasty and balloon kyphoplasty is sparse. In the present work, response surface methodology was used to investigate the direct and interaction effects of variables on three properties of a poly (methyl methacrylate) bone cement (maximum exotherm temperature, residual monomer content (RMC), and degradability) and three properties of a calcium phosphate cement (CPC) (injectability, final setting time (F), and compressive strength). Some main findings were 1) interaction effects were statistically significant for some properties, such as F, but not for others, such as RMC; and 2) values of variables that led to optimum or minimum cement properties; for example, optimum injectability of a CPC (98%) could be attained using a cement with a poly(ethylene glycol) content of 20 wt/wt% and prepared using a powder-to-liquid ratio of 2.0 g mL^{-1}.

TABLE OF CONTENTS

Chapter	Page
1. INTRODUCTION	1
2. BACKGROUND	5
2.1. The spine	5
2.1.1 Anatomy of the spine	5
2.1.2 Functions of the spine	8
2.2 Osteoporosis	8
2.3 Osteoporosis-induced vertebral body compression fractures	9
2.4 Percutaneous vertebroplasty and balloon kyphoplasty	10
2.5 Injectable bone cements for vertebroplasty and balloon kyphoplasty	17
2.5.1 Poly (methyl methacrylate) (PMMA) bone cement	18
2.5.1.1. Constituents and their functions	18
2.5.1.2. Preparation phases	20
2.5.1.3. Polymerization processes	21
2.5.1.4. Problematic properties relevant to vertebroplasty and balloon kyphoplasty	23
2.5.2. Calcium phosphate cement	23
2.5.2.1. Setting reactions	27
2.5.2.2. Problematic properties relevant to vertebroplasty and balloon kyphopslasty	29
2.6 Design of experiments	32
2.6.1. Response surface methodology	35
2.6.2. Advantages and shortcomings of response surface methodology	36
2.6.3. Process optimization	37
3. LITERATURE REVIEW	39
3.1 Injectable bone cements for vertebroplasty and balloon kyphoplasty	39
3.2 Response surface methodology	56
4. CASE STUDIES	60
4.1. Case Study #1: Maximum exotherm temperature of a PMMA bone cement	60
4.1.1. Experimental details	60
4.1.2. Design matrix	61
4.1.3. Empirical relationship and regression analysis	64
4.1.4. Adequacy of regression analysis	65
4.1.5. Residuals and correlation exercises	67
4.1.6. Optimization exercise	70

Chapter Page

4.2. Case Study #2: Residual monomer content of a PMMA bone cement 74
4.2.1. Experimental details 74
4.2.2. Design matrix 75
4.2.3. Empirical relationship and regression analysis 77
4.2.4. Adequacy of regression analysis 79
4.2.5. Residuals and correlation exercises 81
4.2.6. Optimization exercise 84
4.3. Case Study #3: Degradability of a PMMA bone cement 88
4.3.1. Experimental details 88
4.3.2. Design matrix 90
4.3.3. Empirical relationship and regression analysis 93
4.3.4. Adequacy of regression analysis 94
4.3.5. Residuals and correlation exercises 96
4.3.6. Optimization exercise 99
4.4. Case Study #4: Injectability of a calcium phosphate cement 103
4.4.1. Experimental details 103
4.4.2. Design matrix 104
4.4.3. Empirical relationship and regression analysis 107
4.4.4. Adequacy of regression analysis 108
4.4.5. Residuals and correlation exercises 111
4.4.6. Optimization exercise 114
4.5. Case Study #5: Final setting time of a calcium phosphate cement 118
4.5.1. Experimental details 118
4.5.2. Design matrix 119
4.5.3. Empirical relationship and regression analysis 122
4.5.4. Adequacy of regression analysis 123
4.5.5. Residuals and correlation exercises 126
4.5.6. Optimization exercise 129
4.6. Case Study #6: Compressive strength of a calcium phosphate cement 133
4.6.1. Experimental details 133
4.6.2. Design matrix 135
4.6.3. Empirical relationship and regression analysis 137
4.6.4. Adequacy of regression analysis 138
4.6.5. Residuals and correlation exercises 140
4.6.6. Optimization exercise 143

5. CONCLUSIONS AND RECOMMENDATIONS FOR FUTURE STUDIES 147
6. REFERENCES 149

List of Tables

Table		Page
1.	Typical constituents of PMMA bone cement	18
2.	Chemical formula and Ca/P ratio for a sample of calcium phosphate compounds	24
3.	Compositions and manufacturers of a sample of commercially-available CPC brands	25
4.	Summary of studies on direct effect of one or more variables on properties of PMMA bone cement for VP and BKP	40
5.	Summary of a sample of studies on direct effect of one or more variables on properties of calcium phosphate cements	43
6.	Maximum exotherm temperature (T_{max}) of a PMMA bone cement	61
7.	Factors and their levels: maximum temperature of a PMMA bone cement	62
8.	Design matrix and experimental results: maximum exotherm temperature of a PMMA bone cement	63
9.	ANOVA results (response parameter: maximum exotherm temperature (T_{max}), in ^{o}C, of a PMMA bone cement)	65
10.	Residual monomer content (RMC) of a PMMA bone cement	75
11.	Factors and levels; residual monomer content of a PMMA bone cement	76
12.	Design matrix and experimental results : residual monomer of a PMMA bone cement	77
13.	ANOVA results (response: parameter: residual monomer content (RMC), in %, of a PMMA bone cement)	79
14.	Degradability of a PMMA bone cement	89
15.	Factors and their levels: degradabililty of a PMMA bone cement	91
16.	Design matrix and experimental results: degradability of a PMMA bone cement	92

17. ANOVA results (response parameter: degradability (D), in %, of a PMMA bone cement) 94

18. Injectability of a calcium phosphate cement 104

19. Factor and their levels: injectability of a calcium phosphate cement 105

20. Design matrix and experimental results: injectability of a calcium phosphate cement 106

21. ANOVA results (response parameter: injectability (I), in %, of a calcium phosphate cement) 109

22. Final setting time of a calcium phosphate cement 119

23. Factors and their levels: final setting time of a calcium phosphate cement 120

24. Design matrix and experimental results: final setting time of a calcium phosphate cement 121

25. ANOVA results (response parameter: final setting time (F), in min) of a calcium phosphate cement) 124

26. Compressive strength (UCS) of a calcium phosphate cement 134

27. Factors and their levels; compressive strength of a calcium phosphate cement 135

28. Design matrix and experimental results: compressive strength of a calcium phosphate cement 136

29. ANOVA results (response parameter: compressive strength (UCS), in MPa, of a calcium phosphate cement) 139

List of Figures

Figure		Page
1.	The five regions of the spinal column.	5
2.	The three main parts of a vertebra.	6
3.	A schematic drawing showing a vertebral body before and after vertebroplasty	11
4.	A schematic drawing of a standard transpedicular puncture during vertebroplasty with a medical needle trajectory through the pedicle.	12
5.	Injection of cement through a needle into a fractured vertebral body.	12
6.	A schematic drawing of the bone tamp insertion step in balloon kyphoplasty.	14
7.	A schematic drawing of the steps of bone tamp removal, bone filler device. insertion through a cannula, and cement injection into the cavity created in the vertebral body in balloon kyphoplasty.	15
8.	Schematic presentation of a summary of the main steps in balloon kyphoplasty	16
9.	Schematic drawing illustrating the initiation of polymerization of a PMMA bone cement.	22
10.	Schematic drawing of a ‘black box’ process model.	33
11.	The normal probability plot of the maximum exotherm temperature results for a PMMA bone cement.	68
12.	The correlation plot of the maximum exothermic temperature (T_{max}) results for a PMMA bone cement.	69
13.	The response surface plot (A) and the contour plot (B) for the influence of barium sulfate content (BA) and quaternary amine comonomer content (QU) on the maximum exothermic temperature T_{max} of a PMMA bone cement.	71-73
14.	The normal probability plot of the residual monomer content results for a PMMA bone cement.	82

15. The correlation plot of the residual monomer content results for PMMA bone cement. 83

16. The response surface plot (A) and the contour plot (B) for the influence of barium sulfate content (BA) and quaternary amine comonomer content (QU) on the residual monomer content (RMC) of a PMMA bone cement. 85-87

17. The normal probability of the degradability results for a PMMA bone cement. 97

18. The correlation plot of the degradability results for a PMMA bone cement. 98

19. The response surface plot (A), contour plot (B) for influence of PMMA cement powder content, bioactive glass particles content, and chitosan particles content on the degradability of a PMMA bone cement. 100-102

20. The normal probability plot of the injectability results for a calcium phosphate cement. 112

21. The correlation plot of the injectability results for a calcium phosphate cement 113

22. The response surface plot (A), contour plot (B) for influence of PEG content and powder-to-liquid ratio on the injectability of a calcium phosphate cement 115-117

23. The normal probability plot of the final setting time results for a calcium phosphate cement. 127

24. The correlation plot of the final setting time results for a calcium phosphate cement. 128

25. The response surface plot (A), contour plot (B), and desirability plot (C) for the influence of PEG content and PLR on the final setting time of a calcium phosphate cement. 130-132

26. The normal probability plot of the compressive strength results for a calcium phosphate cement. 141

27. The correlation plot of the compressive strength results for a calcium phosphate cement. 142

28. The response surface plot (A), contour plot (B), and desirability plot for the influence of sodium phosphate content and powder-to-liquid ratio on the compressive strength of a calcium phosphate cement. 144-146

CHAPTER 1

INTRODUCTION

Osteoporosis is a serious and potentially life-threatening disease. It is postulated to be one of the main causes of an increase in the fragility of bone and an accompanying decrease in its strength [1]. Thus, the consequence of osteoporosis is an increase in susceptibility to fracture of bones, particularly vertebral bodies in the mid-thoracic, lower-thoracic, and higher-lumbar levels of the spine [2]. There is a high incidence of these spinal fractures, usually referred to as vertebral compression fractures (VCFs) [3]. The impact of VCF(s) on patient quality of life can be substantial, resulting in pain and deformity, which limit mobility and adversely affect ability to perform activities of daily living [4].

Treatment of VCF(s) includes conservative (non-surgical) and surgical methods. Examples of conservative treatments are bed rest, analgesia for pain, and bracing for support [5]. Surgery is used when conservative treatment(s) fail to provide adequate pain relief. Current surgical practice involves use of a minimally invasive procedure, namely, vertebroplasty (VP) or balloon kyphoplasty (BKP) [6].

In VP, the surgeon utilizes fluoroscopy to visually guide a needle through the pedicle of the collapsed vertebral body (VB) bilaterally and inject a bolus of an injectable bone cement (IBC) to strengthen and stabilize the fractured bone. The cement typically hardens within minutes. VP helps in relieving pain by providing mechanical support and stability to the collapsed VB [7]. BKP begins with the placement of a cannula on the VB and then, using a transpedicular or parapedicular approach and guided by fluoroscopy, a tube is inserted into the center of the VB to

the site of the fracture, and a balloon tamp is introduced through the tube into the space and inflated. After that, the balloon is deflated and removed and the resulting cavity that is formed is filled with a bolus of an IBC, which hardens within minutes, stabilizing the VB [8].

A key variable that affects the outcome of either VP or BKP is the type of IBC used. The IBCs that are widely used in these procedures are PMMA bone cement and calcium phosphate cement (CPC), each of which has its attractive features and shortcomings [9]. A PMMA bone cement is biocompatible and bioinert, is easy to handle, has adequate mechanical strength, is reasonably priced, and is very familiar to spine surgeons and interventional radiologists. However, a PMMA bone cement does not allow for direct apposition of new bone, lacks the potential to remodel and/or integrate with the adjacent bone, and, usually, is encapsulated by a thin fibrous layer after implantation. Other shortcomings of PMMA bone cement are a high polymerization (exothermic) temperature and the potential for monomer toxicity. A CPC is nontoxic, resorbs gradually and is replaced by new host bone via creeping substitution, cures via an endothermic reaction, and does not cause tissue necrosis and/or neural injury secondary to curing. However, the biomechanical properties of a CPC in a load-bearing situation are of concern; for example, its compressive strength is substantially lower than that of a PMMA bone cement. Other shortcomings of a CPC compared to PMMA bone cement include its lower viscosity, shorter setting time, lower injectability, lower radiopacity, and higher cost.

There are a host of literature reports on the direct effects of many relevant variables on various properties of PMMA bone cements and CPCs [10]. In contrast,

there are very few reports on interactive effects of two or more variables on the properties of either of these types of cements [11]. The purpose of the present study was to investigate the direct and interactive effects of a number of variables on different properties of a PMMA bone cements and of a CPC, leading to the computation of the values of the variables that yield the optimum value for a given cement property. The cement properties considered in the present study are a sample of ones that need to be improved; namely, maximum exothermic temperature, residual monomer content, and degradability in the case of a PMMA bone cement and injectability, setting time, and compressive strength in the case of a CPC. The investigations were carried out using response surface methodology (RSM) [12].

The thesis is organized into five chapters. Key aspects of all the background topics relevant to the study are presented in Chapter 2. These topics are anatomy and functions of the spine, osteoporosis, VCFs, VP and BKP, PMMA bone cements, CPCs, design of experiments, and RSM. Reviews of the literature on the influence of variables on properties of PMMA bone cements used in or proposed for use in VP and BKP, influence of variables on the properties of CPCs, and applications of RSM to PMMA bone cements and CPCs are presented in Chapter 3. Details of six case studies, in which RSM was used to determine the optimum value of a cement property, are given in Chapter 4. In each case study, the format comprises a description of the experimental method used to determine the cement property; the collection of the property results, as a function of the variables considered; the results of the RSM work; and a discussion of the RSM findings. The final chapter in the

thesis, Chapter 5, contains a statement of the study conclusions and recommendations for future study.

CHAPTER 2

BACKGROUND

2.1. The spine

2.1.1. Anatomy of the spine

The spine, which consists of 33 individual vertebrae (bony members) (Fig. 1), is an inverted S-shaped curve, with the top part being convex and called the cervical region (C1-C7), the middle part being concave and called the thoracic region (T1-T12), and the bottom part being convex and called the lumbar region (L1-L5) [13]. Only the top 24 of these vertebrae are moveable because ligaments and muscles connect them. Distal to the lumbar region are the sacrum (five fused bones) and the coccyx (four fused bones).

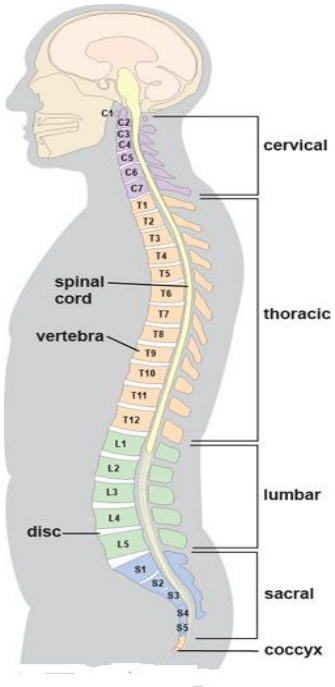

Fig. 1. The five regions of the spinal column [13].

Each moveable vertebra (Fig. 2) has three functional parts: a drum-shaped body (vertebral body (VB)), which has a broad transverse surface area and, as such, is designed to bear weight and withstand applied compression loads (shown as purple); an arch-shaped bone that protects the spinal cord (shown as green); and star-shaped processes designed as outriggers for muscle attachment (shown as tan).

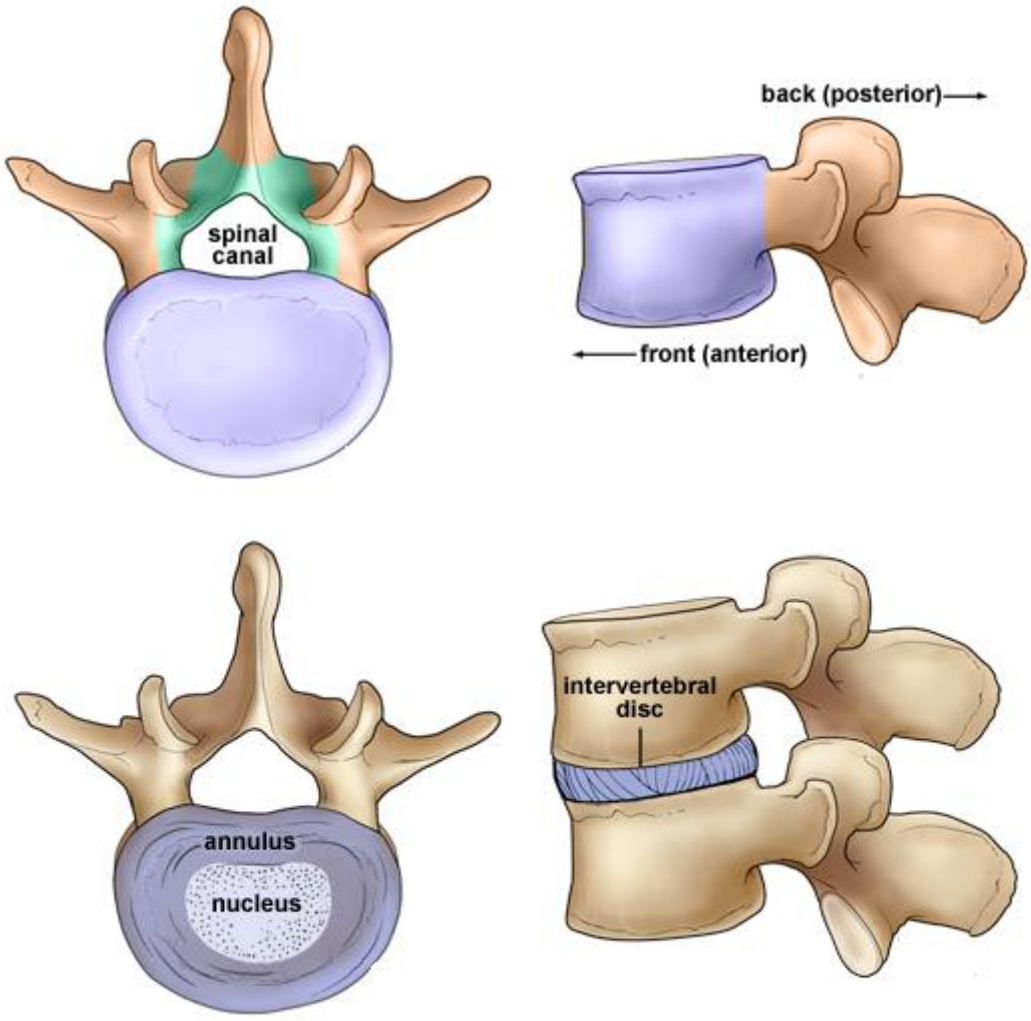

Fig. 2. The three main parts of a vertebra [13].

In each spinal region, the vertebrae have unique features that help them perform various functions. The cervical vertebrae support the weight of the head (~ 45 N). The neck has the greatest range of motion because of two specialized cervical vertebrae that connect to the skull. The first of these (C1), called the atlas, connects directly to the skull and allows for the nodding or "yes" motion of the head, while the other (C2), called the axis, allows for the side-to-side or "no" motion of the head. The thoracic vertebrae hold the rib cage and protect the heart and the lungs. The range of motion in the thoracic spine is limited. The lumbar spine bears the weight of the body and service loads. Thus, the lumbar vertebrae are larger than those in the cervical and thoracic regions. The main function of the sacrum is to connect the spine to the hip bones (iliac bones). The sacrum and the iliac bones form a ring called the pelvic girdle. The bones of the coccyx or tailbone provide attachment for the ligaments and the muscles of the pelvic floor.

Each pair of moveable vertebrae is separated by an intervertebral disc (IVD), which consists of two main parts, namely, the annulus fibrosus and the nucleus pulposus (Fig. 2). The annulus is comprised of criss-crossing fibers that pull against the outward force of the nucleus to hold the shape of the disc. The nucleus is filled with a fluid (an incompressible gel) that provides elastic resistance between the vertebrae. The fluid is absorbed when a person is lying down and is pushed out when he/she is moving upright [13].

2.1.2. Functions of the spine

The spine performs a number of functions: it provides support for the body, acts as the body's shock absorber, helps the body to remain balanced, gives flexibility to the body (thereby allowing motions of extension, flexion, left lateral bending, right lateral bending, clockwise-acting axial torsion, and counterclockwise-acting axial rotation), and protects the spinal cord [13].

2.2. Osteoporosis

Osteoporosis, which is the most prevalent bone disease, is defined as a systematic skeletal disease characterized by low bone mass and disruption or deterioration of the microarchitecture of bone tissue (thinning of the bone), culminating in an increase of the fragility of the bone (decrease in bone strength) [14-16]. Thus, osteoporosis increases susceptibility to fracture of bones, particularly in the spine (vertebral bodies in the mid-thoracic, lower-thoracic, and higher-lumbar levels), pelvis, wrist, humerus, and wrist. In more detail, the pathophysiology of osteoporosis is marked by an imbalance between bone production by osteoblasts and bone resorption by osteoclasts. In normal bone, there is a balance between these two processes, whereas, in osteoporotic bone, there is an increase in osteoclastic bone resorption due to an overall decrease in osteoblastic bone production and/or a direct increase in bone resorption [17, 18]. Among the risk factors for osteoporosis are age > 45 years, gender (being female), low body weight, smoking, and use of certain medications, such as oral glucocorticoids, anti-clotting drugs like heparin, cyclosporine drugs that treat immune system disorders, and drugs used to treat prostate cancer [19]. Dual-energy x-ray absorptiometry (DEXA) is the most widely used clinical method of screening for osteoporosis. A diagnosis of osteoporosis is given when a

person's bone mineral density (BMD), measured using DEXA, is at least 2.5 standard deviations below the mean value for a "young normal" adult population of the same gender [19-21]. Other osteoporosis diagnostic methods, such as calcaneal quantitative ultrasound, quantitative computer tomography, and use of biochemical markers (urine and serum), are also available but, at the moment, are not widely used in the clinical setting [19-21].

There are no symptoms of osteoporosis until bone fracture(s) occur. Thus, prevention is very important. This may involve, for example, lifestyle choices, such as not smoking and exercising on a frequent basis, and increasing calcium and/or vitamin D intake. When, however, a diagnosis of osteoporosis is given, treatment methods include use of pharmacotherapies (such as alendronate and calcitonin), muscle stretching, and ingestion of a dietary supplement [16, 19].

Osteoporosis is a major public health issue everywhere in the world but, particularly, in developed nations. For example, in the United States, it was reported that, in 2005, more than 2 million people suffered fractures related to osteoporosis and the direct cost associated with treating these fractures was about $22 billion [14]. With the graying of the population, both incidence and cost of treatment are expected to rise sharply, with one estimate of the rate of rise between 2005 and 2025 being 50% from its 2005 level [14].

2..3 Osteoporosis-induced vertebral body compression fractures

In the adult spine, the cancellous bone in the VB carries the majority (55%) of the applied axial compressive loads [22]. The compressive strength of cancellous bone is directly proportional to the squared of its density (ρ) [22-24]. With osteoporosis, there is a marked decrease in ρ; as such, there is a high incidence of compression fractures of

VBs, usually referred to as vertebral compression fractures (VCFs), in osteoporotic patients. Since the thoracic and thoracolumbar regions of the spine have a natural kyphotic curvature, VBs in these regions are the most common sites of VCFs [25]. In the United States, there are 700,000 VCFs every year, with hospitalization for about 115,000 cases [26].

2.4. Percutaneous vertebroplasty and balloon kyphoplasty

In cases where the pain due to VCFs is severe, persistent, and unresponsive to conservative treatments, such as medications, bed rest, wearing of back braces, and ingestion of narcotic analgesics, the only treatment option is surgical vertebral augmentation [27]. Such a procedure involves the percutaneous administration of a dough/paste of an injectable bone cement (IBC), usually a highly-radiopaque poly (methyl methacrylate) (PMMA) bone cement or a calcium phosphate cement (CPC), into the fractured VB, under fluoroscopic guidance [28,29]. The two variants of this technique in clinical use today are vertebroplasty (VP) and balloon kyphoplasty (BKP) [28-31].

In VP, the fractured VB is accessed percutaneously with a high-caliber needle positioned using a transpedicular or paravertebral approach (Figs. 3 and 4) [29, 32-33]. Since VCFs are most commonly observed between the T8 and L2 levels, typically, about 3-8 mL of the bone cement dough is injected directly into the collapsed/fractured VB(s) (Fig. 5). Once cured, the cement provides bone augmentation and stabilization, thereby preventing further collapse and movement. For VP, some of the critical factors that affect outcome are proper patient selection, correct needle placement, good timing of cement injection, and careful fluoroscopic control of injection of the cement dough/ paste [25, 26, 33, 34]. Complications of VP include infections and cement leak into body tissues and

organs (a phenomenon known as cement extravasation). Some of the cement leaks have clinical importance; for example, epidural overflow of ABC may cause spinal cord compression; leaks into an IVD may increase the risk of fracture(s) of VB(s) adjacent to the one(s) being treated; and leaks into paravertebral veins can lead to pulmonary cement embolism [24,30,35]. However, other leaks, such as leaks into paravertebral soft tissues, do not have clinical significance [24, 30, 35].

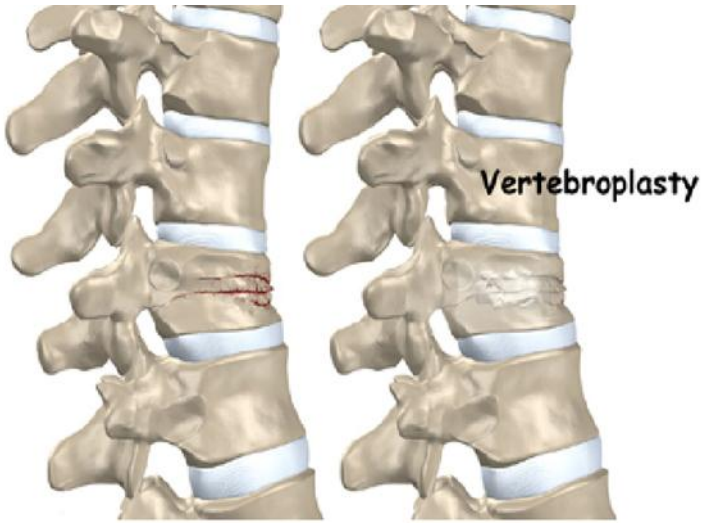

Fig. 3. A schematic drawing showing a vertebral body before and after vertebroplasty [33].

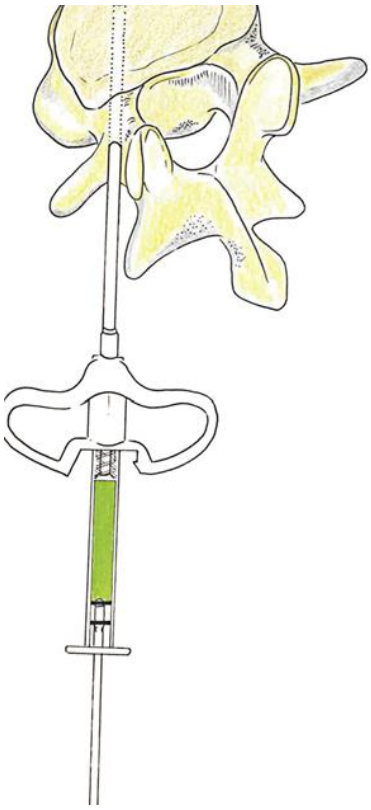

Fig. 4. A schematic drawing of a standard transpedicular puncture during vertebroplasty with a medial needle trajectory through the pedicle [29].

Fig. 5. Injection of cement through a needle into a fractured vertebral body [33].

There are five steps involved in BKP (Figures 6-8) [29, 30, 36-38]. First, a balloon-like device (called a bone tamp) is placed in the fractured/collapsed VB, through a channel created by a drill in it. Second, a guide wire or biopsy needle is advanced into the VB, via a transpedicular or extrapedicular approach. Third, the bone tamp is inflated slowly until either the normal height of the VB is restored or the balloon reaches its maximum volume, whichever occurs first. Fourth, the bone tamp is deflated and removed, the cement is mixed (to yield a bolus), and the cement cannulae are prefilled, allowing the cement to partially cure in the cement cannulae. Fifth, the cement cannulae are positioned in the center of the cavity created by the bone tamp and then the bolus of the cement is slowly extruded into the cavity, under continuous lateral fluoroscopic guidance. This technique permits a low-pressure fill. One major challenge in BKP is that, because the cement is injected while it is highly viscous, the surgeon has to know the setting time of the cement before performing the treatment so that he/she would know when the cement is ready to be injected. One shortcoming of BKP is the pressure associated with inflation of the bone tamp is high enough to compact the cancellous bone around the tamp. One major risk of BKP is allergic reaction to the contrast agent used to visualize the bone tamp as it is being inflated. Complications of BKP include extravasation, pulmonary embolism, nerve root or spinal cord compression by the cement, epidural haematoma, infection, and transient fever [27, 29, 30, 39].

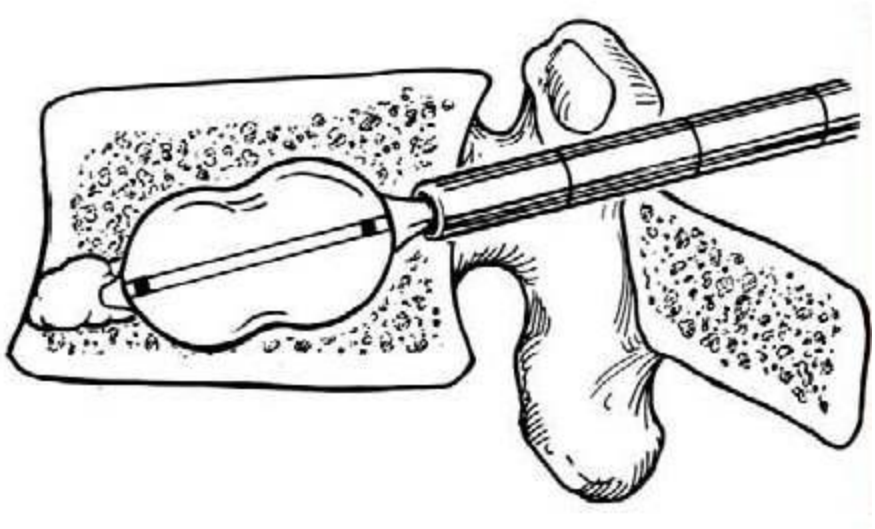

Fig. 6. A schematic drawing of the bone tamp insertion step in balloon kyphoplasty [32].

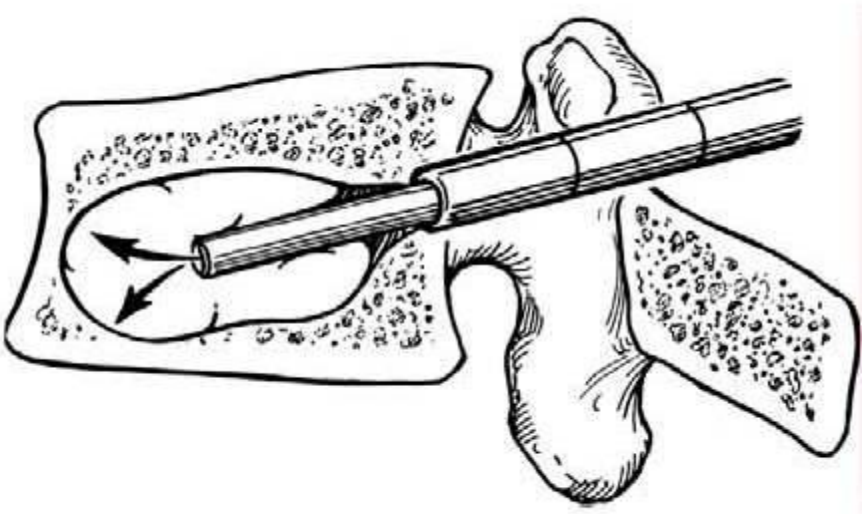

Fig. 7. A schematic drawing of the steps of bone tamp removal, bone filler device insertion through a cannula, and cement injection into the cavity created in the vertebral body in balloon kyphoplasty [32].

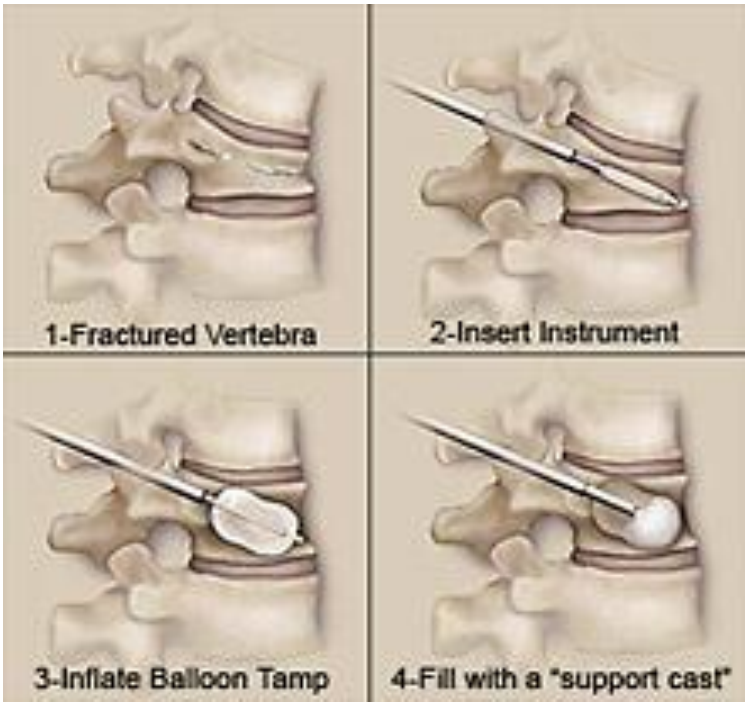

Fig. 8. Schematic presentation of a summary of the main steps in balloon kyphoplasty [40].

There are three key differences and two similarities between VP and BKP in terms of clinical outcomes. The first difference is that the incidence of cement extravasation is significantly lower in BKP compared to VP (0-13.5% versus 2-67% of cases) [31, 37]. There are two reasons for this difference. One is that in BKP, the cement is injected into a cavity created in the fractured VB, rather than directly into the fractured VB as is done in VP. The other is that, in BKP, a very powerful plunger is used and the cement is injected while it is in a very viscous state, whereas, in VP, no plunger is used, and, so, the cement is injected while it is in a low-viscous state. The second difference is that restoration of height of the treated VB(s) is significantly higher when BKP is used compared to VP is used (28% versus 96% of cases) [31, 41]. The third difference is that the incidence of adjacent-level fractures is markedly lower in BKP than in VP, a consequence of the

former method being more successful in restoring the overall spinal balance [41, 42]. The first similarity between VP and BKP is that there are many reports that the procedure is effective; that is, each leads to significant improvements in a patient's functional abilities, enhanced performance of activities of daily living, and significant reduction in pain over the short- to medium-term [36]. The second similarity is that although, for each method, the mechanism of pain relief is not exactly known, it is believed to be achieved by way of two different actions: fracture stabilization as the cement hardens and heat necrosis of the nerve endings at the fracture site [41, 43].

2.5. Injectable bone cements for vertebroplasty and balloon kyphoplasty

Two types of IBC are widely used for VP and BKP, namely, a PMMA cement that has a high amount of radiopacifier and a CPC [44]. A PMMA bone cement is biocompatible and bioinert, is easy to handle, has adequate mechanical strength, is reasonably priced, and is very familiar to spine surgeons and interventional radiologists. However, a PMMA bone cement does not allow for direct apposition of new bone, lacks the potential to remodel and/or integrate into adjacent bone, and, usually, is encapsulated by a thin fibrous layer after implantation. Other drawbacks of a PMMA bone cement are high polymerization temperature (which may lead to thermal necrosis of the periprosthetic tissue) and the potential for chemical necrosis of the periprosthetic tissue (which arises from toxicity of the residual monomer). A CPC is nontoxic and has the potential to resorb gradually and be replaced by new host bone via creeping substitution. Several animal studies have shown that a CPC is highly osteoconductive and, *in vivo*, undergoes gradual remodeling. In addition, curing of a CPC is an endothermic process and does not cause tissue necrosis and/or neural injury secondary to curing. However, the

mechanical properties of a CPC in a load-bearing situation are of concern because they are lower than those of a PMMA bone cement. Other shortcomings of a CPC include low viscosity (and, hence, low injectability), potential for separation of the solid phase from the liquid phase during extrusion of the paste through the syringe, limited radiopacity, and high cost [45].

2.5.1. Poly (methyl methacrylate) (PMMA) bone cement

A PMMA bone cement is a two-component material, comprising a powder (pre-polymerized PMMA and/or methyl methacrylate (MMA) co-polymer beads, a radiopacifier, and an initiator of the polymerization reaction) and a liquid (methyl methacrylate (MMA) monomer, an accelerator of the polymerization reaction, and a inhibitor of the polymerization reaction) [46] (Table 1).

Table 1
Typical constituents of a plain PMMA bone cement [46]

Powder[a]	Liquid[b]
Poly (poly methyl methacrylate) (PMMA) beads (87.30 wt/wt%)	Methyl methacrylate (MMA) (99.1 vol/vol%)
Benzoyl peroxide (BPO) (2.7 wt/wt%)	N, N-dimethyl para-toluidine (DMPT) (0.9 vol/vol%)
Barium sulfate ($BaSO_4$) (10.0 wt/wt%)	Hydroquinone (HQ) (75 ppm)

[a]Total mass = 40.00 g
[b]Total volume = 14.13 mL

2.5.1.1. Constituents and their functions

Barium and zirconium are two elements capable of blocking x-rays. In sulfate form ($BaSO_4$) or oxide form (ZrO_2), each material forms inert powders that are insoluble in water, chemically stable, and non-reactive, making them useful as additives for materials

that need to appear opaque under x-ray visualization. $BaSO_4$ is a fine, white, inert powder that is also used as a contrast medium in x-ray photography of the digestive tract. ZrO_2 is a white, heavy, amorphous, odorless and tasteless, infusible, water-insoluble powder. It is also used as a pigment for paints and in the manufacture of refractory crucibles. BPO is a white, crystalline powder that is capable of decomposing into two highly reactive peroxide molecules. These reactive molecules are known as free radicals, which initiate the polymerization reaction that makes bone cement thicken and finally harden. MMA is a colorless liquid, which is also used as a building block for making acrylic plastics. DMPT acts like a catalyst and serves to decompose the BPO into the free radical molecules that subsequently cause polymerization. HQ is capable of polymerizing by itself very slowly over time. It is added to the liquid component to stabilize the monomer and to prevent it from undergoing self-polymerization.

There is a large number of commercially-available plain PMMA bone cement brands, with the differences between them being in 1) the relative amounts of the constituents in the powder and in the liquid; and 2) the presence or absence of additives, such as a coloring agent (chlorophyll) in the powder and/or the liquid and an antibiotic in the powder.

With respect to the radiopacifier, clinical practice in VP and BKP is to use either a cement brand that has a high radiopacifier content (typically, 30 wt/wt% of the dry powder weight) or one that has a low radiopacifier content (typically, 12-15 wt/wt%) but to which additional radiopaque substances (for example, more $BaSO_4$ or ZrO_2 or 2-3 wt/wt% of another radiopacifier, such as tantalum powder) have been added. This is

necessary to facilitate visualization under fluoroscopy and to monitor cement extravasation [47, 48].

2.5.1.2. Preparation phases

There are four preparation or handling phases, namely, mixing, waiting, working, and hardening [49]. The mixing phase starts with the addition of the liquid to the powder (or vice versa, depending on the cement brand) and ends when the dough is homogenous and stirring becomes effortless. When the liquid and the powder are mixed, the liquid wets the surface of the pre-polymerized beads in the powder. Because PMMA is a polymer that dissolves in its monomer, the pre-polymerized beads swell and some of them dissolve completely during mixing. This dissolution results in a substantial increase in the viscosity of the mixture; however, at this stage, the viscosity is relatively low. At the end of the mixing phase, the mixture is a homogenous mass and the cement is sticky and has a consistency similar to that of toothpaste.

In the waiting phase, there is further swelling of the beads, thereby allowing polymerization to proceed. This leads to an increase in the viscosity of the mixture. During this phase, the cement turns into a sticky dough. This dough is subsequently tested with gloved fingers every 5 seconds, using a different part of the glove on another part of the cement surface on each testing occasion. This process provides an indication of the end of the waiting phase when the cement is neither “sticky” nor “hairy.”

The beginning of the working phase occurs when the cement is no longer sticky, but is of sufficiently low viscosity to enable the surgeon to apply the cement. During this period, polymerization continues and the viscosity continues to increase; in addition, the reaction exotherm associated with polymerization leads to the generation of heat in the

cement. In turn, this heat causes thermal expansion of the cement, while there is a competing volumetric shrinkage of the cement as the monomer converts to the denser polymer. During the working phase, the viscosity of the cement must be closely monitored because with a very low viscosity, the cement would not be able to withstand bleeding pressure. This would result in blood lamination in the cement, which causes the cement to weaken. In total joint replacement, this phase is completed when the cement does not join without folds during continuous kneading by hand.

In the hardening phase, polymerization stops and the cement cures to a hard consistency. The temperature of the cement continues to be elevated, but then slowly decreases to body temperature. During this phase, the cement continues to undergo both volumetric and thermal shrinkage as it cools to body temperature. In total joint replacement, the cement is ready for placement in the bone bed when two cement balls are touched to each other and they stick together.

2.5.1.3. Polymerization processes

When the cement powder and liquid are mixed (using the powder-to-liquid ratio (PLR) recommended by the cement brand manufacturer), two different processes are started [50]. First, the powder takes up the liquid, forming a more or less viscous fluid or dough. This phenomenon occurs because of the swelling and dissolution processes of the powder and the monomer, physical processes that are important for the working characteristics of the cement. Second, a chemical process is initiated, which is responsible for the final hardening of the bone cement. BPO and DMPT interact to produce free radicals in the so-called initiation reaction (Fig. 9). These radicals are able to start the polymerization of MMA by adding to the polymerizable double-bond of the

monomer molecule. This results in a growing polymer chain that builds up macromolecules. Because of the high number of radicals generated, many fast-growing polymer chains are formed and, therefore, there is a fast conversion of MMA to PMMA. If two growing polymer chains meet, the chains are terminated by combining both, thus resulting in an unreactive polymer molecule. The polymerization of MMA is an exothermic reaction, resulting in a temperature increase in the curing of the cement.

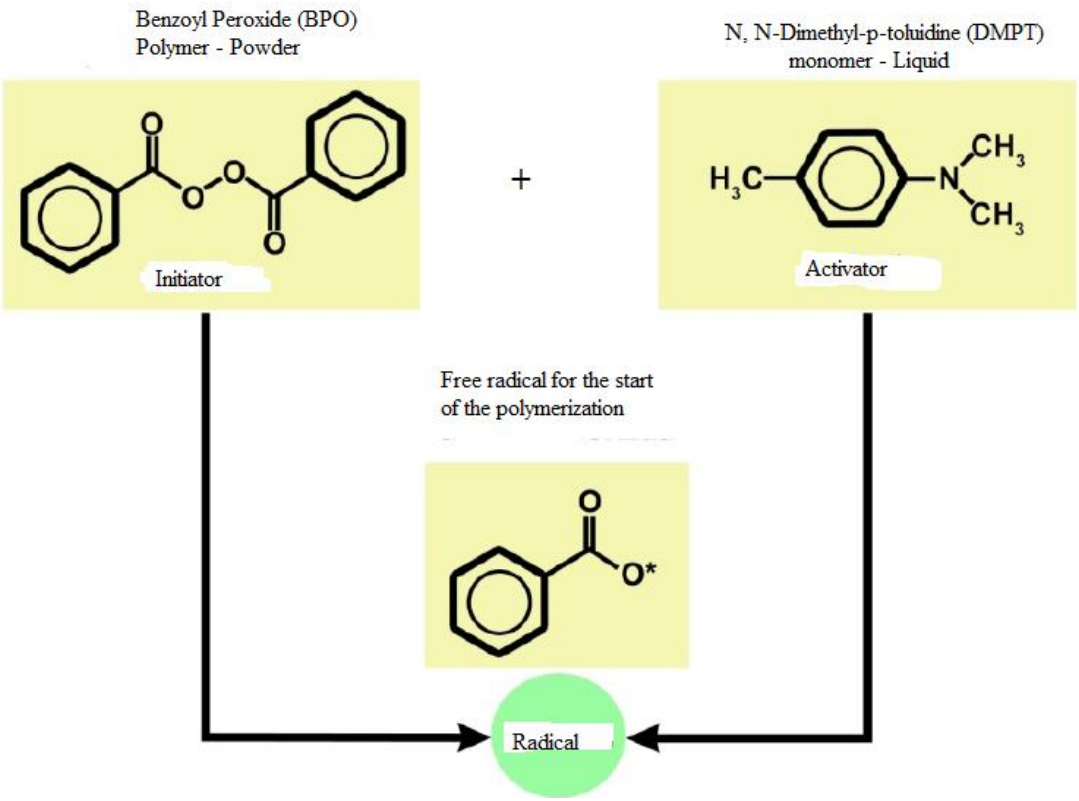

Fig. 9. A schematic drawing illustrating the initiation of polymerization of a PMMA bone cement [50].

2.5.1.4. Problematic properties relevant to vertebroplasty and balloon kyphoplasty

These properties are high exothermic temperature (T_{max}), high incidence of micropores, high residual monomer content (RMC), and very poor degradability. T_{max} as high as 100^{o} C have been reported during mixing of some cement brands. Consequences of high T_{max} include thermal necrosis and evaporation of the monomer, which, in turn, may lead to creation of micropores in the curing cement. Micropores may also may result from flow and wetting during mixing of the powder and the liquid, leading to air entrapment and formation of CO_2 formation. Typically, after ~15 minutes after polymerization, RMC is ~3-5%, which may decrease to ~1-2% with increase in time after polymerization. High RMC can cause chemical necrosis of periprosthetic tissues. Poor degradability means that the cement is not resorbed into the surrounding bone, resulting in lack of osseointegration. [49, 50, 51, 52]

2.5.2. Calcium phosphate cement

Calcium phosphate cement (CPC) was first reported, in 1987, by Brown and Chow [53]. Nowadays, however, the term "CPC" refers to a very large family of materials that contain Ca and P in various forms (Table 2). There is an array of commercially-available CPC brands (Table 3).

Table 2
Chemical formula and Ca/P ratio for a sample of calcium phosphate compounds [54]

Compound	Formula	Ca/P ratio
Amorphous calcium phosphate (ACP)	$Ca_xH_y(PO_4)_z \cdot nH_2O$	1.25-1.55
Biphasic calcium phosphate (BCP)	$Ca_3(PO_4)_2 + Ca_{10}(PO_4)_6(OH)_2$	1.50-1.67
Carbonated apatite (dahlite) (CA)	$Ca_5(PO_4,CO_3)_3$	1.67
Calcium deficient hydroxyapatite (CDHA)	$Ca_{10-x}(HPO_4)_x(PO_4)_{6-x}(OH)_{2-x}$ $0 < x < 1$	1.50-1.67
Dicalcium phosphate anhydrous (monetite) (DCPA)	$CaHPO_4$	1.00
Dicalcium phosphate dihydrate (brushite) (DCPD)	$CaHPO_4 \bullet 2H_2O$	1.00
Hydroxyapatite (HA)	$Ca_{10}(PO_4)_6(OH)_2$	1.67
Monocalcium phosphate monohydrate (MCPM)	$Ca(H_2PO_4)_2 \bullet H_2O$	0.50
Octacalcium phosphate (OCP)	$Ca_8(H_2PO_4)_6 \bullet 5H_2O$	1.33
Precipitated hydroxyapatite (pHA)	$Ca_{10-x}(HPO_4)_x(PO_4)_{6-x}(OH)_{2-x}$ $0 < x < 1$	1.50-1.67
α-tricalcium phosphate (whitlockite) (α-TCP)	$\alpha\text{-}Ca_3(PO_4)_2$	1.50
β-tricalcium phosphate (whitlockite) (β-TCP)	$\beta\text{-}Ca_3(PO_4)_2$	1.50
Tetracalcium phosphate (hilgenstockite) (TTCP)	$CaO \bullet Ca_3(PO_4)_2$	2.00

Table 3
Compositions and manufacturers of a sample of commercially-available CPC brands [55]

Brand	Composition (Manufacturer)
α-BSM (Bone Substitute Material)	Amorphous CaP + DCPD (ETEX, Cambridge, MA, USA)
Biopex	75 wt/wt% α-TCP + 18wt/wt% TTCP + 5 wt/wt% DCPD + 2 wt/wt% HA (Mitsubishi Materials Co., Saitama, Japan)
BoneSave	80 wt/wt% tricalcium phosphate (TCP) + 20 wt/wt% HA (Stryker-Howmedica-Osteonics, Mahwah, NJ, USA)
BoneSource BVF	TTCP; dicalcium phosphate (DCP) (Stryker-Howmedica-Osteonics)
ChronOS Inject	42 wt/wt % β-TCP + 21 wt/wt % MCPM + 3 wt/wt % β-TCP granules + 5 wt/wt % magnesium hydrogen phosphate + <1 wt/wt % sodium hydrogen phosphate and $MgSO_4$ (Synthes, Inc., West Chester, PA, USA)
Calcibon	α-TCP + $CaHPO_4$ + $CaCO_3$ + pHA (Biomet Europe, Dordrecht, The Netherlands)
Eurobone	TCP (F-H Orthopedics, Heimsbrum, France)
Norian SRS	α-TCP, $CaCO_3$, MCPM (Synthes, Inc.)

A CPC consists of two parts: a powder mix, which contains dry calcium phosphate particles, and an aqueous or wetting solution, which, in many cases, is de-ionized distilled water. The CPC is formed by the cementing action of acidic and basic calcium phosphate compounds on wetting the powder with the aqueous solution. Dissolution of the particles (quickly or slowly, depending on the composition and pH of the aqueous solution) and mass transport are the primary functions of the aqueous solution, in which the dissolved reactants form a supersaturated (very far away from the equilibrium) microenvironment with regard to precipitation of the final products. The relative stability and solubility of various calcium phosphates is the major driving force for the setting reactions that occur in these cements. Mixing of the powder and the aqueous solution, in a suitable proportion, gives a self-setting mass. That is, the mixing induces various chemical transformations, where crystals of the initial calcium phosphate(s) rapidly dissolve(s) and precipitate(s) into crystals of CDHA or DCPD, with possible formation of intermediate precursor phases (for example, ACP and OCP). During precipitation, the newly formed crystals grow and form a web of intermingling microneedles or microplatelets of the final products, thus providing mechanical rigidity to the hardened cements. In other words, entanglement of the newly formed crystals is the major manifestation of setting. For the majority of apatite cements, water is not a reactant in the setting reaction; therefore, only a small quantity of water is needed for setting of the cement.

The hardening reaction of the cement, which forms nanocrystalline HA as the product, is isothermic and occurs at physiologic pH so tissue damage does not occur during the setting reaction [56]. Because CPC is brittle, it is used for non-load-bearing

applications, such as dental and cranio-facial applications. CPC has two significant advantages over pre-formed, sintered ceramics. First, the CPC paste can be sculpted during surgery to fit the contours of the application (for example, a wound or in VP or BKP). Second, the nanocrystalline HA structure of the CPC makes it osteoconductive, causing it to be gradually resorbed and replaced with new bone. Recent work with CPC has focused on improving its mechanical properties, making premixed cements, making the cement macroporous, and seeding it with cells and growth factors [56].

2.5.2.1. Setting reactions

Setting of a CPC is a continuous process that always starts with dissolution of the initial compounds in an aqueous system [54]. This process supplies calcium and phosphate ions into the solution, where they interact chemically and precipitate in the form of either the end-products or precursor phases, which causes the cement setting. Some researchers showed that when TTCP and DCPA powders are mixed in double-distilled water, both powders dissolve. The dissolved calcium and phosphate ions in the solution then precipitate in the form of CDHA on the surface of the powders. The precipitate can be either a gel or a conglomerate of crystals. Therefore, the hardening mechanism is either a sol-gel transition of ACP or entanglement of the precipitated crystals of other calcium phosphates [54].

The chemical reactions that take place during the setting of a CPC depend on its chemical composition; however, only two major chemical types of setting reactions are possible [54]. The first type occurs according to the classical rules of an acid-base interaction; that is, an acidic calcium phosphate reacts with a basic one to produce a neutral compound. The following CPC cement is a typical example because TTCP

(basic) reacts with DCPA (slightly acidic) in an aqueous suspension to form a precipitated poorly crystalline HA (slightly basic):

$$Ca_4(PO_4)_2O + CaHPO_4 \rightarrow Ca_5(PO_4)_3OH \qquad (1)$$

Formation of HA according to Eq. (1) releases neither acidic nor basic byproducts. Thus, the liquid phase of the cement remains at a near constant pH of 7.5 for the TTCP +DCPD formulation and 8.0 for the TTCP + DCPA formulation. Another example of the acid-base interaction involves β-TCP (almost neutral) reacting with MCPM (acidic) to form DCPD (slightly acidic):

$$\beta\text{-}Ca_3(PO_4)_2 + Ca(H_2PO_4)_2 \cdot H_2O + 7H_2O \rightarrow 4CaHPO_4 \cdot 2H_2O \qquad (2)$$

The second type of setting reaction might be defined as hydrolysis of a metastable calcium phosphate in aqueous media. As the result, both the initial and final compounds have the same Ca/P ionic ratio. The solid part of such a formulation might be considered a single-phase cement powder. Cements made of ACP + an aqueous solution, α-TCP + an aqueous solution, β-TCP + an aqueous solution, nanocrystalline TTCP + an aqueous solution, or γ-radiated TTCP + an aqueous solution are typical examples, with each of them re-crystallizing to CDHA upon contact with water:

$$3Ca_3(PO_4)_2 \cdot nH_2O \rightarrow Ca_9(PO_4)_5(HPO_4)OH + (3n-1)H_2O \quad (3)$$

$$3\alpha\text{-}Ca_3(PO_4)_2 + H_2O \rightarrow Ca_9(PO_4)_5(HPO_4)OH \quad (4)$$

2.5.2.2. Problematic properties relevant to vertebroplasty and balloon kyphoplasty

These properties are inappropriate setting/hardening times, poor rheological parameters, lack of macroporosity, and inadequate mechanical properties. CPCs should set slowly enough to provide sufficient time to finalize the surgical procedure but fast enough to prevent delaying it. Ideally, good mechanical properties should be reached within minutes after initial setting. Two main experimental approaches are used to study the cement setting process: a batch approach and a continuous approach**.** In the batch approach, the setting reaction is stopped at various times and the resulting samples are analyzed. There are currently two standardized methods that use this approach; namely, the Gillmore needle method (ASTM C266-89) [57] and the Vicat needle method (ASTM C191-92) [58]. Each method involves visually examining the surface of a cement sample to decide whether it has set, with setting denoted when no mark can be seen on the surface after indentation by the needle. A light and thick needle is used to measure initial setting time (I) while a heavy and thin needle is to determine final setting time (F). In a clinical procedure, the cement paste should be implanted before I and terminated after F. The cement should not be deformed between times I and F because at that stage of the setting process any deformation could induce cracks in the cement. The setting process may be monitored in real time by non-destructive methods (the continuous

approach), such as pulse echo ultrasound, isothermal differential scanning calorimetry, and alternating current impedance spectroscopy [59]. It should be noted that the setting time for a CPC often corresponds to an earlier stage in the overall setting reaction, typically 5 – 15 % of the overall reaction, while the end of the cement setting is typically reached after several days.

The two most important rheological properties of calcium phosphate pastes are viscosity and injectability. The viscosity of the cement dough when it is delivered from the syringe to the fractured VB must not be too high (otherwise manual injection would be very difficult) or too low (which would increase the likelihood of extravasation of the cement). Viscosity in the range of 100 – 2,000 Pa·s is considered to be adequate [60]. Mechanical mixing, for example, using an electric mixing machine, allows a cement paste to be obtained within 80 s and enables a rapid and reliable filling of the application syringe [61]. Besides, a cement powder and an aqueous solution might be placed into a syringe and mixed inside a shaker to produce a consistent cement paste of the desired viscosity [62]. Mechanical mixing has been found to decrease both the mean viscosity of the curing cement paste and variability in the viscosity at a given time [63].

Potential problems that may arise during injection of a CPC cement paste into the fractured VB bone include particles might be flushed away into the blood stream, syringe plugging, cannula plugging, phase separation, and paste extravasation [64]. The primary cause of syringe plugging is high permeability of the solid bed for the liquid, where the liquid continuously flows faster than the particles. The cause of cannula plugging is too large particles, typically more than one-third of the cannula diameter. Phase separation (sometimes called filter pressing) is a phenomenon in which there is de-mixing into a thin

paste, which is extruded, and a thick mass, which remains inside the syringe. That is, the liquid comes out of the syringe but a good amount of the powder particles remain in it. Phase separation is avoided when the cement paste has good cohesion, which can be accomplished by, for example, adding cohesion promoters (such as 1 % aqueous solution of sodium alginate) to the cement aqueous solution [65]. One of the causes of cement paste extravasation into neighboring tissues is its low viscosity.

The ease of injection of the cement paste is defined as its injectability. Specifically, in the context of VP and BKP, cement injectability is the ability of the cement paste to be extruded through a small hole of a long needle (typical dimensions of 1 mm diameter and 10 cm length) either directly into the fractured vertebral body (in the case of VP) or into the cavity created in the fractured vertebral body by the bone tamp (in the case of BKP). There are a number of options available for improving cement injectability, examples being use of a shorter cannula with a larger diameter and a cement in which the powder has large particles [66].

In theory, CPCs can be prepared with almost any porosity. However, for most commercially-available CPC brands, pore size is, typically, 8 – 12 μm in diameter and, after the cement is set, about 40 – 50 % of its volume is occupied by pores [67]. The pore dimensions of hardened cements are too small to allow fast bone ingrowth. In other words, the cement lacks sufficient macroporosity. After injection, bone cells are able to degrade the hardened cements layer-by-layer only, starting at the bone-cement interface throughout its inner part [68].

Having a ceramic origin, the set products of all CPCs are brittle and, as such, the cements have low compressive strength (typically, 10-100 MPa), very low impact

resistance, and a very low tensile strength (typically, 1-10 MPa). There are a number of ways of improving the mechanical properties of CPCs, a popular one being addition of water-soluble polymers to the liquid; for example, ultimate compressive strengths of composites of α-BSM with bovine serum albumin and polycations (polyethylenimine and polyallylamine hydrochloride) were up to two and six and times, respectively, greater than that of α-BSM [69].

2.6. Design of experiments

In an experiment, one or more process variables (or factors) can be deliberately changed in order to observe the effect the changes have on one or more response variables. The design-of-experiments (DOE) method is an efficient procedure for planning experiments so that the data obtained can be analyzed to yield valid and objective conclusions [70,71].

DOE begins with determining the objectives of an experiment and selecting the process factors for the study. An experimental design is the laying out of a detailed experimental plan in advance of doing the experiment. Well-chosen experimental designs maximize the amount of information that can be obtained (results collected), for a given amount of experimental effort.

The statistical theory underlying DOE generally begins with the concept of process models. It is common to begin with a process model of the "black box" type, with several discrete or continuous input factors that can be controlled (that is, varied at will by the experimenter) and one or more measured output responses. The output responses are assumed to be continuous. Experimental data are used to derive an empirical (approximation) model linking the outputs and the inputs. These empirical models

generally contain first- and second-order terms. Often, the experimenter has to account for a number of uncontrolled factors that may be discrete, such as different machines or operators, and/or continuous, such as ambient temperature or humidity (Fig. 10).

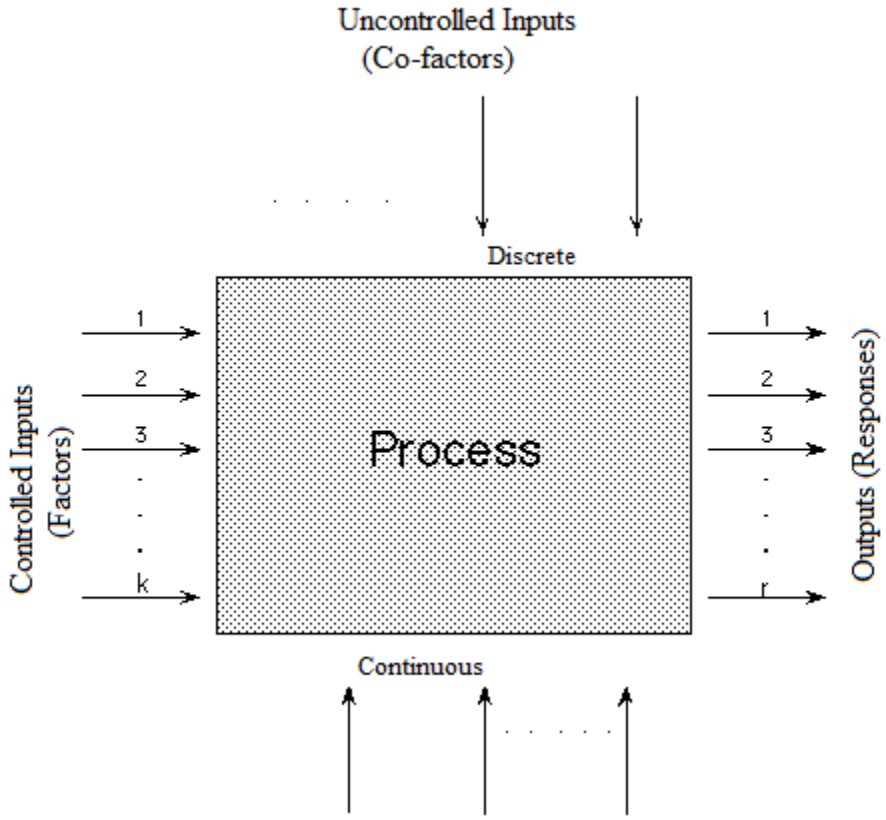

Fig. 10. A schematic drawing of a "black box" process model [71].

The most common fit of an empirical model to experimental data takes either a linear form or a quadratic form. A linear model with two factors, X_1 and X_2, can be written as

$$Y = \beta_0 + \beta_1 X_1 + \beta_2 X_2 + \beta_{12} X_1 X_2 + \text{experimental error}, \quad (5)$$

where Y is the response for given levels of the main effects, X_1 and X_2, and the X_1X_2 term is included to account for a possible interaction effect between X_1 and X_2. The constant, β_0, is the response of Y when both main effects are 0.

A linear model with three factors X_1, X_2, X_3 and one response, Y, can be written as

$$Y = \beta_0 + \beta_1 X_1 + \beta_2 X_2 + \beta_3 X_3 + \beta_{12} X_1 X_2 + \beta_{13} X_1 X_3 + \beta_{23} X_2 X_3 + \beta_{123} X_1 X_2 X_3 + \text{experimental error} \quad (6)$$

The three terms with single Xs are the main effects terms. There are 3 two-way interaction terms and 1 three-way interaction term. When the experimental data are analyzed, all unknown β parameters are estimated and the coefficients of the X terms are tested to see which ones are significantly different from 0.

A second-order (quadratic) model (typically used in response surface DOE with suspected curvature) does not include the three-way interaction term but adds three more terms to the linear model. Thus, the expression becomes

$$Y = \beta_0 + \beta_1 X_1 + \beta_2 X_2 + \beta_3 X_3 + \beta_{12} X_1 X_2 + \beta_{13} X_1 X_3 + \beta_{23} X_2 X_3 + \beta_{11} X_1^2 + \beta_{22} X_2^2 + \beta_{33} X_3^2 + \text{experimental error} \quad (7)$$

Clearly, a full model could include many cross-product (or interaction) terms involving squared Xs. However, in general, these terms are not needed and most DOE software defaults to leaving them out of the model.

2.6.1. Response surface methodology

Response surface methodology (RSM) is a DOE tool that allows a detailed statistical analysis of a problem in which a response of interest is influenced by several variables [71,72]. With this tool, the values of variables that lead to an optimized value of the response may be obtained. In most RSM problems, the true response function, f, is unknown. In order to develop a proper approximation for f, the experimenter usually starts with a low-order polynomial in some small region. If the response can be defined by a linear function of independent variables, then the approximating function is a first-order model. However, if there is a curvature in the response surface, then a higher-degree polynomial should be used; for example, the approximating function with two variables is called a second-order model.

In general, all RSM problems use either a first- or a second-order model or a mixture of the two. In each model, the levels of each factor are independent of the levels of the other factors. In order to get the most efficient result in the approximation of polynomials, proper experimental design must be used to collect data. Once the data are collected, the method of least squares is used to estimate the parameters in the polynomials. The response surface analysis is performed by using the fitted surface. Response surface designs are types of designs for fitting a response surface.

To summarize, then, RSM involves 1) understanding the topography of the response surface (local maximum, local minimum, and ridge lines), and 2) finding the region

where the optimum response occurs. The goal is to move rapidly and efficiently along a path to get to a maximum or a minimum response so that the response is optimized.

2.6.2. Advantages and shortcomings of response surface methodology

RSM has several advantages, four of which are highlighted here. First, it helps to establish a relationship (called the approximate function) between the response variable (Y) and the input/control variables X_1, X_2, X_3,….,X_k that can be used to predict response values for given settings of the control variables. Second, it helps to determine, through hypothesis testing, the significance of the factors whose levels are represented by X_1, X_2, X_3,….,X_k Third, it helps to determine the optimum settings of the control variables that result in a maximum (or a minimum) response over a certain region of interest. Fourth, it provides a way of rigorously choosing a few points in a design space to efficiently represent all possible points and, as such, reduces the number of experimental runs required for studying the significance of different factors that may affect the response of interest.

Four shortcomings of RSM are now described. First, large variation in the factors can be misleading (error, bias, no replication). Second, estimating the accuracy of an approximation is challenging; in other words, determining the magnitude of the approximation errors is difficult. Third, RSM is a local analysis; the developed response surface is invalid for regions other than the studied ranges of factors. Fourth, RSM is sensitive to system noise. In RSM, it is assumed that the experimental noise factors are controllable during process development for purposes of a designed experiment. This assumption reduces the robustness of RSM models. In this respect, Taguchi has modified RSM and developed a new approach known as robust parameter design (RPD)

methodology that makes RSM models insensitive (or robust) to changes in a set of uncontrollable factors [70,72].

2.6.3. Process optimization

The optimal region to which to run a process is usually determined after a sequence of experiments has been conducted and a series of empirical models obtained. In many engineering and science applications, experiments are conducted and empirical models are developed with the objective of improving the response of interest. From a mathematical point of view, the objective is to find the operating conditions (or factor levels) X_1, X_2, ..., X_k that maximize or minimize the system response variables Y_1, Y_2, ...Y_r. In experimental optimization, different optimization techniques are applied to the fitted response equations. Provided that the fitted equations approximate adequately the true (unknown) system responses, the optimum operating conditions of the model will be close to the optimum operating conditions of the true system.

The experimental optimization of response surface models differs from classical optimization techniques in at least three ways. First, experimental optimization is an iterative process; that is, experiments conducted in one set of experiments result in fitted models that indicate where to search for improved operating conditions in the next set of experiments. Thus, the coefficients in the fitted equations (or the form of the fitted equations) may change during the optimization process. In classical optimization, the functions to optimize are supposed to be fixed and given. Second, the response models are fitted from experimental data that usually contain random variability due to uncontrollable or unknown causes. This implies that an experiment, if repeated, will result in a different fitted response surface model that might lead to different optimum

operating conditions. Therefore, sampling variability should be considered in experimental optimization. In classical optimization, the functions are deterministic and given. Third, in response models, the fitted responses are local approximations, implying that the optimization process requires the input of the experimenter (a person familiar with the process). Classical optimization is always automated in the form of some computer algorithm.

CHAPTER 3

LITERATURE REVIEW

3.1. Injectable bone cements for use in vertebroplasty and balloon kyphoplasty

There is a large body of literature on the direct effect of one or more intrinsic or extrinsic variables on a wide collection of properties of both PMMA bone cements and CPCs for use in VP and BKP. Intrinsic variables refer to compositional parameters, such as presence or absence of reinforcing fillers in the cement powder, whereas extrinsic variables refer to preparation/fabrication parameters, such as PLR. Key features of a sample of these literature reports are given in Tables 4 and 5. The observations from this review are 1) of the properties of PMMA bone cement that were characterized as "problematic" (see sub-section 2.5.1.4), only T_{max} and RMC have been investigated [75,76,81-83]); and 2) there have been many studies involving properties of CPC that were characterized as "problematic" (see sub-section 2.5.2.2).

Table 4
Summary of studies on direct effect of one or more variables on properties of PMMA bone cement for VP and BKP

Cement property/properties	Variable(s)	Influence	Reference
Compressive modulus of elasticity (E_c); compressive yield strength (YS)	Addition of 2% aqueous solution of sodium hyaluronate (0-50%) to cement liquid	Decrease in each property	Boger et al. [73]
E_c; ultimate compressive strength (UCS)	Addition of radiopacifier to cement powder (15 wt/wt% of ZrO_2, $BaSO_4$, Lipiodol) or to cement liquid (7.5 mL of Lopamiro or Ultravist)	Influence complex	Boger et al. [74]
E_c; YS; maximum exotherm temperature (T_{max});	Addition of castor oil (2.5-12.0 wt/wt%) to cement liquid	Decrease in each property	Lopez et al. [75]
YS; E_c; T_{max}; initial viscosity; setting time (t_{set})	Addition of bone marrow (0-7 mL) to cement liquid	Except for initial viscosity, each property decreased	Arens et al. [76]
Viscosity-mixing time profile	Ambient temperature under which test was conducted (T_{amb})	Mean time to reach a selected viscosity decreased with increase in T_{amb}	Boger et al. [77]

Table 4
Summary of studies on direct effect of one or more variables on properties of PMMA bone cement for VP and BKP

Cement property/properties	Variable(s)	Influence	Reference
Polymerization rate, at 37 ^{o}C; fatigue limit	PLR	Increase in PLR led to a significant increase in polymerization rate; influence of PLR on fatigue limit not significant	Lewis et al. [78]
Injectability; water intake; UCS; ultimate bending strength (UBS) (3-point flexure); E_c; bending modulus (E_b) (3-point flexure); impact strength	Addition of an antibiotic (5 wt/wt% ciprofloxacin alone or in combination with another antibiotic (3 wt/wt% vancomycin)) to cement powder	Injectability decreased; water intake increased; UCS unaffected; E_c increased; UBS unaffected; E_b unaffected; impact strength decreased	Hernandez et al. [79]
Viscosity-mixing time profile	Mixing method (manual versus oscillatory)	At any mixing time, viscosity significantly lower when cement was oscillatory mixed	Baroud et al. [63]
Setting temperature (T_{set}); t_{set}; T_{max}; time at maximum temperature (t_{max})	Mixing method (manual versus oscillatory)	No significant influence on any of the properties	Baroud et al. [80]
Injectability; UCS; E_c; residual monomer content (RMC)	Surface treatment of $MTiO_3$ particles (M: Ba or Sr) added to the cement powder as radiopacifier (none vs silanated)	Silanation led to increases in each property, with the exception of RMC, which was unaffected	Carrodeguas et al. [81]

Table 4
Summary of studies on direct effect of one or more variables on properties of PMMA bone cement for VP and BKP

Cement property/properties	Variable(s)	Influence	Reference
UCS; viscosity; T_{max}; t_{set}	Size of ZrO_2 spheres added as radiopacifier (microsphers vs nanospheres)	UCS and viscosity lower when microspheres were used; T_{max} and t_{set} are both unaffected With each type of sphere, viscosity increased with increase in sphere content	Rodriguez et al. [82]

In addition to the studies reviewed above (Table 4), Carrodeguas et al. [81] determined the t_{dough}, t_{set}, T_{max}, RMC, UCS, E_c, and injectability of 8 cements. The compositions of these cement differed in terms of the following variables: amount of PMMA, $MTiO_3$ (M = Ba or Sr), and BPO in the powder; amount of MMA and 4-N,N-dimethylamino benzyl alcohol in the liquid; and PLR. Thus, it is difficult to isolate the influence of a given variable on a given cement property.

Table 5
Summary of a sample of studies on direct effect of one or more variables on properties of calcium phosphate cements

Cement property/ properties	Variable(s)	Influence(s)	Reference
Viscosity	Mixing method (manual versus oscillatory mixing)	For one cement (ChronOS Inject), viscosity significantly lower when cement was oscillatory mixed; for another cement (Bioplex), change was not significant	Baroud et al. [63]
Injectability	Resting time; that is, time over which cement set without further mixing	Injectability decreased with increase in resting time	Vlad et al. [83]
Injectability	Agitation at a given resting time (none versus mixing at 1600 rpm for 30 s)	Agitation led to significant decrease in injectability	
UBS (3-point flexure); E_b (3-point flexure); WOF (3-point flexure)	Amount of chitosan lactate in the liquid	For a given PLR, each property increased with increase in chitosan content	Weir et al. [84]
	PLR	For a given chitosan content, each property increased with increase in PLR	

Table 5
Summary of a sample of studies on direct effect of one or more variables on properties of calcium phosphate cements

Cement property/ properties	Variable(s)	Influence(s)	Reference
UCS; energy-to-failure (compression test) (ETF)	Addition of a water-soluble polymer (PAH, PEI, PDMAC, SPS, PEO) or bovine serum albumin (BSA) to the cement paste during setting	Influence depended on the additive; e. g., PAH and PEI composites showed very large increase; PDMAC and SPS composites showed slight drop; PEO composites showed little or no increase; and BSA composites show large increase. In general, ETF results followed the same trends as the UCS results	Mickiewicz et al. [85]
Injectability; doughing time (t_d); initial setting time (I); final setting time (F)	PLR	Increase in each property with decrease in PLR	Khairoun et al. [66]
	Addition of Na_2HPO_4 to cement liquid [SPC]	At a given PLR, decrease in each property with increase in [SPC]	
I; F; UCS	PLR	At a given [SPC], I increased, F increased, and UCS decreased with decrease in PLR	Khairoun et al. [86]
	Addition of Na_2HPO_4 to cement liquid [SPC]	At a given PLR, each property decreased with increase in Na_2HPO_4 content	

Table 5
Summary of a sample of studies on direct effect of one or more variables on properties of calcium phosphate cements

Cement property/ properties	Variable(s)	Influence(s)	Reference
Injectability; UCS	Addition of a fine-particle-sized filler [dicalcium phosphate anhydrous (DCPA), titanium dioxide (TiO_2), or calcium carbonate] to cement powder PLR	At a given PLR, filler increased injectability At a given filler content, injectability decreased markedly with increase in PLR At a given PLR, addition of DCPA or TiO_2 filler did not significantly influence UCS	Gbureck et al. [87]
Setting time (T); diametral tensile strength (DTS)	Addition of an antibiotic (flomoxef sodium) to cement powder	T increased and DTS decreased with addition of antibiotic Very slight increase in T but sharp decrease in DTS with increase in antibiotic content	Takechi et al. [88]
F; DTS	Sterilization of cement powder (steam; dry heat; EtO gas; γ-irradiation)	Sterilization led to higher F and lower DTS With γ-irradiation, F increased and DTS decreased with increase in dose	Tekechi et al. [89]
Injectability; UBS (3-point bend); E_b (3-point bend)	PLR	Injectability decreased, UBS increased, and E_b increased with increase in PLR	Burguera et al. [90]

Table 5
Summary of a sample of studies on direct effect of one or more variables on properties of calcium phosphate cements

Cement property/ properties	Variable(s)	Influence(s)	Reference
Injectability	PLR	Property increased with decrease in PLR	Bohner et al. [91]
	Liquid composition (water vs 1% polyacrylic acid sodium salt (PAA) vs 0.2% xanthan)	At a given PLR, injectability was in order: PAA > xanthan > water	
Injectability; UCS	PLR	At a given PLR, injectability with water lower than with citrate. Same trends for UCS	Gbureck et al. [92]
	Liquid composition (tri-sodium citrate vs water)	With each liquid, UCS increased with increase in PLR	
I; F	PLR	Each time decreased with increase in PLR	Barralet et al. [93]
UCS	Addition of sodium citrate solution or citric acid solution to cement liquid	At a given PLR, UCS decreased with increase in sodium citrate concentration but independent of citric acid concentration	

Table 5
Summary of a sample of studies on direct effect of one or more variables on properties of calcium phosphate cements

Cement property/ properties	Variable(s)	Influence(s)	Reference
UCS	Pre-compaction pressure of cement paste (PLR = 3.3 and 500 nM of additive solution)	Influence complex	
UCS	α-TCP content of cement powder	Property increased linearly with increase in α-TCP content	Nilsson et al. [94]
Injectability; I; F; UCS; UBS (4-point bend)	Addition of (poly (4-HMA) to cement liquid	Influence depended on the 4-HMA content; e. g., with 5 wt/wt%, injectability increased but after a longer period it decreased; I decreased; F decreased; UCS increased; and UBS increased relative to values when there was no 4-HMA	Ginebra et al. [95]
Injectability	Addition of an adjuvant, such as sodium glycerophosphate, lactic acid, or glycerol to cement liquid	With each additive, property increased	Leroux et al. [96]

Table 5
Summary of a sample of studies on direct effect of one or more variables on properties of calcium phosphate cements

Cement property/ properties	Variable(s)	Influence(s)	Reference
Injectability; viscosity	Addition of carboxymethyl cellulose (CMC), agarpolymer (AGAR), and sodium alginate (SA) to cement powder	With each additive, injectability increased and viscosity decreased Influence of additive content on injectability depended on additive; e. g., with CMC, injectability increased with increased content but that was not the case with AGAR.	Alves et al. [65]
I; injectability; UCS	A porogen (acetic acid versus citric acid) dissolved in the cement liquid	Porogen led to significant decreases of I and UCS Cement prepared with citric acid showed better injectability compared to CPC prepared with acetic acid	Herasaki et al. [97]
UCS	Addition of gelatin to cement powder	Property increased up to gelatin content of 8 wt/wt% after which it decreased	Fujishiro et al. [98]
	Addition of wt/wt% of either $CaTiO_3$ or HA powder to cement powder	Property increased	

Table 5
Summary of a sample of studies on direct effect of one or more variables on properties of calcium phosphate cements

Cement property/ properties	Variable(s)	Influence(s)	Reference
T; injectability; UBS (4-point flexure); WOF (4-point flexure); E_b (4-point flexure)	Composition of liquid (aqueous sodium phosphate vs aqueous sodium phosphate-HPMC)	With sodium phosphate, both T and injectability decreased with increase in content	Burguera et al. [99]
		With sodium phosphate-HPMC, marginal influence of content on T, UBS, WOF, and E_b while injectability increased with content up to 0.5 mass% after which it stayed unaffected	
UCS	Pressure applied to cement paste in mold (p_{comp})	With water, increase in property with increase in p_{comp}; with phosphate, decrease in property with increase in p_{comp}	Burguera et al. [100]
	Composition of liquid (water vs sodium phosphate solution)	For a given p_{comp}, UCS higher when water was used compared to when phosphate was used	

Table 5
Summary of a sample of studies on direct effect of one or more variables on properties of calcium phosphate cements

Cement property/ properties	Variable(s)	Influence(s)	Reference
UCS; fracture toughness (J_{IC}); DTS	Addition of fibers (carbon, polypropylene, nylon 66) to cement powder For a given fiber, volume fraction (V_f)	UCS decreased with addition of each of the fibers. Influence on J_{Ic} depended on the fiber; thus, with both C and nylon, it increased with increase in V_f but with propylene, it was practically constant with increase in fiber content until 5% after which it decreased Influence on DTS depended on the fiber; thus, with C, it increased up to fiber content of 3 wt/wt% after which it decreased ; with each of the other two fibers, influence was marginal	dos Santos et al. [101]

Table 5
Summary of a sample of studies on direct effect of one or more variables on properties of calcium phosphate cements

Cement property/ properties	Variable(s)	Influence(s)	Reference
UCS; compressive fracture energy; E_c	Composition of liquid (polypeptide graft copolymer vs polypeptide micelle)	With polypeptide graft solution, E_c decreased with polypeptide content regardless of liquid composition With polypeptide graft solution, influence on each of the other two properties depended on the property, the liquid composition, and the polypeptide content With polypeptide micelle solution, influence on each of the properties depended on the property, the liquid composition, and the polypeptide content	Lin et al. [102]
DTS	Addition of $NaHCO_3$ to cement powder	Property decreased	Miyamoto et al. [103]

Table 5
Summary of a sample of studies on direct effect of one or more variables on properties of calcium phosphate cements

Cement property/ properties	Variable(s)	Influence(s)	Reference
UCS; T	Ca/P ratio of cement powder Composition of liquid ($NaHPO_4$ vs water)	UCS decreased with decrease in Ca/P ratio; With each liquid, T was not significantly affected by Ca/P ratio At a given Ca/P ratio, when $NaHPO_4$ was used, UCS was, on average, lower than when water was used; T was significantly higher when water was used	Burguera et al. [104]
I; injectability; UCS	Fluidicant (citric acid (CA) versus no fluidicant)	I unaffected but injectability increased when CA was used When CA used, I increased with increase in CA content, up to ~1.8 wt/wt%, after which it decreased. Same pattern seen for injectability results 1.5 wt/wt% CA retarded evolution of UCS	Sarda et al. [105]
UCS; Weibull compressive modulus	Compaction pressure (p_{comp})	Each property increased with increase in p_{comp}	Barralet et al. [106]
Injectability; I	Addition of gelatin microspheres to cement	Each property increased slightly (25-45%)	Habraken et al. [107]

Table 5
Summary of a sample of studies on direct effect of one or more variables on properties of calcium phosphate cements

Cement property/ properties	Variable(s)	Influence(s)	Reference
DTS; UCS	Time of paste in mold during setting; p_{comp} PLR; liquid composition (distilled water vs phosphate solution)	Influence of each variable was small but significant With water, DTS unaffected but UCS decreased with decrease in PLR. With phosphate, each property was unaffected	Chow et al. [108]
Resorption of implants in the diaphysis of femoral bones of New Zealand white rabbits	Amount of Zn-containing TCP powder in cement powder	Marked decrease in property with increase in Zn content	Ito et al. [109]
I; F	Addition of tantalum pentoxide (Ta_2O_5) as radiopacifier	Each time increased with addition of a radiopacifier	Hoekstra et al. [110]

Table 5
Summary of a sample of studies on direct effect of one or more variables on properties of calcium phosphate cements

Cement property/ properties	Variable(s)	Influence(s)	Reference
UBS (3-point flexure); WOF (3-point flexure); E_b (3-point flexure); UCS; I; F; injectability	Addition of high-strength β-TCP aggregates to cement powder	With addition, UBS, WOF, E_b, UCS increased, I decreased, F decreased, injectability decreased With increase in β-TCP aggregates content, UCS increased up to content of 20 wt/wt% and then decreased; but I, F, and injectability each dropped continuously	Gu et al. [111]
UCS	Molar ratio of monocalcium phosphate monohydrate (MCPM) to hydroxyapatite in cement	UCS when ratio = 4:1 > UCS when ratio = 2:3 > UCS when ratio = 2:5	Alge et al. [112]
I; UCS	Addition of a liposoluble statin, simvastatin (SIM), to the cement powder	No significant effect on I by either SIM or SDS	Yin et al. [113]
	Addition of an air-entraining agent, sodium doceyl sulfate (SDS), to the cement liquid	With no SDS, SIM had no significant influence on UCS; with 300 mM SDS, UCS decreased with increase in SIM	

Table 5
Summary of a sample of studies on direct effect of one or more variables on properties of calcium phosphate cements

Cement property/ properties	Variable(s)	Influence(s)	Reference
I; F; UCS	Amount of colloidal silica suspension added to cement liquid	I decreased, F decreased, and UCS increased significantly For cements that contained the colloid, I decreased, F decreased, and UCS increased continuously with increase in colloid content	Heraskai et al. [114]
UBS; E_b; WOF	Amount of bovine collagen (BC) in cement powder PLR	At a given value of BC, both UBS and E_b increase but little effect on WOF, with increase in PLR At a given PLR, small decrease in UBS, small increase in Eb, and large increase in WOF, with increase in BC	Moreau et al. [115]

MC3T3E1: clonal murine calvarial cells; PAH: poly(allylamine hydrochloride);

PEI: poly(ethylenimine); PDMAC: poly(diayldimethylammonium chloride);

SPS: poly(sodium 4-styrenesulfonate); PEO: poly(ethylene oxide);

4-HMA: a methacrylamide derived from 4-aminosalicylic acid; HPMC: hydroxypropyl methylcellulose.

In addition to the above-reviewed studies (Table 5), Lopez-Heredia et al. [116] determined I, F, injectability, UCS, specific compressive strength (= UCS/density), indirect strength (ITS) (using the Brazilian test method), and specific indirect tensile strength (= ITS/density) of 7 cements. However, differences in the compositions of the cements (amounts of fibrin, fibrinogen, and thrombin) and the amount of liquid used in preparing the cement pastes make it difficult to isolate the influence of a variable (fibrin amount and thrombin type (long-setting variant versus fast-setting variant) on a cement property.

3.2. Response surface methodology

There are a multitude of reports in the literature on the application of RSM to a very large array of fields of study, ranging from materials science to fuel processing technology and from manufacturing engineering to renewable energy. Some aspects of a small sample of these reports are now presented.

Thirumalaikumarasamy el al. [117] reported on the influence of atmospheric plasma spraying parameters (input energy (IE), stand-off distance (SOD), and powder feed rate (PFR)) on the porosity level of an alumina coating on AZ31B magnesium alloy. The optimum (minimum achievable) porosity level was determined to be 4.44 vol/vol%, with this being obtained when IE, SOD, PFR were 22.27 kW, 11.30 cm, and 21.50 g min^{-1}, respectively.

In the case of friction-stir-welded AA6061–T6 aluminum alloy joints, Rajakumar et al. [118] developed empirical relationships that relate six friction stir welding input parameters (rotational speed (RS), welding speed (WS), axial force (AF), shoulder diameter (SD), pin diameter (PD), and tool hardness (TH)) to three properties of

the joints (tensile strength, hardness, and corrosion rate). The combination of the values of these process parameters that would simultaneously maximize tensile strength, maximize hardness, and minimize corrosion rate were computed to be RS = 1,100 rev min^{-1}, WS = 80 mm min^{-1}, AF = 8 kN, SD = 15 mm, PD = 5 mm, and TH = 45 HRc.

Bhushan [119] investigated the effects of cutting speed (CS), feed rate (FR), depth of cut (DC) and nose radius (NR) on power consumption and tool life in computerized numerically-controlled turning of a composite (7075 Al alloy reinforced with 15 wt/wt% SiC particle size: 20-40 μm) using a 6615-grade tungsten carbide cutting tool. The minimum power consumption (1,116 watt-hours) and maximum tool life (6.6 min) were found to occur with CS = 90 m min^{-1}, FR= 0.15 mm rev^{-1}, DC = 0.20 mm, and NR = 0.42 mm.

Gil et al. [120] used RSM for optimizing carbon adsorbents for the highest possible CO_2 capture capacity of activated carbons. Carbon precursors were prepared by incorporating potassium chloride (KCl) into the Re and No1 cured resins, which were impregnated with KCl at ambient temperature (ReKCla and No1KCla precursors) or boiled with a saturated KCL solution (ReKClb and No1KClb precursors).
The No1KCla-600 carbonized was prepared from No1KCla precursor carbonized at 600^{o} C and the No1KClb-1000 carbonized material was prepared from No1KClb precursor carbonized at 1000^{o} C. The blend of olive stone to resin mixed with hexa methylene teramine (28.6 wt/wt%) and heated at 170^{o} C for 30 min resulted in the No2OS precursor. The No2OS precursor was carbonized at 1000^{o} C to obtain the No2OS-1000 carbonized material. The activation parameters (temperature and burn-off

degree) did not influence the capture capacity of the evaluated carbonized materials in a uniform way. Thus, 1) for No1KCla-600, the maximum CO_2 capture capacity was 9.3 wt/wt% and it was reached at an activation temperature of 809^o C and a burn-off degree of 22%; and 2) for No1KClb-1000 and No2OS-1000, the maximum CO_2 capture capacity and activation temperature were 7.5 wt/wt% and 800^o C and 7.3 wt/wt% and 942^{o}C, respectively, regardless of the burn-off degree.

In an RSM optimization study involving air cyclones used as separators, which rely on centrifugal forces to separate particles from a gas stream, Elsayed et al. [121] found that the combination of cyclone geometrical parameters that led to the minimum pressure drop were as follows: vortex finder diameter = 0.487 m, inlet height = 0.628 m, inlet width = 0.203 m, vortex finder length = 0.733 m, total cyclone height = 4.852 m, cylinder height = 1.633 m, and cone tip diameter = 0.383 m.

Cisneros-Pineda et al. [122] used RSM to investigate the effect of the amount of $BaSO_4$ and the amount of a co-monomer, diethyl amino ethyl methacrylate on the properties of a PMMA bone cement. The interaction between these two variables produced significant effect on a number of cement properties, such as T_{max}, setting time, RMC, and injectability.

Direct and interaction effects of three variables on a number of properties of a PMMA bone cement were studied by Lopez et al. [11]. The variables were the amount of BPO, the amount of a crosslinking agent (ethylene glycol dimethacrylate (EGDMA)), and PLR. The cement properties were UCS, E_c, t_{dough}, $t_{setting}$, T_{max}, t_{ons}, and the critical curing rate (CCR). t_{ons} is time at the onset of cure and it is defined as the time when the complex viscosity increased sharply. CCR is defined as the slope of the complex viscosity-versus-

mixing time curve at $t_{ons.}$ There were significant direct effects of the amount of EGDMA on compressive strength, the amount of EGDMA on t_{set}, the amount of BPO on t_{set}, the amount of EGDMA on T_{max}, and PLR on T_{max}. Furthermore, there were significant interactive effects between the amount of EGDMA and the amount of BPO on both t_{dough} and CCR.

O'Hara et al. [123] used DOE to determine the factors that have the greatest effect on the mechanical and handling properties of an apatitic calcium phosphate cement. The optimum predicted values were compressive strength = 26 MPa, injectability = 30%, I = 6 min, and F = 13 min. These property values were obtained with a cement powder that contained no HA, a cement liquid of 5 wt% Na_2HPO_4, and a PLR of 2.86 g mL^{-1}. It was found that the material properties were interrelated; for example, increasing compressive strength had a negative effect on the handling properties and vice versa. The authors did not include a statistical analysis of the interaction effects.

Direct and interaction effects of compositional variables on the ultimate compressive strength of CPC composites comprising calcium phosphate, multi-walled carbon nanotubes (MWCNTs), and bovine serum albumin (BSA) were studied by Low et al. [124]. The optimum compressive strength of the composite was found to be 12.5 MPa, which was achieved when the composition of the composite was 84.5 wt/wt% calcium phosphate, 0.5 wt/wt% of MWCNTs, and 15 wt/wt% BSA.

CHAPTER 4
CASE STUDIES

4.1. Case Study #1: Maximum exotherm temperature of a PMMA bone cement

4.1.1. Experimental details

A radiolucent cement powder was used, while the liquid was that in a commercially-available brand used for BKP (KyphX® HV-R™; Medtronic Spinal & Biologics, Memphis, TN, USA) but modified by addition of a quaternary amine co-monomer (QACM). The cement powder and liquid were mixed in a polyethylene bowl that was open to the laboratory atmosphere.

The maximum exotherm temperature (T_{max}) of the cement was determined by using the protocols given in ISO 5833 standard [125]. After mixing the cement powder and liquid, the dough was poured into a circular ultra-high-molecular-weight polyethylene (UHMWPE) mold (diameter and height = 60 mm and 20 mm, respectively), equipped with a thermocouple, positioned with its junction 3.0 ± 0.5 mm above the base of the mold. An UHMWPE cover (8 mm thick) was placed over the dough in the mold to squeeze out excess dough. The mold was placed in a thermostatically-controlled water bath, with the temperature maintained at 37^{o} C. A record of the temperature of the cement as a function of polymerization time, up to the point when the cement was fully polymerized, taken continuously, was exported to a data acquisition system. T_{max} was computed from this temperature-versus-time record, per ISO 5833. The results are given in Table 6.

Table 6
Maximum exotherm temperature (T_{max}) of a PMMA bone cement

$BaSO_4$ content (wt/wt%)	QACM content (wt/wt%)	T_{max} (^oC)
0	5	79
0	10	75
5	5	84
5	15	62
15	0	85
15	10	78
15	20	50
25	5	58
25	15	49
30	5	88
30	10	69

4.1.2. Design matrix

Two factors (explanatory variables) were considered for their influence on the maximum exothermic temperature (T_{max}) of a PMMA bone cement; namely, $BaSO_4$ content (BA) and quaternary amine co-monomer content (QU). For each factor, 5 values were used; thus, there were 11 data points.

For the RSM work (Design-Expert®, Version 8; Star-Ease, Inc., Minneapolis, MN), therefore, it was appropriate to use the two-factors, five-levels, central composite design matrix (rotatable option). The values of the factors used and the corresponding level for

each factor are given in Table 7 while, in Table 8, the 11 data points are presented both as coded values and as raw values.

Table 7
Factors and their levels: maximum exotherm temperature of a PMMA bone cement

Factor	Unit	Coded levels				
		-1.414	-1	0	+1	+1.414
$BaSO_4$ content (BA)	wt./wt.%	0.00	5.00	15.00	25.00	30.00
Quaternary amine comonomer content (QU)	wt./wt.%	0.00	5.00	10.00	15.00	20.00

Table 8
Design matrix and experimental results: maximum exotherm temperature of a PMMA bone cement

Cement	Coded values		Raw values		Maximum exotherm temperature
	BA	QU	BA	QU	T_{max}
			(wt/wt%)	(wt/wt%)	(^{o}C)
A	-1.414	-1	0	5	79
B	-1.414	0	0	10	75
C	-1	-1	5	5	84
D	-1	+1	5	15	62
E	0	-1.414	15	0	85
F	0	0	15	10	78
G	0	+1.414	15	20	50
H	+1	-1	25	5	58
I	+1	+1	25	15	49
J	+1.414	-1	30	5	88
K	+1.414	0	30	10	69

4.1.3. Empirical relationship and regression analysis

The second-order polynomial (regression) equation used to represent the response surface (T_{max}) is given by

$$T_{max} = b_o + \sum b_i X_i + \sum b_{ij} X_i X_j + \sum b_{ii} X_i^2, \quad (8)$$

where X_i and X_j are the two factors.

Thus, the selected polynomial could be expressed as

$$T_{max} = b_o + b_1 (BA) + b_2 (QU) + b_{12} (BA)(QU) + b_{11} (BA)^2 + b_{22} (QU)^2 \quad (9)$$

where b_o is the mean of the responses; b_1 and b_2 are the regression coefficients that characterize the direct effects of the factors; b_{12} is the regression coefficient that characterizes the interaction effect of the factors; and b_{11} and b_{22} are the regression coefficients that characterize the quadratic effects of the factors.

With the computed values of the coefficients, it is found the quadratic models given above were aliased. In experimental design, when two interactions, or a main effect and an interaction, share the same column, and so cannot be individually analyzed, then their effects are termed “aliased”. Hence, the linear model is used in RSM and Eq. (9) becomes

$$T_{max} = 91.514 - 0.265(BA) - 1.858(QU) \quad (10)$$

4.1.4. Adequacy of regression model

Analysis of variance (ANOVA) of the regression model was performed and the results (Table 9) were used to examine the adequacy of the model. The desired level of confidence was considered to be adequate provided that 1) the calculated value of the F ratio of the model developed did not exceed the standard tabulated value of the F ratio and 2) the calculated value of the coefficient of determination (R^2) of the developed relationship exceeded the standard tabulated value of the R^2 for a desired level of confidence (in this case study, 0.64).

Table 9
The ANOVA results (response parameter: maximum exotherm temperature (T_{max}), in ^{o}C, of a PMMA bone cement)

Source	Sum of squares	Df	Mean Square	F value	p-value Prob > F	
Model	1269.28	2	634.64	7.345	0.016	significant
BA	91.56	1	91.56	1.060	0.333	
QU	1177.72	1	1177.72	13.630	0.006	
Residual	691.27	8	86.41			
Cor total	1960.55	10				
Std dev	9.296	R^2	0.6474			
Mean	70.636	Adj R^2	0.5593			
COV (%)	13.160	Pred R^2	0.3801			
		Adeq precision	7.6575			

The model F-value of 7.345 implies the model is significant because there is only a 1.16% chance that a model F-value this large could occur due to noise. The goodness of fit of the model is indicated by the coefficient of determination (R^2), which was found to be 0.6474, which implies that 64.74% of the experimental data were predicted by the model. For a good statistical model, R^2 value should be close to 1.0. The adjusted R^2 value recalculates the model coefficient of determination but, this time, only the significant model terms were considered. The adjusted R^2, 0.5593, was not high enough to confirm the significance of the model. The predicted R^2 is 0.3801, which means that the model could explain 38% of the variability in predicting new T_{max} observations. The parameter, Adeq precision, is a measure of the signal-to-noise ratio, with a value > 4 considered desirable. In this case study, the ratio was 7.6575, which indicated an adequate signal. The coefficient of variation (COV), 13.16%, is low enough to indicate that the deviations between the experimental and the predicted values are low. All of the aforementioned ANOVA results show that the model (Eq. (10)) was adequate and, thus, may be used to navigate the design space.

Values of "Prob > F" less than 0.0500 indicate model terms that are significant. Thus, in this case study, the only significant model term is QU and BA is not significant model term. But the model Eq. (10) is significant and was adequate and hence used as is

$$T_{max} = 91.514 - 0.265(BA) - 1.858(QU) \quad (11)$$

For a given response, the contributions of factors can be ranked from their respective F ratio values provided the degrees of freedom are same for all the input parameters. The larger the F ratio the higher is the significance. From the F ratio values (Table 9), it is seen that QU exerts a greater influence on T_{max} than does BA.

4.1.5. Residuals and correlation exercises

The normal probability plot of the residuals for T_{max} is not perfectly linear (Fig. 11), indicating that the errors (residuals) are not distributed normally. There are extreme positive and negative residuals and, hence, this distribution is "heavy tailed". The relationship between the sample percentiles and theoretical percentiles is not linear and, hence, the condition that the error terms are normally distributed is not met. The match between the predicated and the experimental maximum exothermic temperature T_{max} values is not very good (Fig. 12).

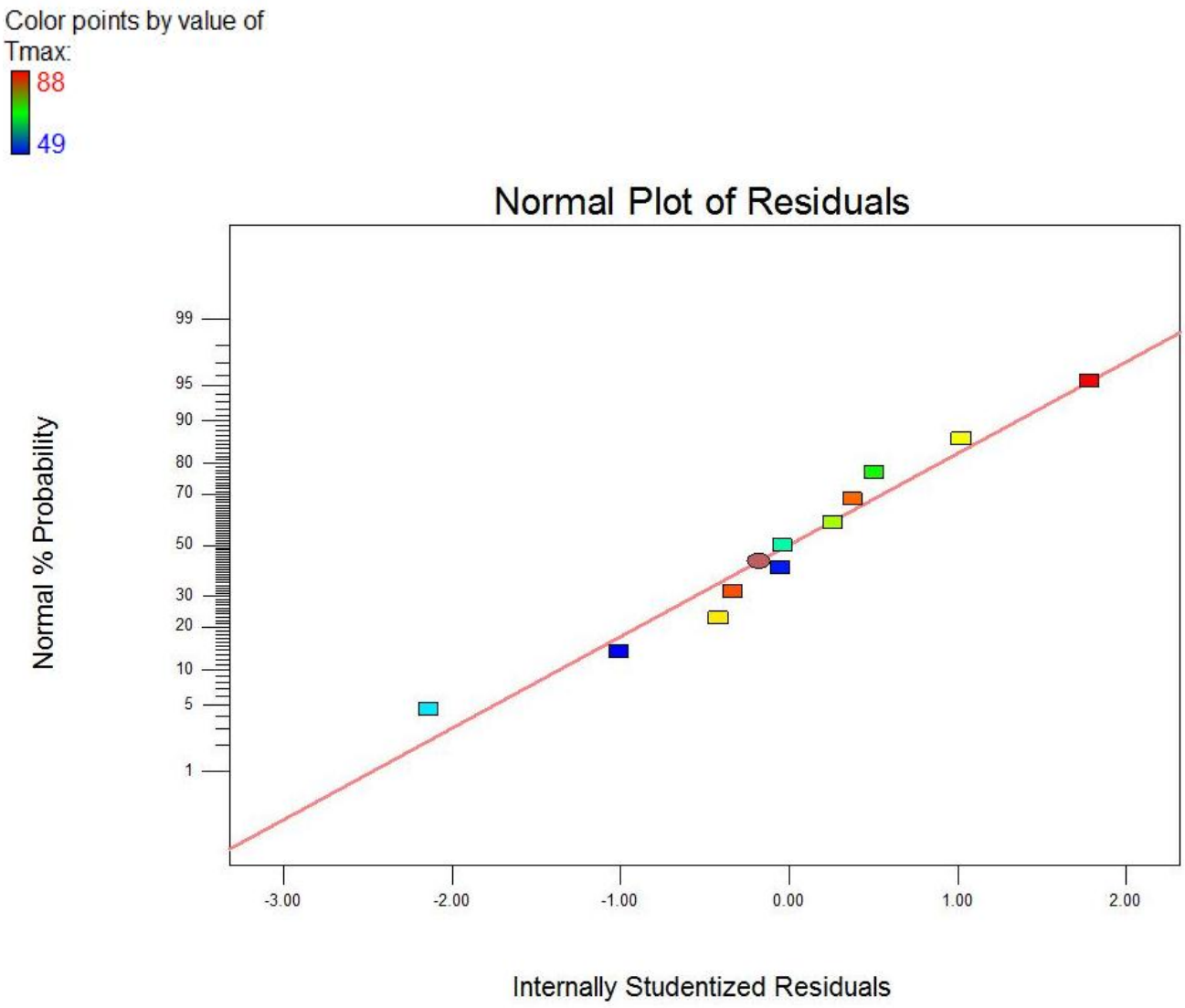

Fig. 11. The normal probability plot of the maximum exotherm temperature results for a PMMA bone cement.

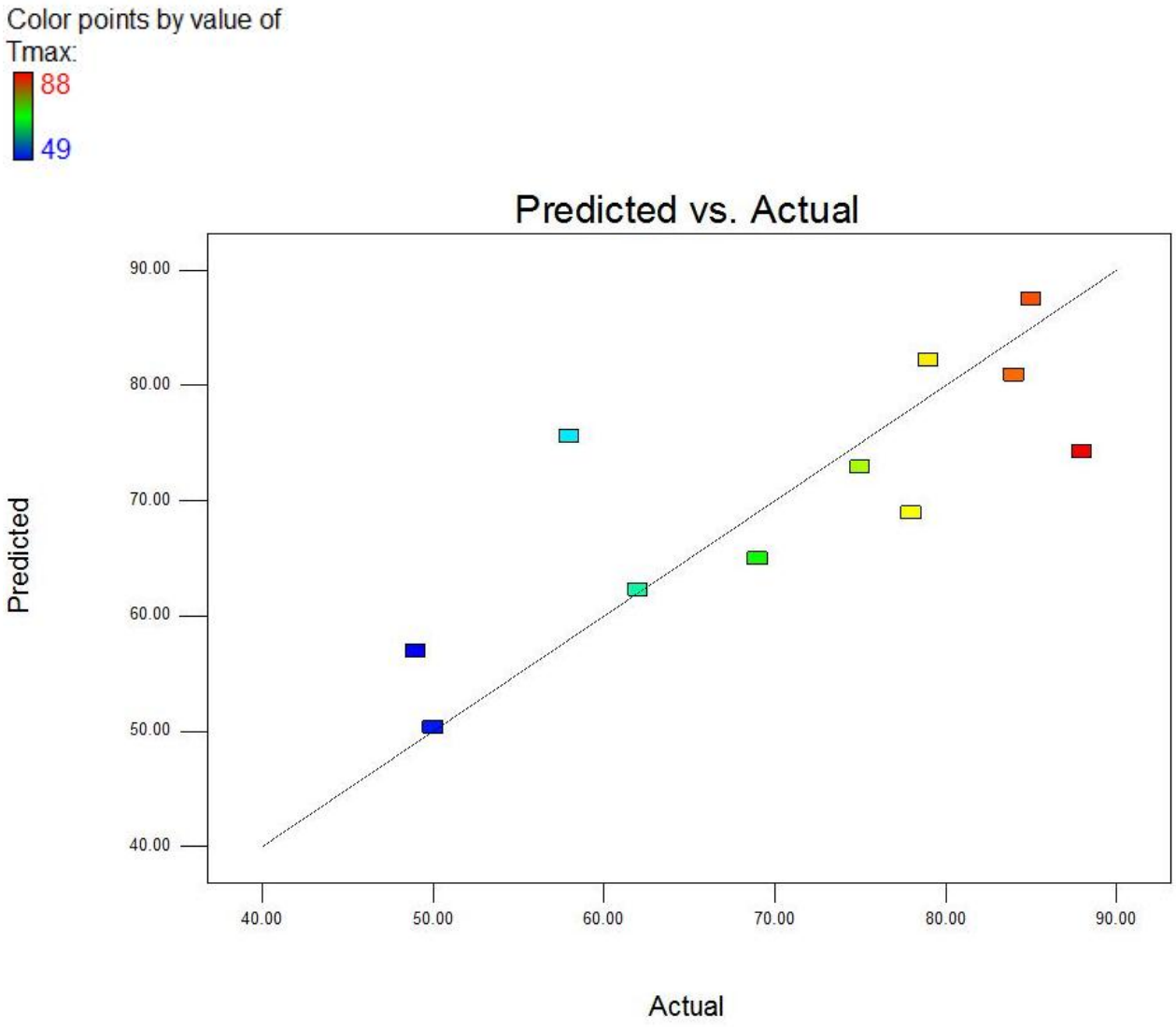

Fig. 12. The correlation plot of the maximum exothermic temperature (T_{max}) results for a PMMA bone cement.

4.1.6. Optimization exercise

To obtain the optimum combination for getting cement the minimum value of T_{max}, response surface, contour, and desirability plots were developed for the proposed model that contained only the significant coefficients (Eq. (11)). A contour plot was produced to display the regions of the optimal factor settings. Either the response surface plot or the contour plot may be used to predict the response (minimum value of T_{max}) for any zone of the experimental domain. As shown on the surface response plot (Fig. 13A), the desired optimum is the minimum value. After identifying the stationary point in a contour plot, it has to be determined if it is the maximum, minimum, target, or saddle point. An analysis of the response surface and contour plots (Figs. 13A and B) found that the indicated minimum value (47.62^{o} C) has a desirability equal to 1.000 (Fig 13C). This minimum value of T_{max} is obtained when BA = 26.51 wt/wt% and QU = 19.82 wt/wt%.

A

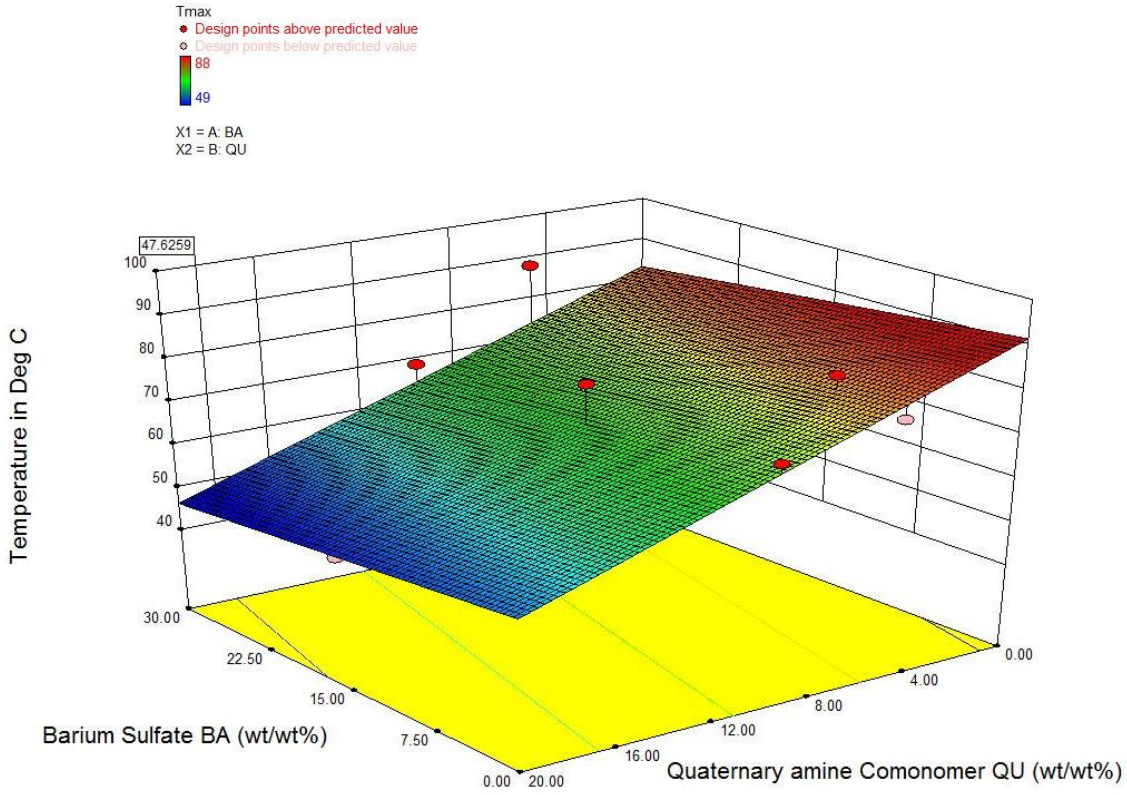
Tmax
Design points above predicted value
Design points below predicted value
88
49
X1 = A: BA
X2 = B: QU
47.6259
100
90
80
70
60
50
40
Temperature in Deg C
30.00
22.50
15.00
7.50
0.00
Barium Sulfate BA (wt/wt%)
0.00
4.00
8.00
12.00
16.00
20.00
Quaternary amine Comonomer QU (wt/wt%)

B

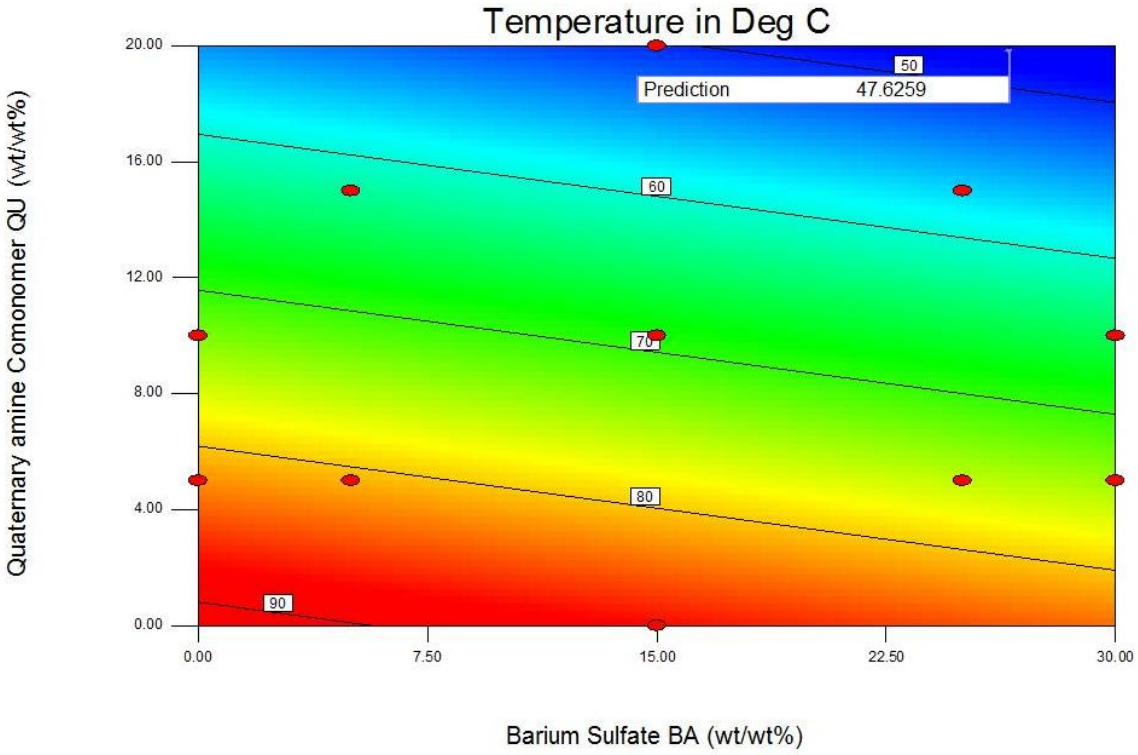
Temperature in Deg C
Prediction 47.6259
50
60
70
80
90
20.00
16.00
12.00
8.00
4.00
0.00
0.00
7.50
15.00
22.50
30.00
Quaternary amine Comonomer QU (wt/wt%)
Barium Sulfate BA (wt/wt%)

C

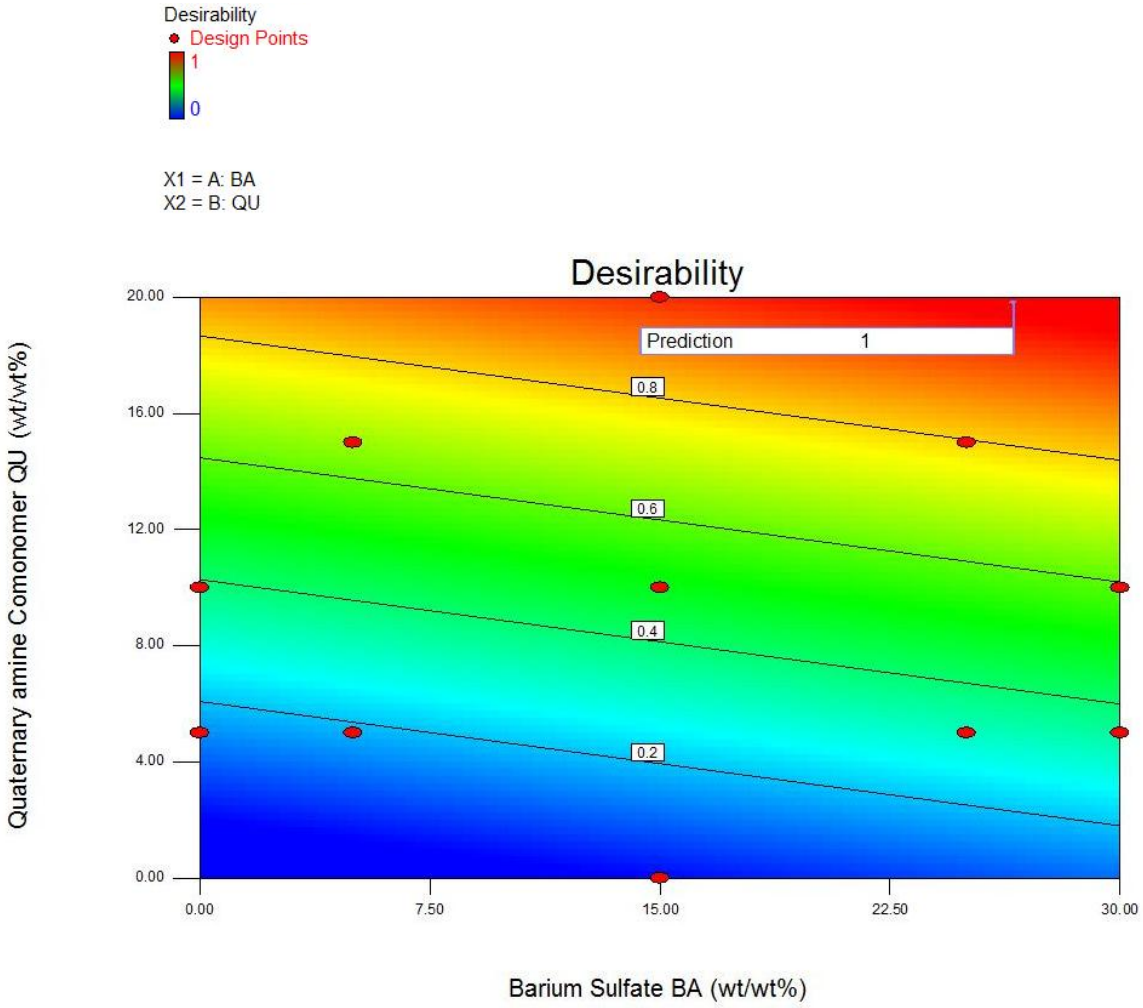

Fig. 13. The response surface plot (A), the contour plot (B) and the desirability plot (C) for the influence of barium sulfate content (BA) and quaternary amine comonomer content (QU) on the maximum exothermic temperature T_{max} of a PMMA bone cement.

4.2. Case Study #2: Residual monomer content of a PMMA bone cement

4.2.1. Experimental details

A radiolucent cement powder was used, while the liquid was that in a commercially-available brand used for BKP (KyphX® HV-R™; Medtronic Spinal & Biologics, Memphis, TN, USA) but modified by addition of a quaternary amine co-monomer (QACM). The cement powder and liquid were mixed in a polyethylene bowl that was open to the laboratory atmosphere.

7 days after preparation of the fully cured cement specimens, a sample (mass 1 g) was cut from a specimen and dissolved in a deuterated chloroform solution (5% w/v) using tetramethylsilane as an internal reference. Then the proton nuclear magnetic resonance (^{1}H-NMR) spectra of the solution was obtained. The residual monomer content (RMC) of the cement was calculated using the expression

$$RMC = 100\ (A_{MMA})/(A_{PMMA} + A_{MMA})\%, \qquad (12)$$

where A_{MMA} is the area in the peak, in the spectrum, that was assigned to the methoxyl protons of the monomer, MMA and QACM (where included) and A_{PMMA} is the sum of the areas of the peaks, in the spectrum, that were assigned to the methoxyl protons of the polymer, PMMA. The results are given in Table 10.

Table 10
Residual monomer content (RMC) of a PMMA bone cement

$BaSO_4$ content (wt/wt%)	Quaternary amine comonomer content (wt/wt%)	RMC (%)
0	5	2.8
0	10	3.5
5	5	2.6
5	15	5.1
15	0	1.3
15	10	4.0
15	20	5.4
25	5	2.4
25	15	5.8
30	5	3.4
30	10	4.7

4.2.2. Design matrix

Two factors (explanatory variables) were considered for their influence on residual monomer content (RMC) of a PMMA bone cement; namely, $BaSO_4$ content (BA) and quaternary amine comonomer content (QU). For each factor, 5 values were used; thus, there were 11 data points.

For the RSM work (Design Expert®, Version 8), therefore, it was appropriate to use the two-factors, five-levels, central composite design matrix (rotatable option). The values of the factors used and the corresponding level for each factor are given in Table 11 while, in Table 12, the 11 data points are presented both as coded values and as raw values.

Table 11
Factors and their levels: residual monomer content of a PMMA bone cement

Factor	Unit	Coded levels				
		-1.414	-1	0	+1	+1.414
$BaSO_4$ Content (BA)	wt./wt.%	0.00	5.00	15.00	25.00	30.00
Quaternary amine comonomer content (QU)	wt./wt.%	0.00	5.00	10.00	15.00	20.00

Table 12
Design matrix and experimental results; residual monomer content of a PMMA bone cement

Cement	Coded values		Raw values		Residual monomer content
	BA	QU	BA	QU	(RMC)
			(wt/wt%)	(wt/wt%)	(%)
A	-1.414	-1	0	5	2.8
B	-1.414	0	0	10	3.5
C	-1	-1	5	5	2.6
D	-1	+1	5	15	5.1
E	0	-1.414	15	0	1.3
F	0	0	15	10	4.0
G	0	+1.414	15	20	5.4
H	+1	-1	25	5	2.4
I	+1	+1	25	15	5.8
J	+1.414	-1	30	5	3.4
K	+1.414	0	30	10	4.7

4.2.3. Empirical relationship and regression analysis

The second-order polynomial (regression) equation used to represent the response surface for RMC is given by

$$RMC = b_o + \sum b_i X_i + \sum b_{ij} X_i X_j + \sum b_{ii} X_i^2, \quad (13)$$

where X_i and X_j are the two factors.

Thus, the selected polynomial could be expressed as

$$RMC = b_o + b_1 (BA) + b_2 (DE) + b_{12} (BA)(DE) + b_{11} (BA)^2 + b_{22} (DE)^2, \quad (14)$$

where b_o is the mean of the responses; b_1 and b_2 are the regression coefficients that characterize the direct effects of the factors; b_{12} is the regression coefficient that characterizes the interaction effect of the factors; and b_{11} and b_{22} are the regression coefficients that characterize the quadratic effects of the factors.

With the computed values of the coefficients, it is found the quadratic models given above were aliased. In experimental design, when two interactions, or a main effect and an interaction, share the same column, and so cannot be individually analyzed, then their effects are termed “aliased”. Hence, the linear model is used in RSM and Eq. (14) becomes

$$RMC = 1.3107 - 0.0246(BA) + 0.2252(QU) \quad (15)$$

4.2.4. Adequacy of regression model

Analysis of variance (ANOVA) of the regression model was performed and the results (Table 13) were used to examine the adequacy of the model. The desired level of confidence was considered to be adequate provided that 1) the calculated value of the F ratio of the model developed did not exceed the standard tabulated value of the F ratio and 2) the calculated value of the coefficient of determination (R^2) of the developed relationship exceeded the standard tabulated value of the R^2 for a desired level of confidence (in this study, 0.906).

Table 13
The ANOVA results (response: parameter: residual monomer content (RMC), in %, of a PMMA bone cement)

Source	Sum of squares	df	Mean square	F value	p-value Prob > F	
Model	18.08	2	9.04	38.77	< 0.0001	significant
BA	0.79	1	0.79	3.38	0.1033	
QU	17.29	1	17.29	74.17	< 0.0001	
Residual	1.86	8	0.23			
Cor total	19.94	10				
Std dev	0.48	R^2	0.9065			
Mean	3.73	Adj R^2	0.8831			
COV (%)	12.95	Pred R^2	0.7847			
		Adeq precision	17.863			

The model F-value of 38.77 implies the model is significant because there is only a 0.01% chance that a model F-value this large could occur due to noise. The goodness of fit of the model is indicated by the coefficient of determination (R^2), which was found to be 0.9065, which implies that 90.65% of the experimental data were predicted by the model. The adjusted R^2 value recalculates the model coefficient of determination but, this time, only the significant model terms were considered. The adjusted R^2, 0.8831, was high enough to confirm the high significance of the model. The predicted R^2 is 0.7847, which means that the model could explain 78% of the variability in predicting new RMC observations is in reasonable agreement with the adjusted R^2 of 0.8831. The parameter, Adeq precision, is a measure of the signal-to-noise ratio, with a value > 4 considered desirable. In this case study, the ratio was 17.863, which indicated an adequate signal. The coefficient of variation (COV), 12.95%, is low enough to indicate that the deviations between the experimental and the predicted values are low. All of the aforementioned ANOVA results show that the model (Eq. (15)) was adequate and, thus, may be used to navigate the design space.

Values of "Prob > F" less than 0.0500 indicate model terms are significant. Thus, in this case study, the only significant model term is QU and BA is non-significant term. Thus, in this case study, the model Eq. (15) was adequate and used as is

$$RMC = 1.3107 - 0.0246(BA) + 0.2252(QU) \qquad (16)$$

For a given response, the contributions of factors can be ranked from their respective F ratio values provided the degrees of freedom are same for all the input parameters. The larger the F ratio the higher is the significance. From the F ratio values (Table 13), it is seen that QU exerts a greater influence on RMC than does BA.

4.2.5. Residuals and correlation exercises

The normal probability plot of the residuals is approximately linear (Fig. 14), indicating that the errors (residuals) are approximated distributed normally. By default, the residuals are studentized; that is, they are converted to a standard deviation scale. Ideally, the normal plot of residuals is a straight line, indicating no abnormalities. The data do not have to match up perfectly with the line. A good rule of thumb is called the 'fat pencil" test. In this case, you can easily put a fat pencil over the line and cover up all the data points, and, hence, the data in Fig. 14 is sufficiently normal. The match between the predicated and the experimental values is very good (Fig. 15). It is observed there is no outlier and every data point is practically on the predicted line.

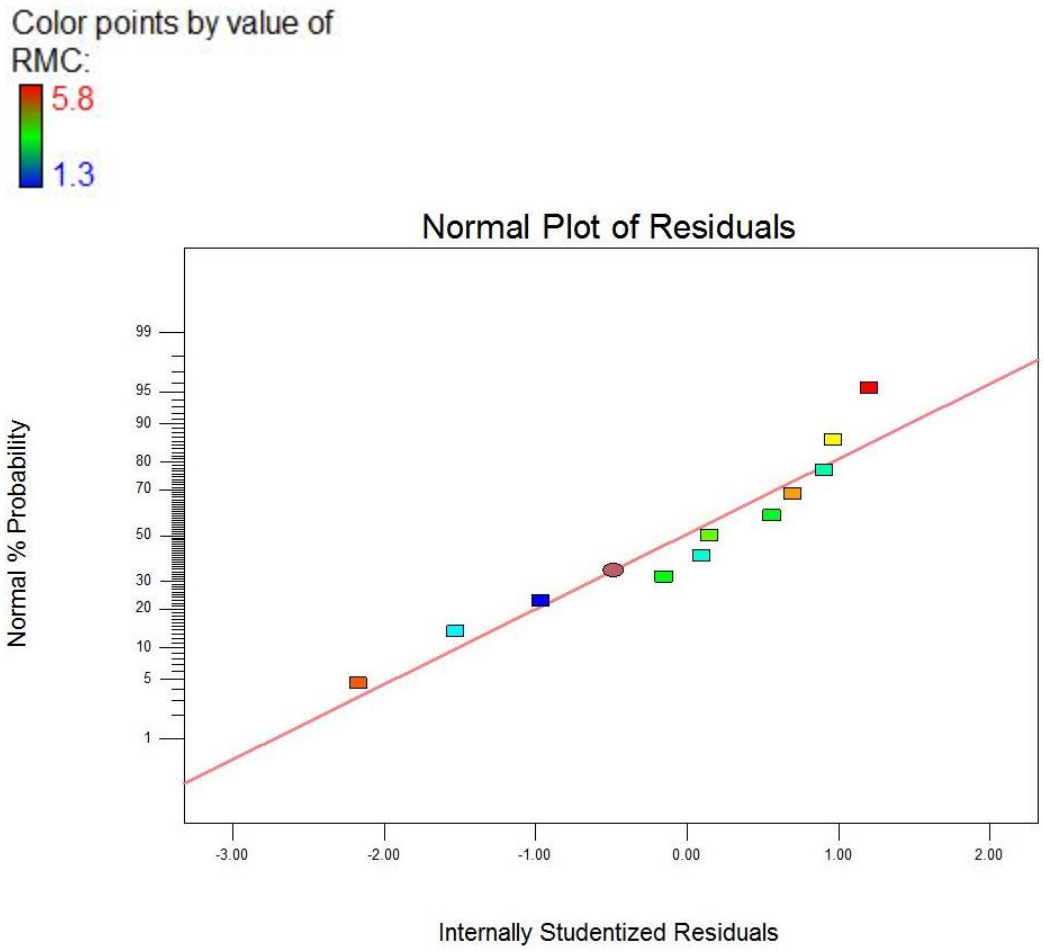

Fig. 14. The normal probability plot of the residual monomer content results for a PMMA bone cement.

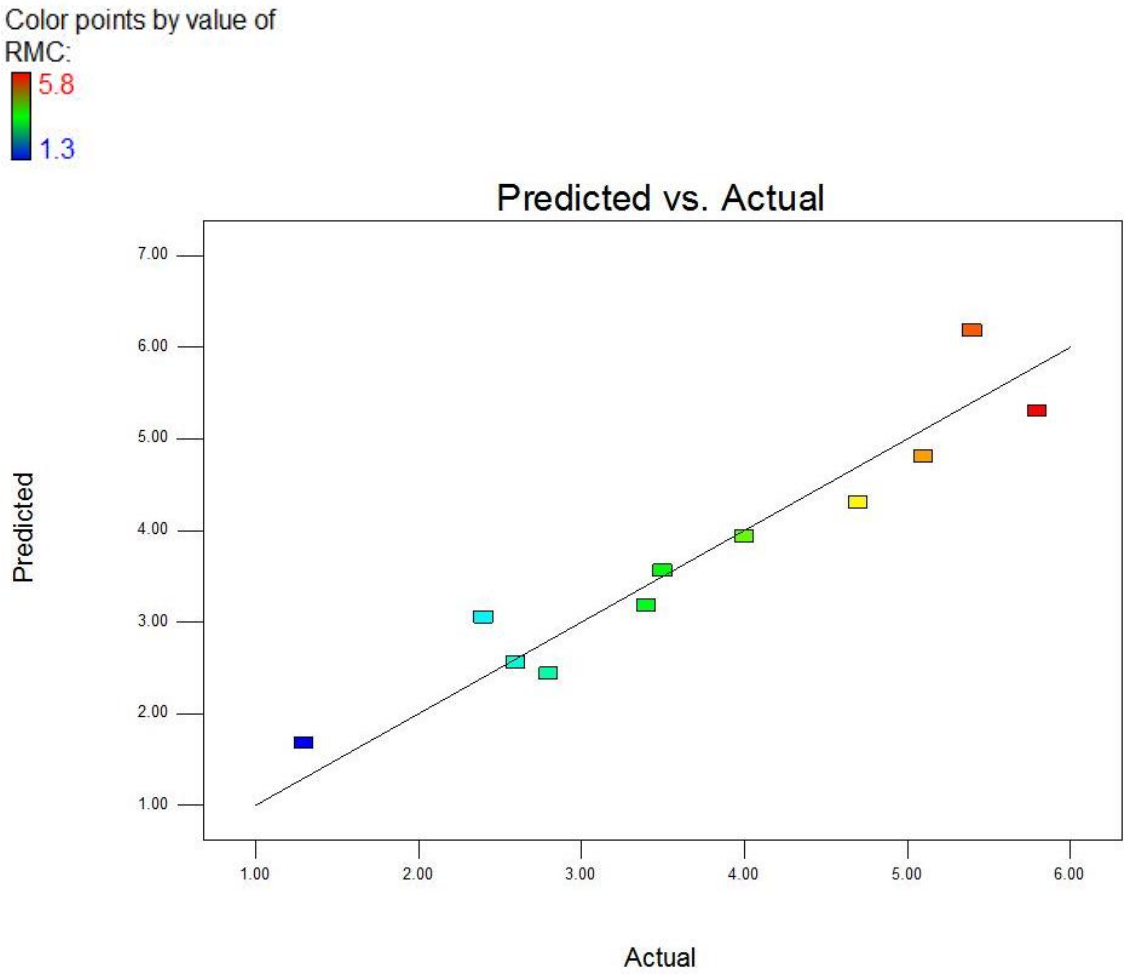

Fig. 15. The correlation plot of the residual monomer content results for a PMMA bone cement.

4.2.6. Optimization exercise

To obtain the optimum combination for getting minimum RMC, response surface, contour, and desirability plots were developed for the proposed model that contained only the significant coefficients (Eq. (16)). A contour plot is produced to display the regions of the optimal factor settings. Either the response surface plot or the contour plot can be used to predict the response (minimum RMC) for any zone of the experimental domain. As shown on the surface response plot, the desired optimum is the minimum value (Fig. 16A). After identifying the stationary point in a contour plot, it has to be determined if it is the maximum, minimum, target, or saddle point. An analysis of the response surface and contour plots (Figs. 16A and B) found that the indicated minimum RSM (1.809%) has a desirability of 1.00 (Fig. 16C). This minimum RMC is obtained when BA = 20.25 wt/wt% and QU = 0 wt/wt%. It is noted that the desirability is equal to 0.886 and, hence, the model may not be good enough to accurately predict the minimum RMC response. Six possible numerical RSM solutions are found and in all cases QU = 0.

A

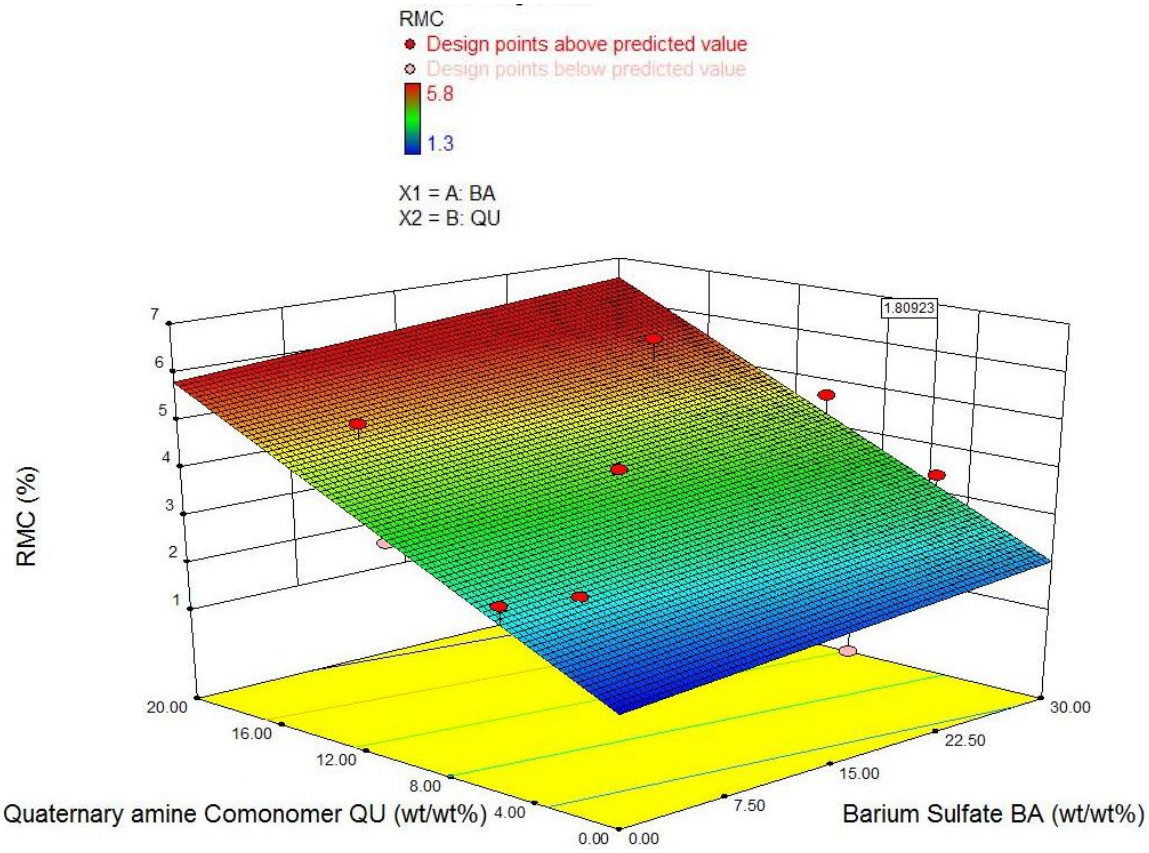
RMC
Design points above predicted value
Design points below predicted value
5.8
1.3
X1 = A: BA
X2 = B: QU
1.80923
RMC (%)
7
6
5
4
3
2
1
20.00
16.00
12.00
8.00
4.00
0.00
Quaternary amine Comonomer QU (wt/wt%)
0.00
7.50
15.00
22.50
30.00
Barium Sulfate BA (wt/wt%)

B

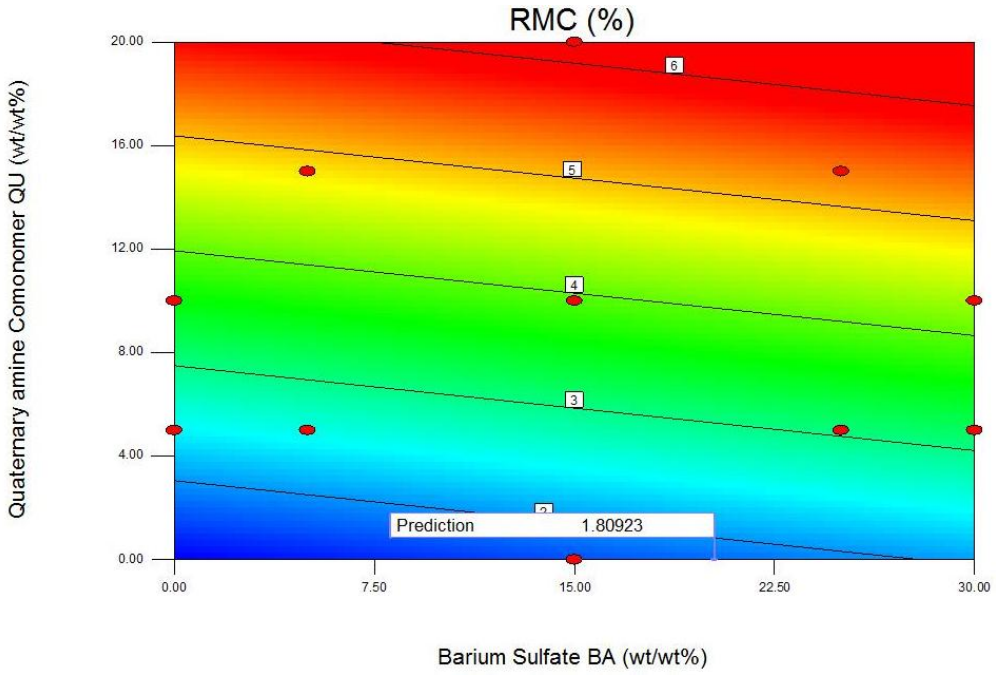
RMC (%)
Quaternary amine Comonomer QU (wt/wt%)
20.00
16.00
12.00
8.00
4.00
0.00
6
5
4
3
Prediction 1.80923
0.00
7.50
15.00
22.50
30.00
Barium Sulfate BA (wt/wt%)

C

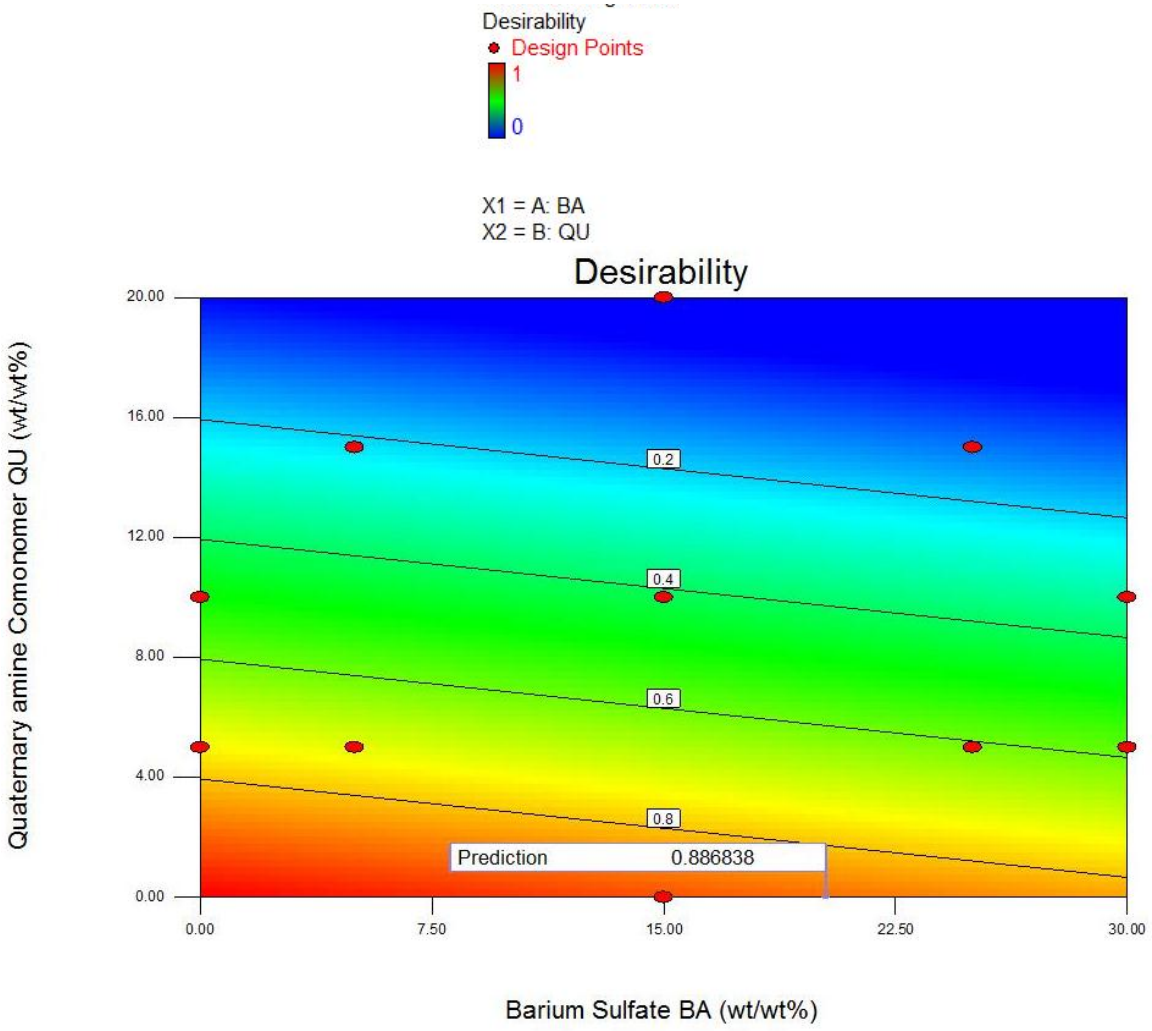

Fig. 16. The response surface plot (A), the contour plot (B) and the desirability plot (C) for the influence of barium sulfate content (BA) and quaternary amine comonomer content (QU) on the residual monomer content (RMC) of a PMMA bone cement.

4.3. Case Study #3: Degradability of a PMMA bone cement

4.3.1. Experimental details

The cement used was a commercially-available brand used for BKP (KyphX® HV-R™; Medtronic Spinal & Biologics, Memphis, TN, USA). The powder was modified by the addition of finely ground spherical glass beads that had its surface treated with 0.2 wt/wt γ methacryloxy propyl trimethoxy silane (mean diameter of glass powder = 3.2 μm) and finely-ground chitosan particles (diameter: 60-600 μm). The cement powder and liquid were mixed in a polyethylene bowl that was open to the laboratory atmosphere.

For this test, a VB augmentation model was used and it comprised a polyurethane (PU) foam (Last-a-Foam® FR-7108; Polymer Tooling Systems, Inc., Exton, PA, USA; density = 128 kg m^{-3}) cube (26 mm sides) into which a centrally-located through-thickness cylindrical hole (diameter, 14 mm) was drilled. The density of this commercially-available material is the same as that suggested for PU foam that models cancellous bones with severe osteoporosis [126]. The cement bolus was injected into the cylindrical hole, which represented the fracture zone in a VB. The volume of cement used in VP or BKP is in the range of 3.5-8.0 mL [127, 128]. With the mean volume of VBs that are commonly augmented using VP or BKP (T6–L5) being 29.4 mL [129], the range of the computed cement volume ratio (C_r) is, thus, 13-27 %. The value of C_r used in the present study (23%) is within this range.

The cube was then immersed in a beaker that contained 1X phosphate buffered saline, after which the beaker was covered and placed in an incubator (Model 610; Fisher Scientific, Inc, Fair Lawn, NJ) that was set at 37^o C. After 10 weeks, the cube was

removed and then imaged using microcomputed tomography. The residual material volume fraction (RMVF) was calculated as the ratio of the volume of residual cement to the volume of the cement cylinder in a region of interest. After that, degradability of the cement was computed thus

$$\text{Degradability} = 100\,(1 - \text{RMVF})\% \qquad (17)$$

For each of the five cements, the test was run four times. The results are given in Table 14.

Table 14
Degradability of a PMMA bone cement

Cement	PMMA powder content (wt/wt%)	Bioactive glass particles content (wt/wt%)	Chitosan particles content (wt/wt%)	Degradability (%)
CONTROL	100	0	0	2.05 ± 0.09
EXPCI	65	31	4	8.63 ± 0.81
EXPCII	51	41	8	19.30 ± 1.24
EXPCIII	40	50	10	26.00 ± 2.16
EXPCIV	31	57	12	36.85 ± 2.94

4.3.2. Design matrix

Three factors (explanatory variables) were considered for their influence on degradability; namely, PMMA powder content (A), bioactive glass particles content (B) and chitosan particles content (C). This is a mixture-type experiment in which the factors are the constituents of the cement powder (in wt/wt%). The constraint on these factors is that their amounts must add up to 100 wt/wt% and, as such, the levels of the factors cannot be chosen independently.

For the RSM work (Design Expert®, Version 8), therefore, it was appropriate to use the three-factors, five-levels, mixture experiment design (IV optimal option). The values of the factors used and the corresponding level for each factor are given in Table 15 while, in Table 16, the 20 data points are presented both as coded values and as raw values.

In mixture design, the purpose of the experiment is to model the blending surface with some form of mathematical equation in order to achieve three objectives. First, predictions of the response for any mixture or combination of the powder constituents can be made empirically. Second, some measure of the influence on the response of each component singly and in combination with other components can be obtained. Third, in all cases, the model has to follow the restriction where the amounts of the constituents add up to 100% wt/wt%.

Table 15
Factors and their levels: degradability of a PMMA bone cement

Factor	Unit	Coded levels				
		-1.68	-1	0	+1	+1.68
PMMA powder content (A)	wt./wt.%	31	41	51	65	100
Bioactive glass particles content (B)	wt./wt.%	0	31	41	50	57
Chitosan particles content (C)	wt./wt.%	0	4	8	10	12

Table 16
Design matrix and experimental results: degradability of a PMMA bone cement

Cement	Coded values			Raw values			Degradability
	A	B	C	A	B	C	(%)
Control	1.000	0.000	0.000	100	0	0	2.140
Control	1.000	0.000	0.000	100	0	0	2.095
Control	1.000	0.000	0.000	100	0	0	2.005
Control	1.000	0.000	0.000	100	0	0	1.960
EXPC I	0.493	0.449	0.058	65	31	4	9.440
EXPC I	0.493	0.449	0.058	65	31	4	9.035
EXPC I	0.493	0.449	0.058	65	31	4	8.225
EXPC I	0.493	0.449	0.058	65	31	4	7.820
EXPC II	0.290	0594	0.116	51	41	8	20.540
EXPC II	0.290	0594	0.116	51	41	8	19.920
EXPC II	0.290	0594	0.116	51	41	8	18.680
EXPC II	0.290	0594	0.116	51	41	8	18.060
EXPC III	0.130	0.725	0.145	40	50	10	28.160
EXPC III	0.130	0.725	0.145	40	50	10	27.080
EXPC III	0.130	0.725	0.145	40	50	10	24.920
EXPC III	0.130	0.725	0.145	40	50	10	23.840
EXPC IV	0.000	0.826	0.174	31	57	12	39.790
EXPC IV	0.000	0.826	0.174	31	57	12	38.320
EXPC IV	0.000	0.826	0.174	31	57	12	35.380
EXPC IV	0.000	0.826	0.174	31	57	12	33.910

4.3.3. Empirical relationship and regression analysis

The second-order polynomial (regression) equation used to represent the response surface (Degradability (D)) is given by

$$D = \sum b_i X_i + \sum\sum b_{ij} X_i X_j, \quad (18)$$

where X_i and X_j are the amount of cement powder constituents.

Thus, the selected polynomial could be expressed as

$$D = b_1 (A) + b_2 (B) + b_3 (C) + b_{12} (A)(B) + b_{13} (A)(C) + b_{23} (B)(C), \quad (19)$$

where b_1, b_2, and b_2 are the regression coefficients that characterize the direct effects of the factors; b_{12}, b_{13}, and b_{23} are the regression coefficients that characterize the interaction effect of the factors.

It is recommended to select the highest order polynomial where the additional terms are significant and the model is not aliased. The quadratic model and higher are aliased. Hence, with the computed values of the coefficients, Eq. (19) becomes

$$D = 0.016(A) - 0.381(B) + 4.608(C) \quad (20)$$

4.3.4. Adequacy of regression model

Analysis of variance (ANOVA) of the regression model was performed and the results (Table 17) were used to examine the adequacy of the model. The desired level of confidence was considered to be adequate provided that 1) the calculated value of the F ratio of the model developed did not exceed the standard tabulated value of the F ratio and 2) the calculated value of the coefficient of determination (R^2) of the developed relationship exceeded the standard tabulated value of the R^2 for a desired level of confidence (in this case study, 0.96).

Table 17
The ANOVA results (response parameter: degradability (D), in %, of a PMMA bone cement

Source	Sum of squares	df	Mean square	F value	p-value Prob > F	
Model	2969.512	2	1484.756	218.15	< 0.0001	significant
Linear Mixture	2969.512	2	1484.756	218.15	< 0.0001	
Residual	115.7056	17	6.806211			
Lack of fit	76.92809	2	38.46404	14.88	0.0003	significant
Pure error	38.7775	15	2.585167			
Cor total	3085.218	19				

Std dev	2.61	R^2	0.9625
Mean	18.57	Adj R^2	0.9581
COV (%)	14.05	Pred R^2	0.9525
		Adeq precision	32.1406

The model F-value of 218.15 implies the model is significant because there is only a 0.01% chance that a model F-value this large could occur due to noise. The goodness of fit of the model is indicated by the coefficient of determination (R^2), which was found to be 0.9625, which implies that 96.25% of the experimental data were predicted by the model. The adjusted R^2 value recalculates the model coefficient of determination but, this time, only the significant model terms were considered. The adjusted R^2, 0.9581, was high enough to confirm the high significance of the model. The predicted R^2 is 0.9525, which means that the model could explain 95% or more of the variability in predicting new degradability observations. This is in excellent agreement with the adjusted R^2 of 0.9581. The parameter, Adeq precision, is a measure of the signal-to-noise ratio, with a value > 4 considered desirable. In this case study, the ratio was 32.1406, which indicated an adequate signal. The coefficient of variation (COV), 14.05%, is low enough to indicate that the deviations between the experimental and the predicted values are low. The "lack of fit F-value" of 14.88 implies the lack of fit is significant. There is only 0.03% chance that a "lack of fit F-value" this large could occur due to noise. Significant lack of fit is bad because we want the model to fit. All of the aforementioned ANOVA results show that the model (Eq. (20)) was adequate and, thus, may be used to navigate the design space.

For a model term, a value of Prob>F less than 0.0500 indicates that it is significant. Thus, in this case study, the linear terms A, B, and C are the significant model terms. In that case, Eq. (20) is of the same order as of equation (19) with no interaction term:

$$D = 0.016(A) - 0.381(B) + 4.608(C) \quad (21)$$

For a given response, the contributions of factors can be ranked from their respective F ratio values provided the degrees of freedom are same for all the input parameters. The larger the F ratio the higher is the significance. From the F ratio values (Table 17), it is seen that the mixture of A, B, and C exerts the greatest influence on degradability.

4.3.5. Residuals and correlation exercises

The residuals from the least squares fit play an important role in judging model adequacy. The normal probability plot of the residuals for D is linear (Fig. 17), indicating that the errors are distributed normally. The match between the predicted and the experimental D values is very good (Fig. 18). This helps us to assess the validity of our model. Fig. 17 is a normal probability plot of the studentized residuals from the quadratic mixture model. This plot is satisfactory for a mixture experiment because the points in a mixture design can have substantial differences in their leverage values. As shown, the residuals plot is, approximately a straight line; thus, the normality assumption is satisfied. In this normal probability plot, there are no data point that can be considered as outliers. Fig. 18 shows a plot of the values of the observed response versus the predicted values. The pairs lie closely along a straight line (the straight line in the graph is a result of a least squares fit). This is a usual indication that the model is a satisfactory fit to the data.

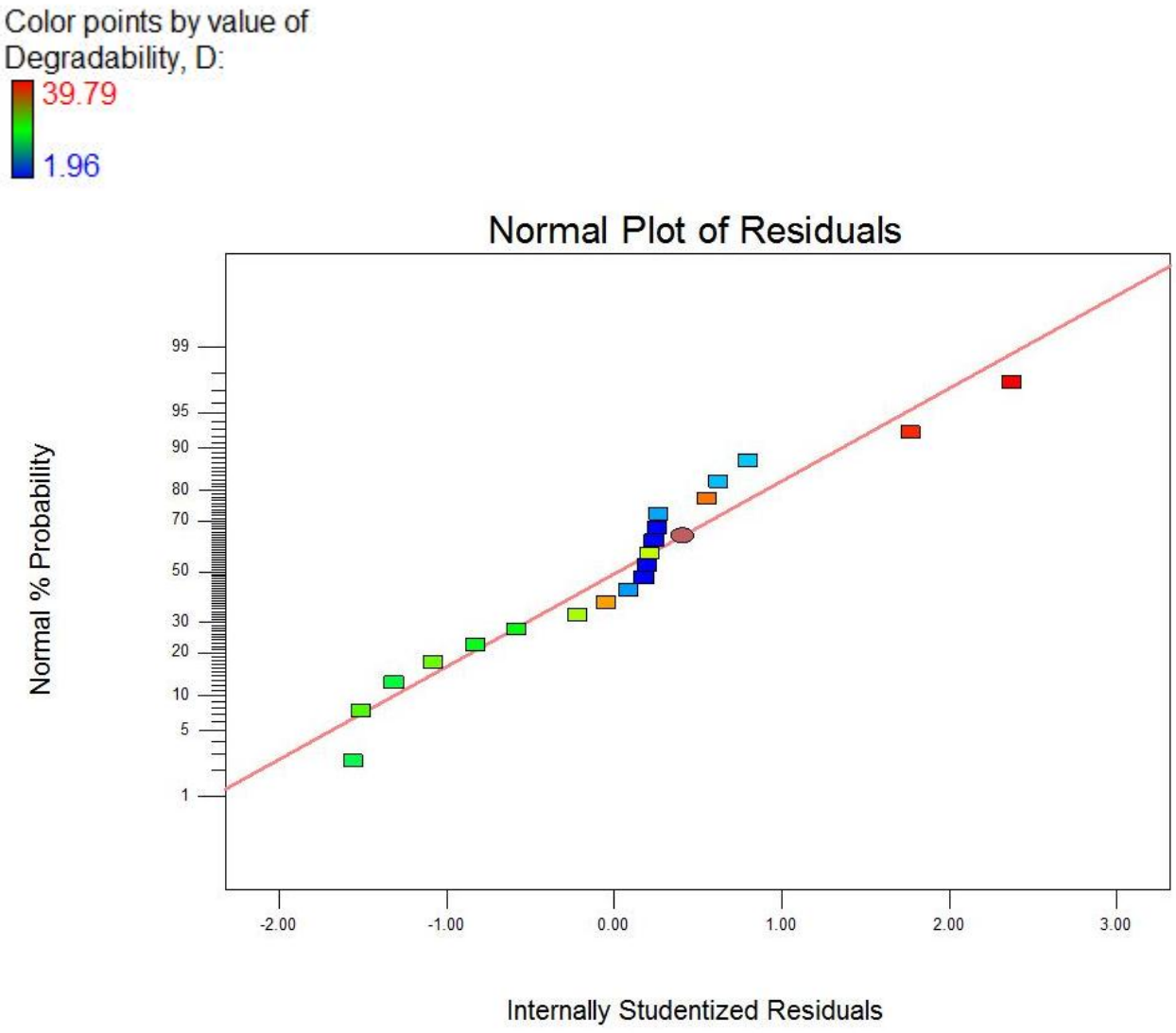

Fig. 17. The normal probability plot of the degradability results for a PMMA bone cement.

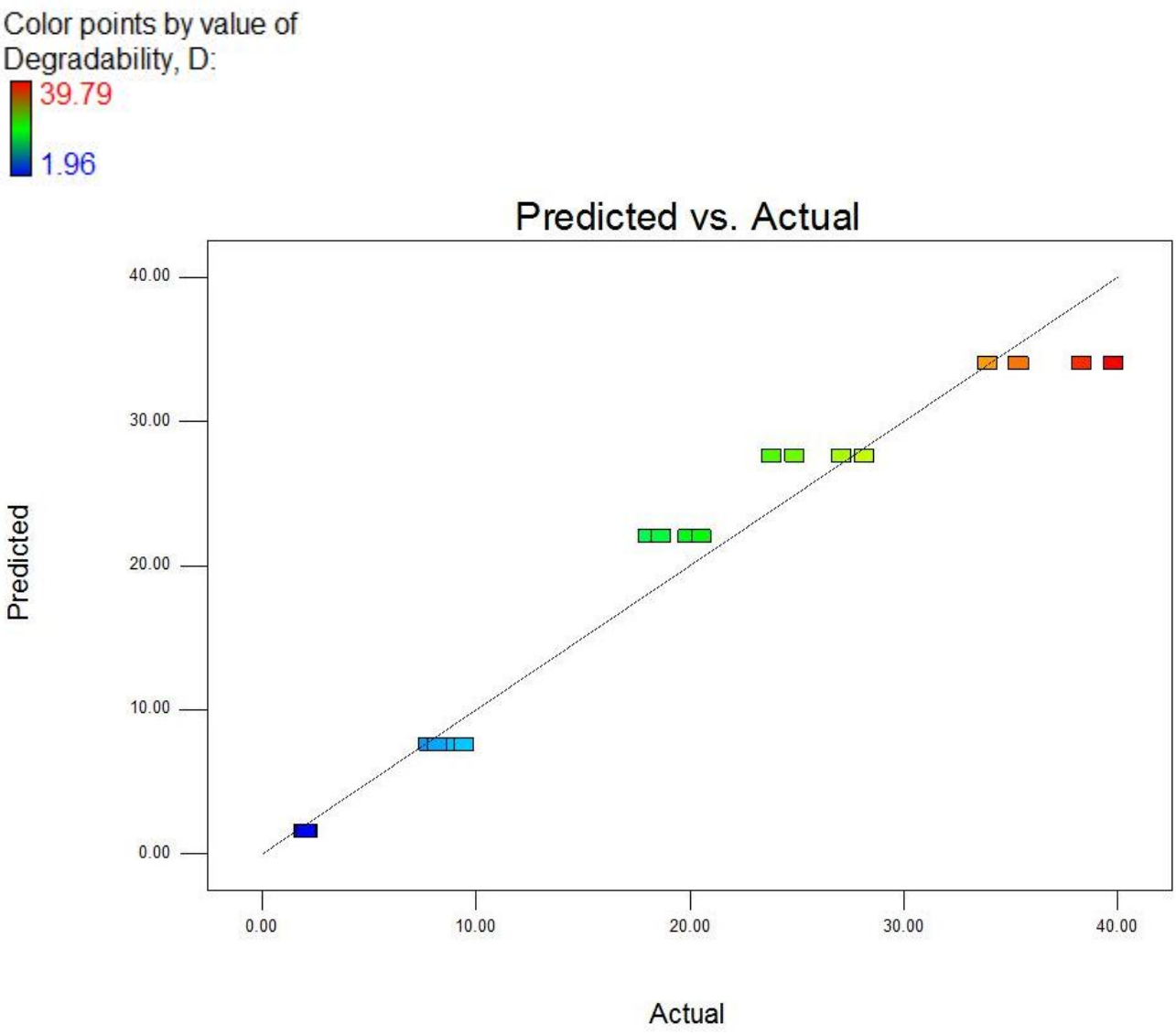

Fig. 18. The correlation plot of the degradability results for a PMMA bone cement.

4.3.6. Optimization exercise

To obtain the optimum combination for maximizing degradability (D) of the cement, response surface, contour, and desirability plots were developed for the proposed model that contained only the significant coefficients (Eq. (21)). A contour plot is produced to display the regions of the optimal factor settings. Either the response surface plot or the contour plot can be used to predict the response (degradability) for any zone of the experimental domain. The right-hand tip of the response plot (Fig. 19A) shows the maximum degradability (in %). After identifying the stationary point in a contour plot, it has to be determined if it is a maximum, minimum, or saddle point. An analysis of the response surface and contour plots (Figs. 19A and B) found that a number of maximum degradability RSM solutions are possible and this needs actual testing to verify the result, based on highest desirability the maximum then was estimated to be 41.19%. The corresponding parameters that yielded this maximum value were A = 50.90 wt/wt%, B = 37.25 wt/wt%, and C = 11.85 wt/wt%. The desirability factor for the optimum solution is 1 (Fig. 19C), indicating that the result is acceptable for optimum value and mixture variables.

A

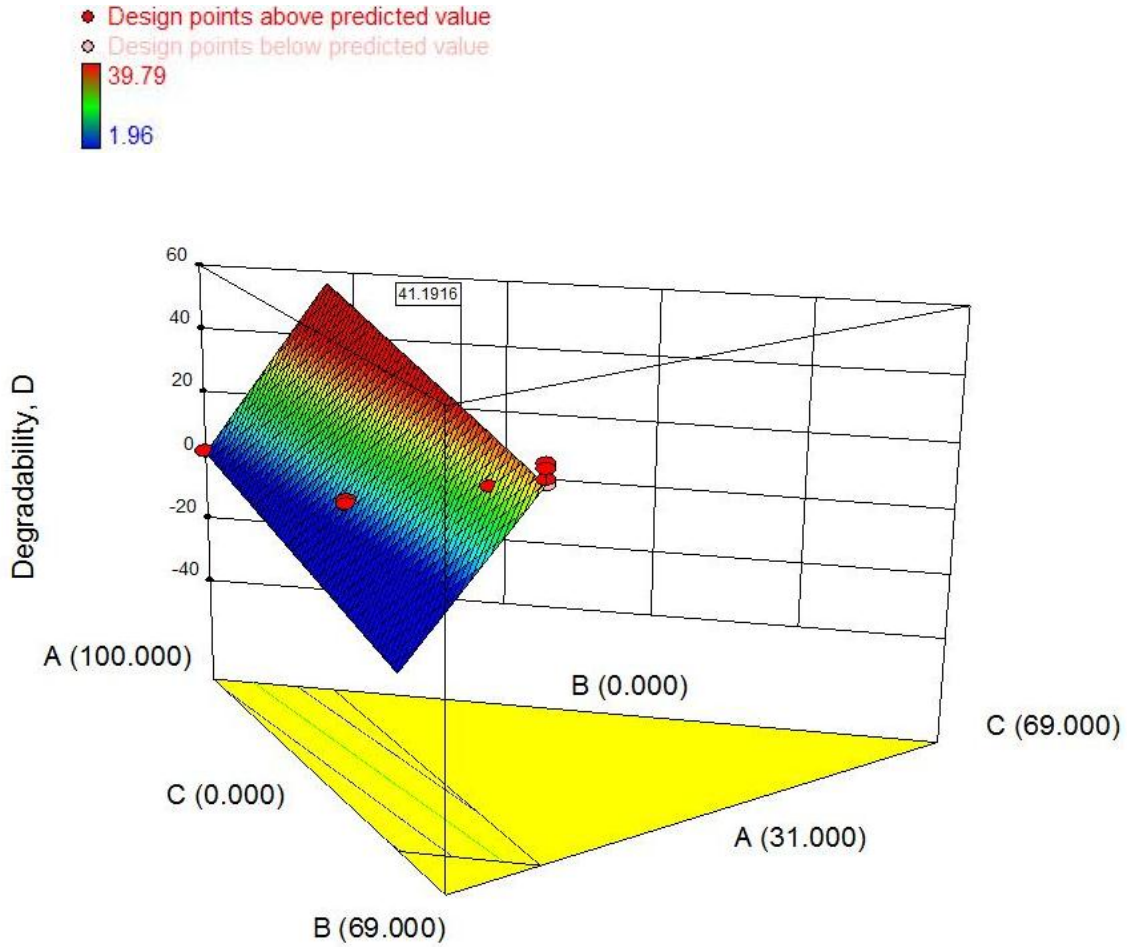
Design points above predicted value
Design points below predicted value
39.79
1.96
Degradability, D
60
40
20
0
-20
-40
41.1916
A (100.000)
B (0.000)
C (69.000)
C (0.000)
A (31.000)
B (69.000)

B

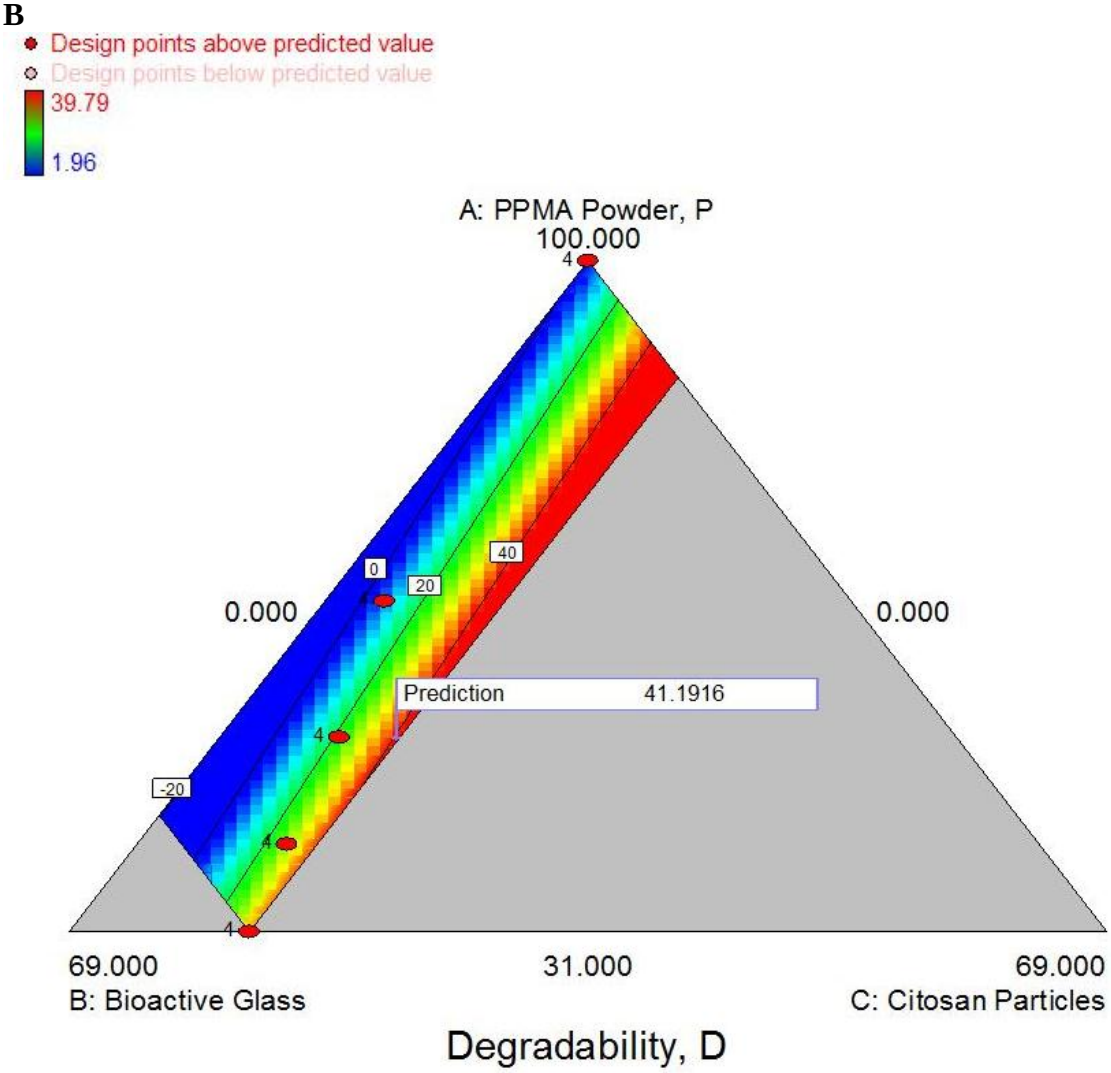
Design points above predicted value
Design points below predicted value
39.79
1.96
A: PPMA Powder, P
100.000
0
20
40
-20
0.000
0.000
Prediction 41.1916
69.000
31.000
69.000
B: Bioactive Glass
C: Citosan Particles
Degradability, D

C

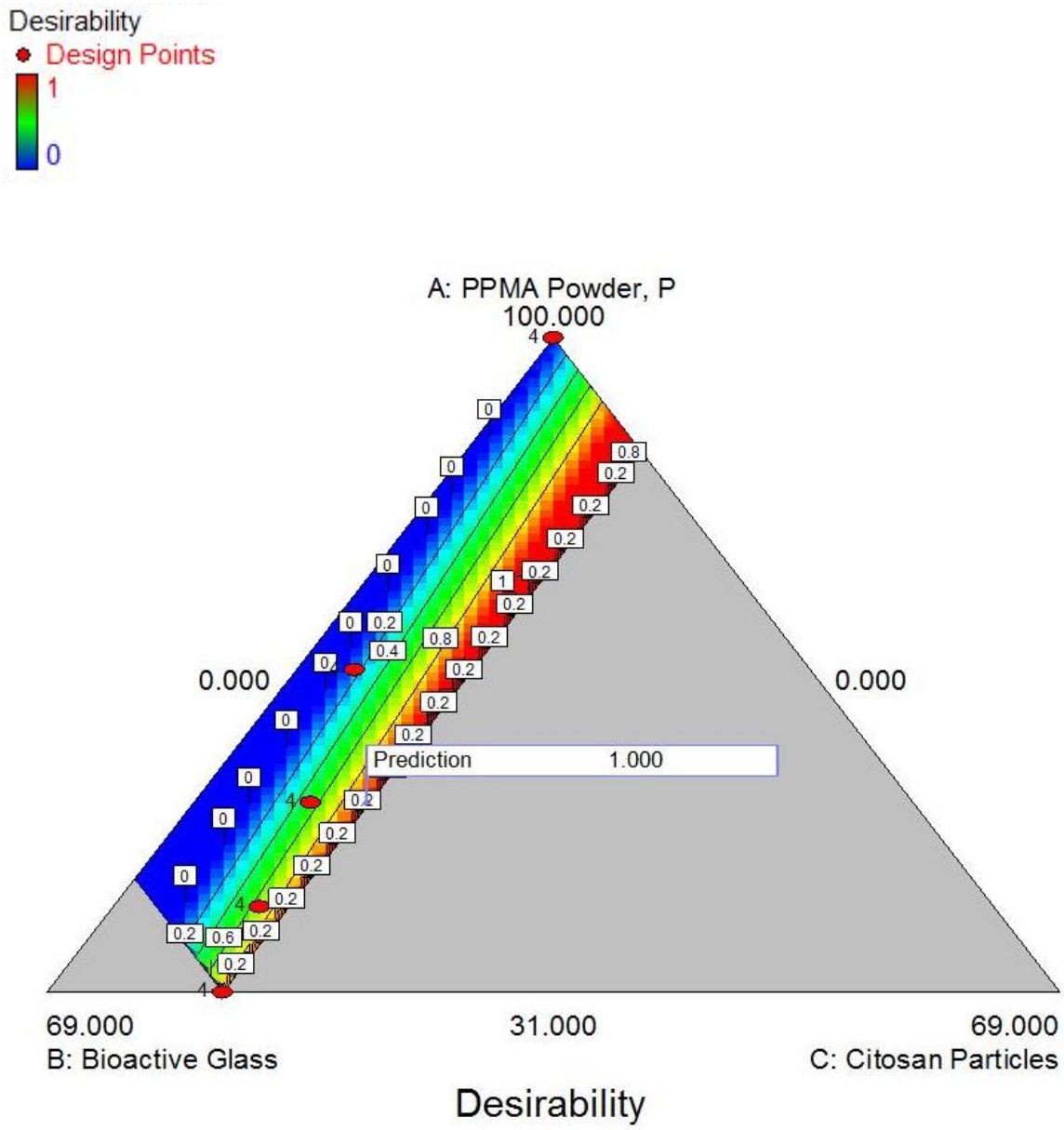

Fig. 19. The response surface plot (A), contour plot (B) and desirability plot (C) for influence of PMMA cement powder content, bioactive glass particles content, and chitosan particles content on the degradability of a PMMA bone cement.

4.4. Case study #4: Injectability of a calcium phosphate cement

4.4.1. Experimental details

The powder constituents of the cement were $CaCO_3$, DCPA, and β–TCP, while the liquid was an aqueous solution of poly (ethylene glycol) (PEG). The powder and liquid were mixed, with a spatula, in a glass dish, until a paste was obtained.

The cement powder and liquid was mixed in a 10-mL disposable syringe fitted with an 11-gage needle (1.1 mm x 30 mm) needle for 45 s. The assembly was then placed in a universal materials testing machine. After 2 min, a force of 300 N was applied to the plunger of the syringe, at a crosshead displacement rate of 10 mm min^{-1}, for 3 min, thereby extruding the paste through the needle. The injectability was calculated using the expression

$$\text{Injectability} = 100 \left(\frac{\text{mass of cement extruded from the syringe}}{\text{original mass of cement paste loaded in the syringe}} \right) \% \quad (22)$$

Each test was run in triplicate. The results are given in Table 18.

Table 18
Injectability of a calcium phosphate cement

PEG content (wt/wt%)	PLR (g mL^{-1})	Injectability (%)
0	2.0	50.6 ± 1.52
10	2.0	76.4 ± 4.54
20	2.0	96.1 ± 3.57
0	3.0	18.7 ± 0.46
10	3.0	40.3 ± 2.20
20	3.0	62.6 ± 2.80
0	3.5	14.8 ± 0.32
10	3.5	26.7 ± 1.48
20	3.5	44.9 ± 2.45

4.4.2. Design matrix

Two factors (explanatory variables) were considered for their influence on injectability; namely, PEG content (PC) and powder-to-liquid ratio (PLR). For each factor, three values were used; thus, there were 27 data points.

For the RSM work (Design Expert®, Version 8), therefore, it was appropriate to use the two-factors, three-levels, central composite design matrix face centered option (CCD option). The values of the factors used and the corresponding level for each factor are given in Table 19 while, in Table 20, the 27 data points are presented both as coded values and as raw values.

Table 19
Factors and their levels: injectability of a calcium phosphate cement

Factor	Unit	Coded levels		
		-1	0	+1
PEG content (PC)	wt./wt.%	0	10	20
Powder-to-liquid ratio (PLR)	g mL^{-1}	2.0	3.0	3.5

Table 20
Design matrix and experimental results: injectability of a calcium phosphate cement

Cement	Coded values		Raw values		Injectability (%)
	PC	PLR	PC	PLR	
A	-1	-1	0	2.0	49.08
A	-1	-1	0	2.0	50.60
A	-1	-1	0	2.0	52.12
B	0	-1	10	2.0	71.86
B	0	-1	10	2.0	76.40
B	0	-1	10	2.0	80.94
C	+1	-1	20	2.0	92.53
C	+1	-1	20	2.0	96.10
C	+1	-1	20	2.0	99.67
D	-1	0	0	3.0	18.24
D	-1	0	0	3.0	18.70
D	-1	0	0	3.0	19.16
E	0	0	10	3.0	38.10
E	0	0	10	3.0	40.30
E	0	0	10	3.0	42.50
F	+1	0	20	3.0	59.80
F	+1	0	20	3.0	62.60
F	+1	0	20	3.0	65.40
G	-1	+1	0	3.5	14.48
G	-1	+1	0	3.5	14.80
G	-1	+1	0	3.5	15.12
H	0	+1	10	3.5	25.22
H	0	+1	10	3.5	26.70
H	0	+1	10	3.5	28.18
I	+1	+1	20	3.5	42.45
I	+1	+1	20	3.5	44.90
I	+1	+1	20	3.5	47.35

4.4.3. Empirical relationship and regression analysis

The second-order polynomial (regression) equation used to represent the response surface (I) is given by

$$I = b_o + \sum b_i X_i + \sum b_{ij} X_i X_j + \sum b_{ii} X_i^2, \qquad (23)$$

where X_i and X_j are the two factors.

Thus, the selected polynomial could be expressed as

$$I = b_o + b_1 (PC) + b_2 (PLR) + b_{12} (PC)(PLR) + b_{11} (PC)^2 + b_{22} (PLR)^2, \qquad (24)$$

where b_o is the average of the responses; b_1 and b_2 are the regression coefficients that characterize the direct effects of the factors; b_{12} is the regression coefficient that characterizes the interaction effect of the factors; and b_{11} and b_{22} are the regression coefficients that characterize the quadratic effects of the factors.

With the computed values of the coefficients, Eq. (24) becomes

$$I = 150.8 + 3.24(PC) - 63.87(PLR) - 0.45(PC)(PLR) + 0.0015(PC)^2 + 6.91(PLR)^2 \qquad (25)$$

4.4.4. Adequacy of regression model

Analysis of variance (ANOVA) of the regression model was performed and the results (Table 21) were used to examine the adequacy of the model. The desired level of confidence was considered to be adequate provided that 1) the calculated value of the F ratio of the model developed did not exceed the standard tabulated value of the F ratio and 2) the calculated value of the coefficient of determination (R^2) of the developed relationship exceeded the standard tabulated value of the R^2 for a desired level of confidence (in this study case, 0.98).

Table 21
ANOVA results (response parameter: injectability (I), in %, of a calcium phosphate cement)

Source	Sum of squares	df	Mean square	F Value	p-value Prob >F	
Model	17358.97	5	3471.79	324.47	< 0.0001	significant
PC	7282.36	1	7282.36	680.60	< 0.0001	
PLR	9343.44	1	9343.44	873.23	< 0.0001	
(PC)(PLR)	142.65	1	142.65	13.33	0.0015	
$(PC)^2$	0.135	1	0.135	0.01	0.9116	
$(PLR)^2$	69.09	1	69.09	6.45	0.019	
Residual	224.69	21	10.70			
Lack of fit	110.99	3	36.699	5.85	0.0057	significant
Pure error	113.70	18	6.32			
Cor total	17583.67	26				
Std dev	3.27	R^2		0.9872		
Mean	47.90	Adj R^2		0.9841		
COV (%)	6.83	Pred R^2		0.9790		
		Adeq precision		55.871		

The model F-value of 324.47 implies the model is significant because there is only a 0.01% chance that a model F-value this large could occur due to noise. The goodness of fit of the model is indicated by the coefficient of determination (R^2), which was found to be 0.9872, which implies that 98.72% of the experimental data were predicted by the model. For a good statistical model, R^2 value should be close to 1.0. The adjusted R^2

value recalculates the model coefficient of determination but, this time, only the significant model terms are considered. The adjusted R^2, 0.9841, was high enough to confirm the high significance of the model. The predicted R^2 is 0.9790, which means that the model could explain 97.9% of the variability in predicting new injectability observations. The parameter, Adeq precision, is a measure of the signal-to-noise ratio, with a value > 4 considered desirable. In this case study, the ratio was 55.87, which indicated an adequate signal. The coefficient of variation (COV), 6.82%, is low enough to indicate that the deviations between the experimental and the predicted I values are low. All of the aforementioned ANOVA results show that the model (Eq. (25)) was adequate and, thus, may be used to navigate the design space. The "lack of fit F-value" of 110.99 implies the lack of fit is significant. There is only a 0.57% chance that a "lack of fit F-value" this large could occur. Significant lack of fit is bad because we want the model to fit. Because the p value is smaller than the significance level $\alpha = 0.05$, there is sufficient evidence at the $\alpha = 0.05$ level to conclude that there is lack of fit.

For a model term, a value of Prob>F less than 0.0500 indicates that it is significant. Thus, in this case study, PC, PLR, $(PLR)^2$ and (PC)(PLR) are each a significant model term but $(PC)^2$ is a non-significant term. Thus the model is acceptable to navigate the design space and Eq. (25) can be used as is

$$I = 150.8 + 3.24(PC) - 63.87(PLR) - 0.45(PC)(PLR) + 0.0015(PC)^2 + 6.91(PLR)^2 \quad (26)$$

For a given response, the contributions of factors can be ranked from their respective F ratio values provided the degrees of freedom are same for all the input parameters. The larger the F ratio the higher is the significance. From the F ratio values (Table 21), it is seen that PLR exerts the greater influence on I. The interaction effects (PC)(PLR) and the square effect $(PLR)^2$ exert less significance compared to the aforementioned main terms.

4.4.5. Residuals and correlation exercises

The normal probability plot of the residuals for I is linear (Fig. 20), indicating that the errors are distributed normally. The match between the predicated and the experimental I values is very good (Fig. 21). This helps us to assess the validity of our model. As shown on the plot, the standardized residual larger than 3 is considered as outliers. In this normal probability plot, there is no data point that can be considered as outliers. But for some value of I near residual value of -1, it is observed the data points deviate from the straight line compared to the other set of data shown around the straight line. Fig. 21 shows the actual value in the horizontal axis where three values are shown for each predicted value.

This is given from the dataset where the minimum, mean, and maximum values are shown for each data set of PC and PLR.

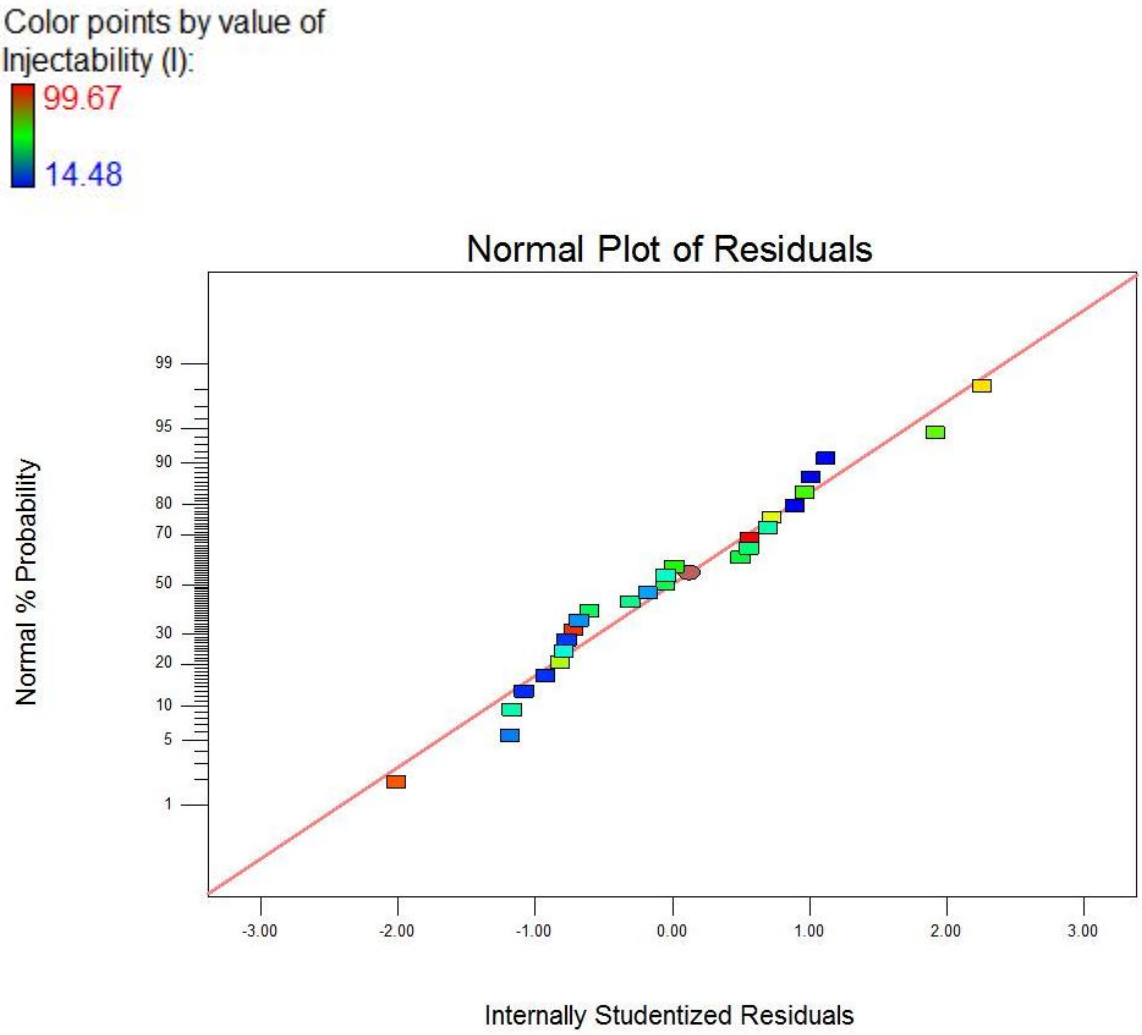

Fig. 20. The normal probability plot of the injectability results for a calcium phosphate cement.

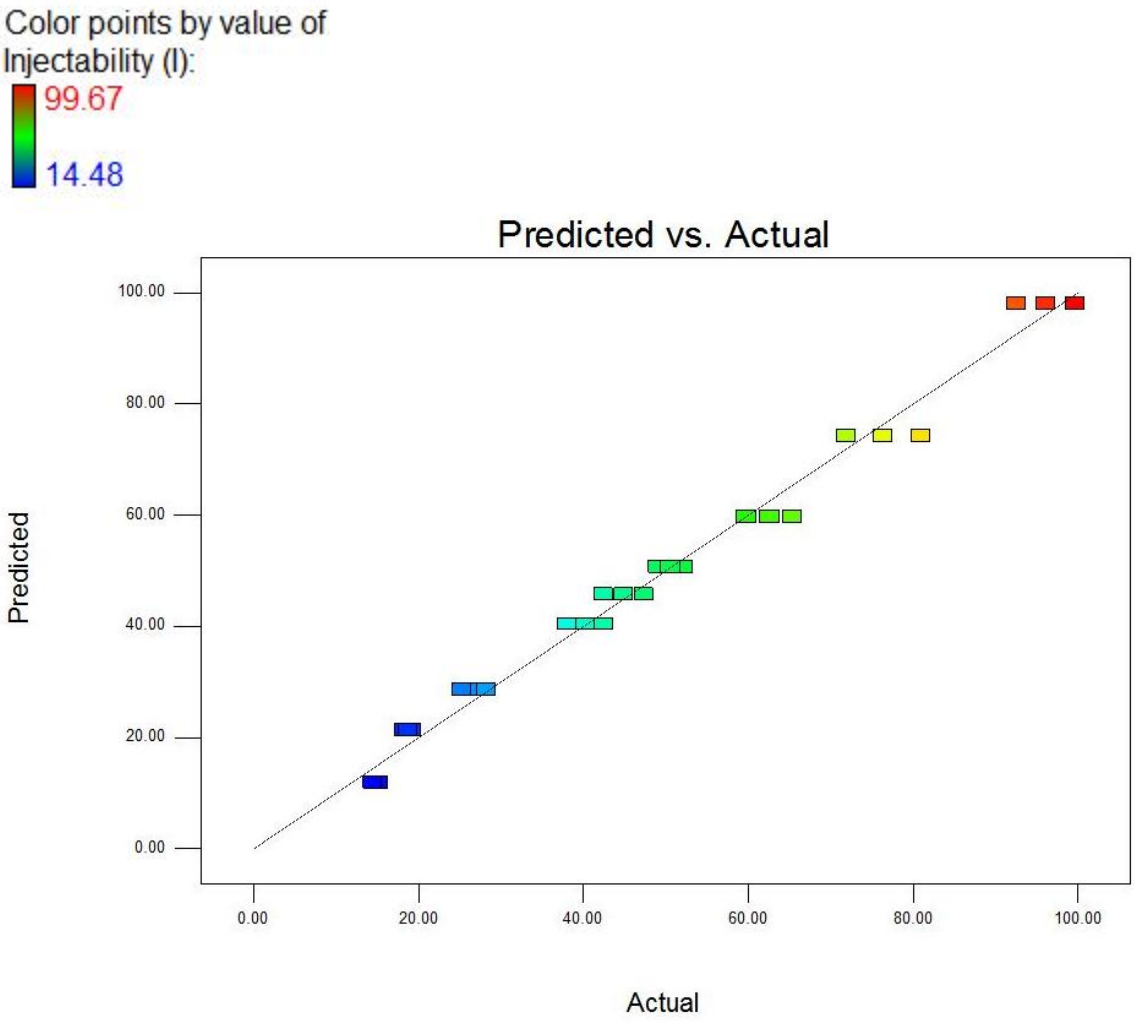

Fig. 21. The correlation plot of the injectability results for a calcium phosphate cement.

4.4.6. Optimization exercise

To obtain the optimum combination for maximizing I of the cement, response surface, contour, and desirability plots were developed for the proposed model that contained only the significant coefficients (Eq. (26)). A contour plot is produced to display the regions of the optimal factor settings. Either the response surface plot or the contour plot can be used to predict the response (I value) for any zone of the experimental domain. The right-hand tip of the response plot (Fig 22A) shows the maximum I value measured in percentage (%). After identifying the stationary point in a contour plot, it has to be determined if it is the maximum, minimum, or saddle point. An analysis of the response surface and contour plots (Fig. 22A and B) found that the maximum I to be 98.1%. The corresponding parameters that yielded this maximum value were PC = 20 wt/wt% and PLR = 2.0 g mL^{-1}. The desirability factor for the optimum solution is 0.981 (Fig. 22C), which indicates that the result is acceptable for optimum value of I.

A

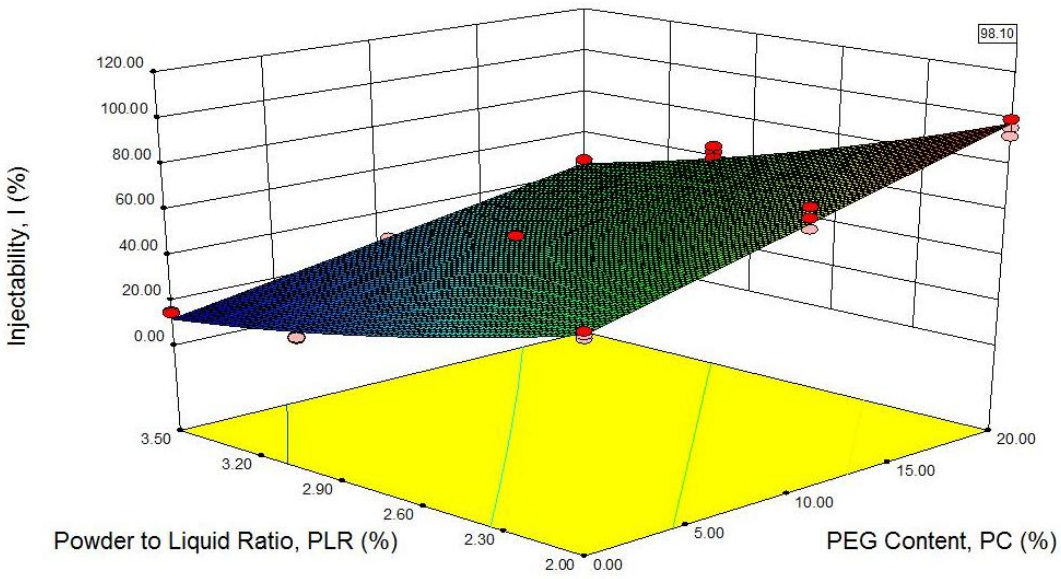
98.10
120.00
100.00
80.00
60.00
40.00
20.00
0.00
Injectability, I (%)
3.50
3.20
2.90
2.60
2.30
2.00
Powder to Liquid Ratio, PLR (%)
0.00
5.00
10.00
15.00
20.00
PEG Content, PC (%)

B

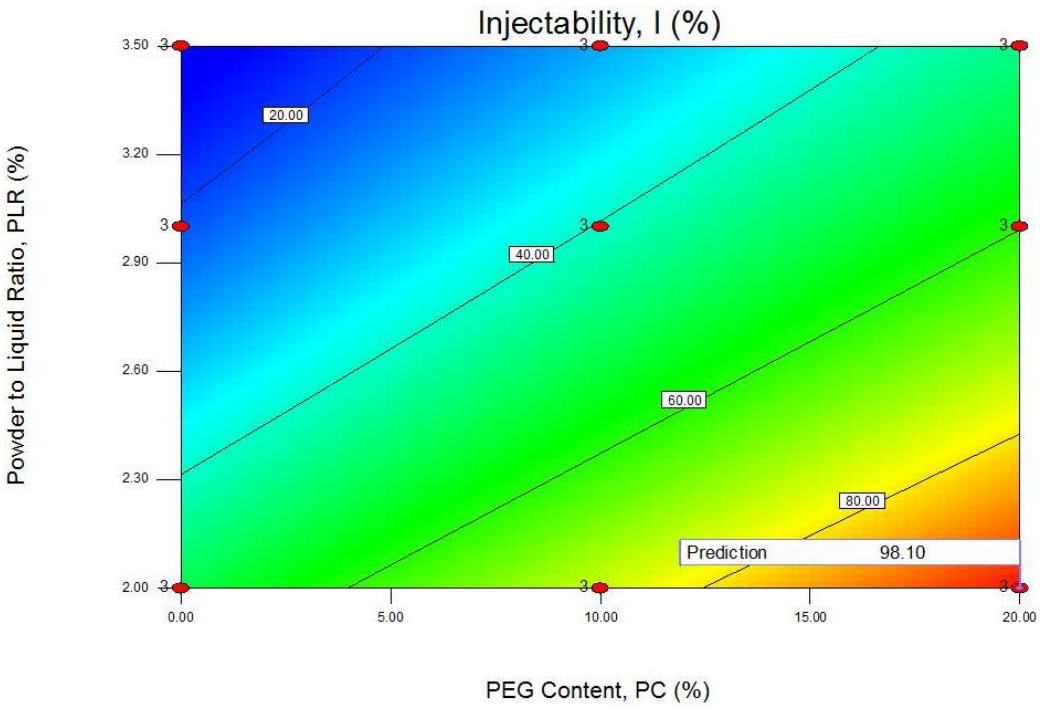
Injectability, I (%)
Powder to Liquid Ratio, PLR (%)
PEG Content, PC (%)
3.50
3.20
2.90
2.60
2.30
2.00
0.00
5.00
10.00
15.00
20.00
20.00
40.00
60.00
80.00
Prediction 98.10

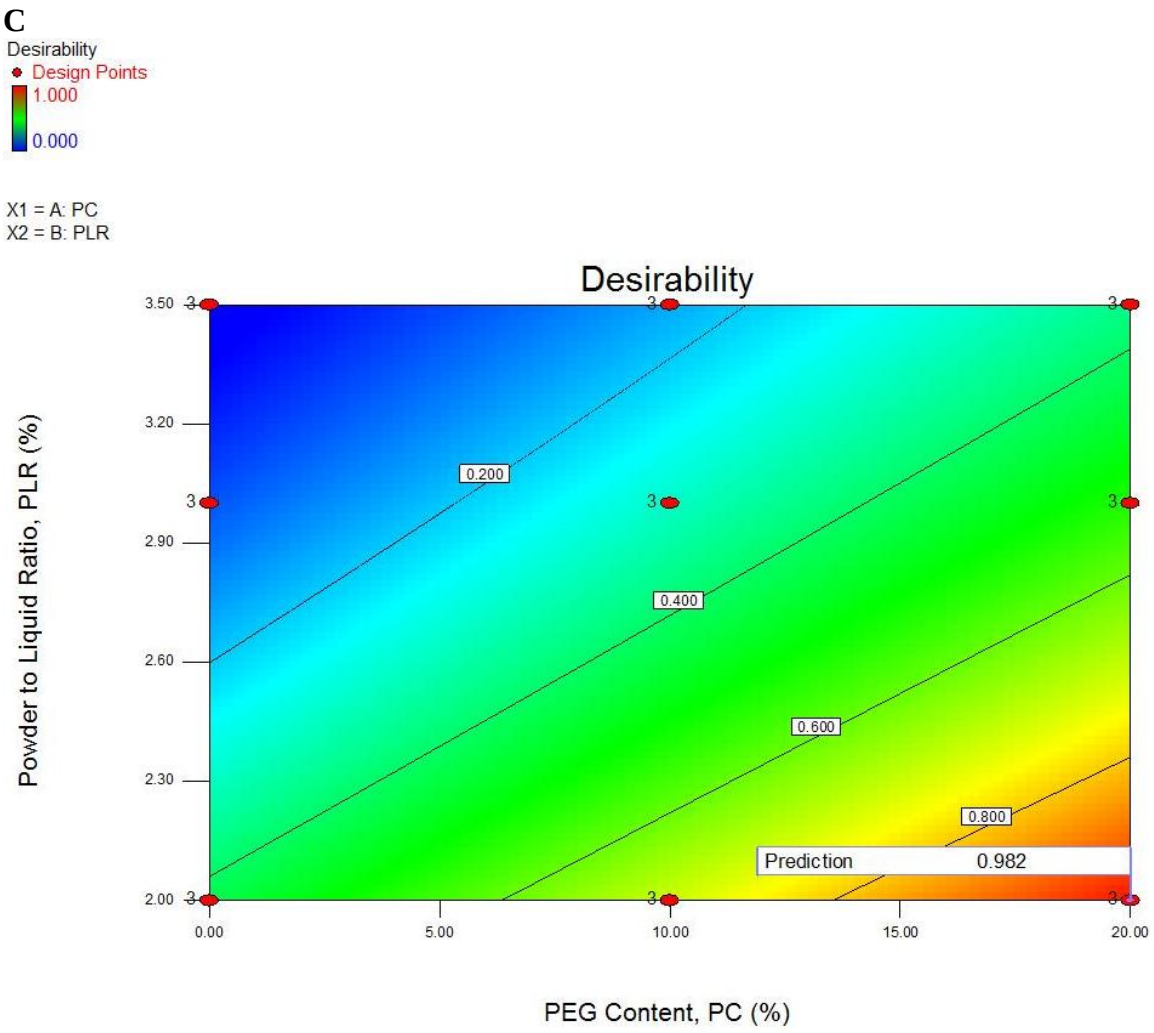

Fig. 22. The response surface plot (A), contour plot (B) and desirability plot (C) for influence of PEG content and powder-to-liquid ratio on the injectability of a calcium phosphate cement.

4.5. Case Study #5: Final setting time of a calcium phosphate cement

4.5.1. Experimental details

The powder constituents of the cement were $CaCO_3$, DCPA, and β–TCP, while the liquid was an aqueous solution of poly (ethylene glycol) (PEG). The powder and liquid were mixed, with a spatula, in a glass dish, until a paste was obtained.

The final setting times were determined using the Gillmore needle method (per ASTM C266-99 [57]).The apparatus comprised a weighted needle (diameter and weight =1.06 mm and 453.6 g, respectively). After mixing the cement powder and liquid, the paste was poured into a PTFE mold (nominal diameter and height = 6 mm and 12 mm, respectively), held at 37^{o} C. The final setting time was denoted as the time taken for the curing cement to bear the weight of the needles without any appreciable indentation to its surface. The surface of the specimen was observed visually every 30 s, until it was deemed that the indentation was negligible. Each test was run in triplicate. The results are given in Table 22.

Table 22
Final setting time of a calcium phosphate cement

PEG content (wt/wt%)	PLR (g mL^{-1})	Final setting time (min)
0	2.0	26.3 ± 0.8
10	2.0	35.4 ± 1.4
20	2.0	42.1 ± 1.3
0	2.5	12.9 ± 0.3
10	2.5	24.6 ± 0.7
20	2.5	36.3 ± 1.6
0	3.5	4.8 ± 0.2
10	3.5	8.6 ± 0.3
20	3.5	13.1 ± 0.30

4.5.2. Design matrix

Two factors (explanatory variables) were considered for their influence on final setting time (F); namely, PEG content (PC) and powder-to-liquid ratio (PLR). For each factor, 9 values were used; thus, there were 27 data points.

For the RSM work (Design Expert®, Version 8), therefore, it was appropriate to use the two-factors, three-levels, central composite design matrix (CCD). The values of the factors used and the corresponding level for each factor are given in Table 23 while, in Table 24, the 27 data points are presented both as coded values and as raw values.

Table 23
Factors and their levels: final setting time of a calcium phosphate cement

Factor	Unit	Coded levels		
		-1	0	+1
PEG content PC)	wt./wt.%	0	10	20
Powder-to-liquid ratio (PLR)	g mL^{-1}	2.0	2.5	3.5

Table 24

Design matrix and experimental results: final setting time of a calcium phosphate cement

Cement	Coded values		Raw values		Final setting time
	PC	PLR	PC	PLR	F
			(wt/wt%)	(g mL^{-1})	(min)
A	-1	-1	0	2.0	27.13
A	-1	-1	0	2.0	26.32
A	-1	-1	0	2.0	25.51
B	0	-1	10	2.0	36.86
B	0	-1	10	2.0	35.43
B	0	-1	10	2.0	34.00
C	1	-1	20	2.0	43.45
C	1	-1	20	2.0	42.11
C	1	-1	20	2.0	40.77
D	-1	0	0	2.5	13.25
D	-1	0	0	2.5	12.94
D	-1	0	0	2.5	12.63
E	0	0	10	2.5	25.29
E	0	0	10	2.5	24.60
E	0	0	10	2.5	23.91
F	1	0	20	2.5	37.92
F	1	0	20	2.5	36.33
F	1	0	20	2.5	34.74
G	-1	1	0	3.5	4.97
G	-1	1	0	3.5	4.80
G	-1	1	0	3.5	4.63
H	0	1	10	3.5	8.88
H	0	1	10	3.5	8.63
H	0	1	10	3.5	8.38
I	1	1	20	3.5	13.43
I	1	1	20	3.5	13.14
I	1	1	20	3.5	12.85

4.5.3. Empirical relationship and regression analysis

The second-order polynomial (regression) equation used to represent the response surface (final setting time (F)) is given by

$$F = b_o + \sum b_i X_i + \sum b_{ij} X_i X_j + \sum b_{ii} X_i^2, \quad (27)$$

where X_i and X_j are the two factors.

Thus, the selected polynomial could be expressed as

$$F = b_o + b_1 (PC) + b_2 (PLR) + b_{12} (PC)(PLR) + b_{11} (PC)^2 + b_{22} (PLR)^2, \quad (28)$$

where b_o is the average of the responses; b_1 and b_2 are the regression coefficients that characterize the direct effects of the factors; b_{12} is the regression coefficient that characterizes the interaction effect of the factors; and b_{11} and b_{22} are the regression coefficients that characterize the quadratic effects of the factors.

With the computed values of the coefficients, it is found the cubic and above models were aliased. In experimental design, when two interactions, or a main effect and an interaction, share the same column, and so cannot be individually analyzed, then their effects are termed “aliased”. Two factors interaction 2FI model is suggested to best fit the model. Hence, the 2FI model is used in RSM and Eq. (28) becomes

$$F = 51.502 + 1.646(PC) – 13.770(PLR) - 0.320(PC)(PLR) \quad (29)$$

4.5.4. Adequacy of regression model

Analysis of variance (ANOVA) of the regression model was performed and the results (Table 25) were used to examine the adequacy of the model. The desired level of confidence was considered to be adequate provided that 1) the calculated value of the F ratio of the model developed did not exceed the standard tabulated value of the F ratio and 2) the calculated value of the coefficient of determination (R^2) of the developed relationship exceeded the standard tabulated value of the R^2 for a desired level of confidence (in this case study, 0.95).

Table 25
The ANOVA results (response parameter: final setting time (F), in min, of a calcium phosphate cement)

Source	Sum of squares	df	Mean square	F value	p-value Prob > F	
Model	4226.24	3	1408.75	252.63	< 0.0001	significant
PC	1035.75	1	1035.75	185.74	< 0.0001	
PLR	3025.33	1	3025.33	542.52	< 0.0001	
(PC)(PLR)	71.84	1	71.84	12.88	0.0016	
Residual	128.26	23	5.58			
Lack of fit	112.71	5	22.54	26.10	< 0.0001	significant
Pure error	15.54	18	0.86			
Cor total	4354.50	26				
Std dev	2.36	R^2	0.9705			
Mean	22.70	Adj R^2	0.9667			
COV (%)	10.40	Pred R^2	0.9604			
		Adeq precision	44.853			

The model F-value of 252.63 implies the model is significant because there is only a 0.01% chance that a model F-value this large could occur due to noise. The goodness of fit of the model is indicated by the coefficient of determination (R^2), which was found to be 0.9705, which implies that 97.05% of the experimental data were predicted by the model. The adjusted R^2, 0.9667, was high enough to confirm the high significance of the model. The predicted R^2 is 0.9604, which means that the model could explain 96% of the

variability in predicting new final setting time observations. The parameter, Adeq precision, is a measure of the signal-to-noise ratio, with a value > 4 considered desirable. In this case study, the ratio was 44.85, which indicated an adequate signal. The coefficient of variation (COV), 10.40%, is low enough to indicate that the deviations between the experimental and the predicted I values are low. All of the aforementioned ANOVA results show that the model (Eq. (29)) was adequate and, thus, may be used to navigate the design space. The "lack of fit F-value" of 22.54 implies the lack of fit is significant. There is only a 0.01% chance that a "lack of fit F-value" this large could occur. Significant lack of fit is bad because we want the model to fit. Because the p-value is smaller than the significance level $\alpha = 0.05$, there is sufficient evidence at the $\alpha = 0.05$ level to conclude that there is lack of fit.

For a model term, a value of Prob>F less than 0.0500 indicates that it is significant. Thus, in this case study, PC, PLR and (PC)(PLR) are the only significant model terms and square terms are not significant. In that case, Eq. (28) reduces to

$$F = 51.502 + 1.646(PC) - 13.770(PLR) - 0.320(PC)(PLR) \quad (30)$$

For a given response, the contributions of factors can be ranked from their respective F ratio values provided the degrees of freedom are same for all the input parameters. The larger the F ratio the higher is the significance. From the F ratio values (Table 3), it is seen that PLR exerts a greater influence on the final setting time than does PC but the

interaction term (PC)(PLR) exerts far less influence on the final setting time compared to the main terms, PC and PLR.

4.5.5. Residuals and correlation exercises

The normal probability plot of the residuals for final setting time is linear (Fig. 23), indicating that the errors are distributed normally. The match between the predicted and the experimental values is very good (Fig. 24).

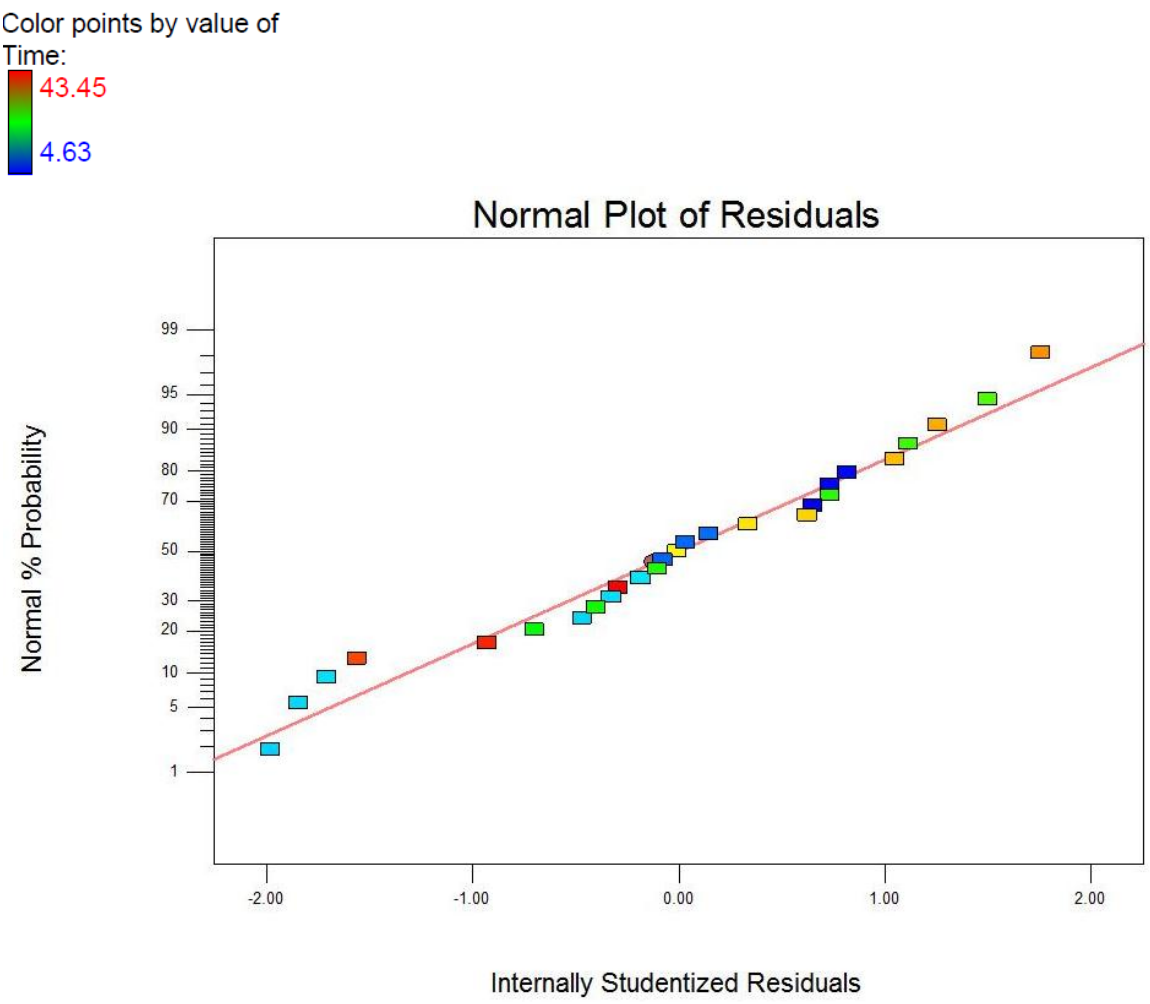

Fig. 23. The normal probability plot of the final setting time results for a calcium phosphate cement.

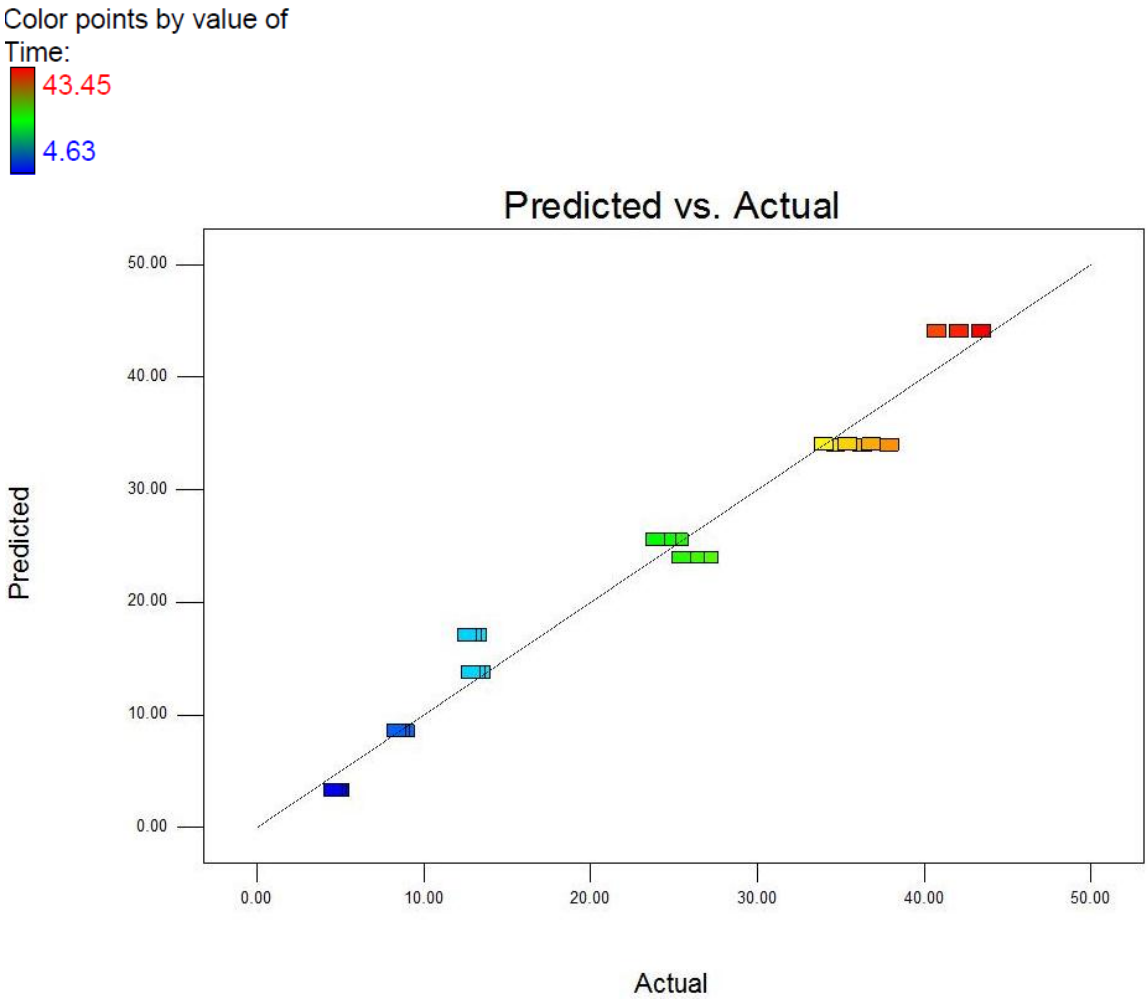

Fig. 24. The correlation plot of the final setting time results for a calcium phosphate cement.

4.5.6. Optimization exercise

To obtain the optimum combination for obtaining a final setting time of 15 min [54], response surface, contour, and desirability plots were developed for the proposed model that contained only the significant coefficients (Eq. (4)). A contour plot is produced to display the regions of the optimal factor settings. Either the response surface plot or the contour plot can be used to predict the response (target final setting time of 15 min) for any zone of the experimental domain. As shown on the surface response plot (Fig. 25A), the desired optimum is a target value rather than showing the maximum achievable setting time. After identifying the stationary point in a contour plot, it has to be determined if it is the maximum, minimum, target, or saddle point. An analysis of the response surface and contour plots (Figs. 25A and B) found that the indicated target point (15 min) has high desirability compared to other location with same target setting time in minutes (Fig. 25C). The corresponding parameters that yielded this 15 min target final setting time value desired were PC = 3.96 wt/wt% and PLR = 2.86 g mL^{-1}.

However, there are 33 possible numerical RSM solutions that gives the target final setting time of 15 min and, thus, multiple solutions are expected where the contour plot for 15 min have multiple options as shown on the RSM contour plot.

A

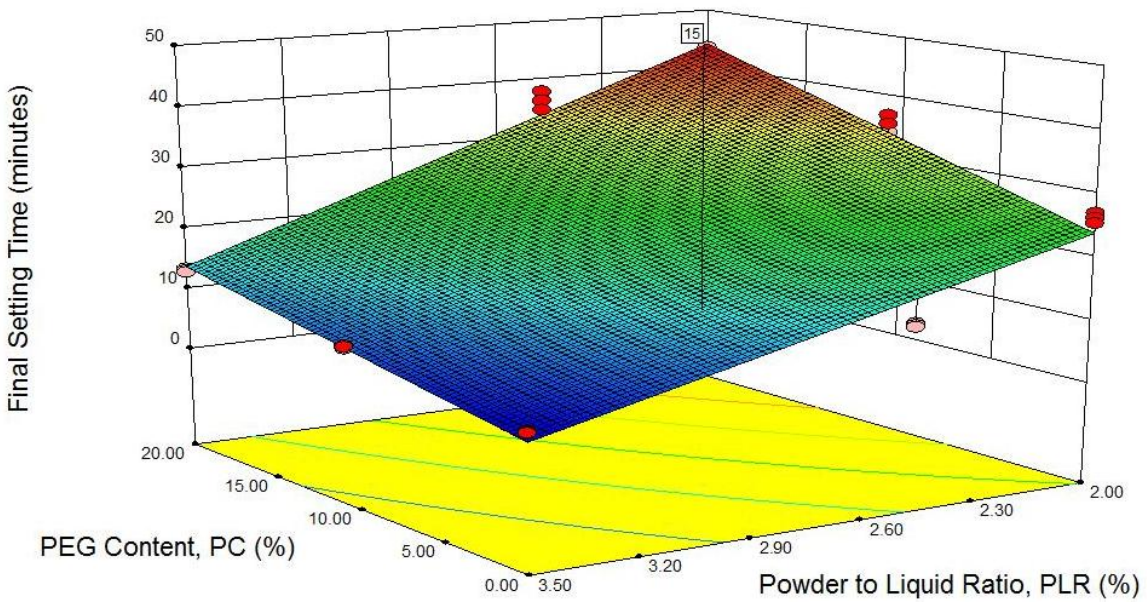
Final Setting Time (minutes)
50
40
30
20
10
0
15
20.00
15.00
10.00
5.00
0.00
PEG Content, PC (%)
3.50
3.20
2.90
2.60
2.30
2.00
Powder to Liquid Ratio, PLR (%)

B

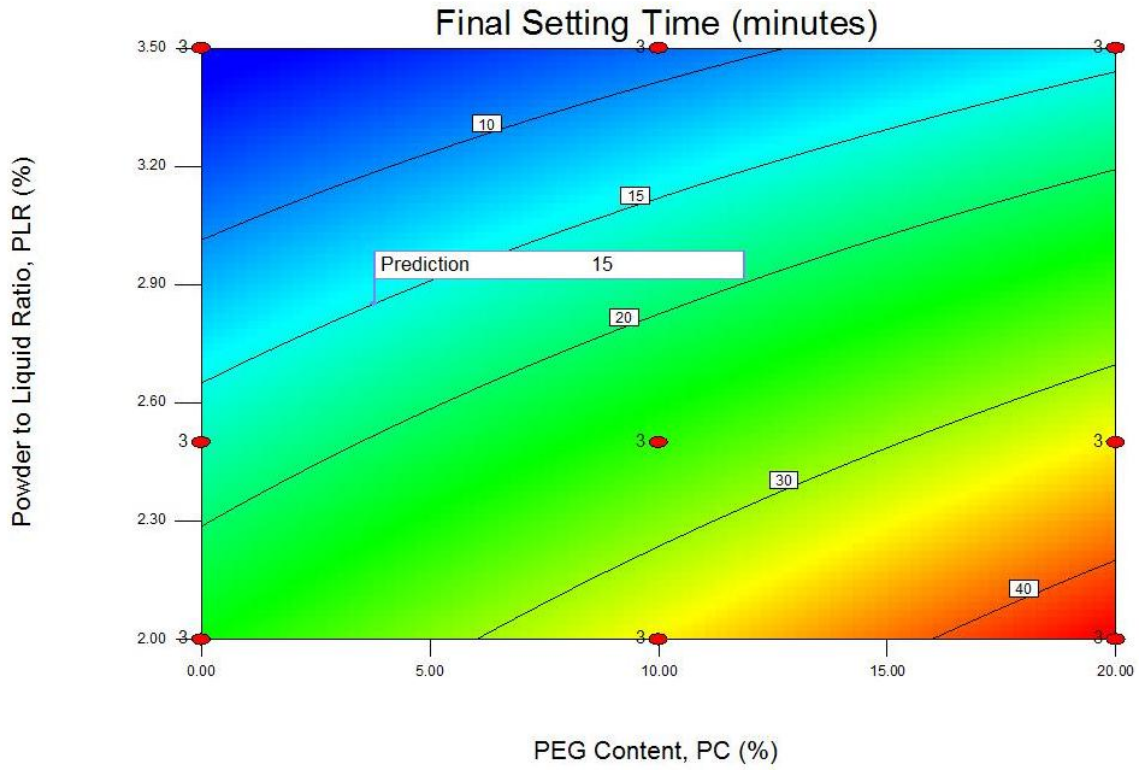
Final Setting Time (minutes)
Powder to Liquid Ratio, PLR (%)
PEG Content, PC (%)
Prediction 15
10
15
20
30
40
3.50
3.20
2.90
2.60
2.30
2.00
0.00
5.00
10.00
15.00
20.00

C

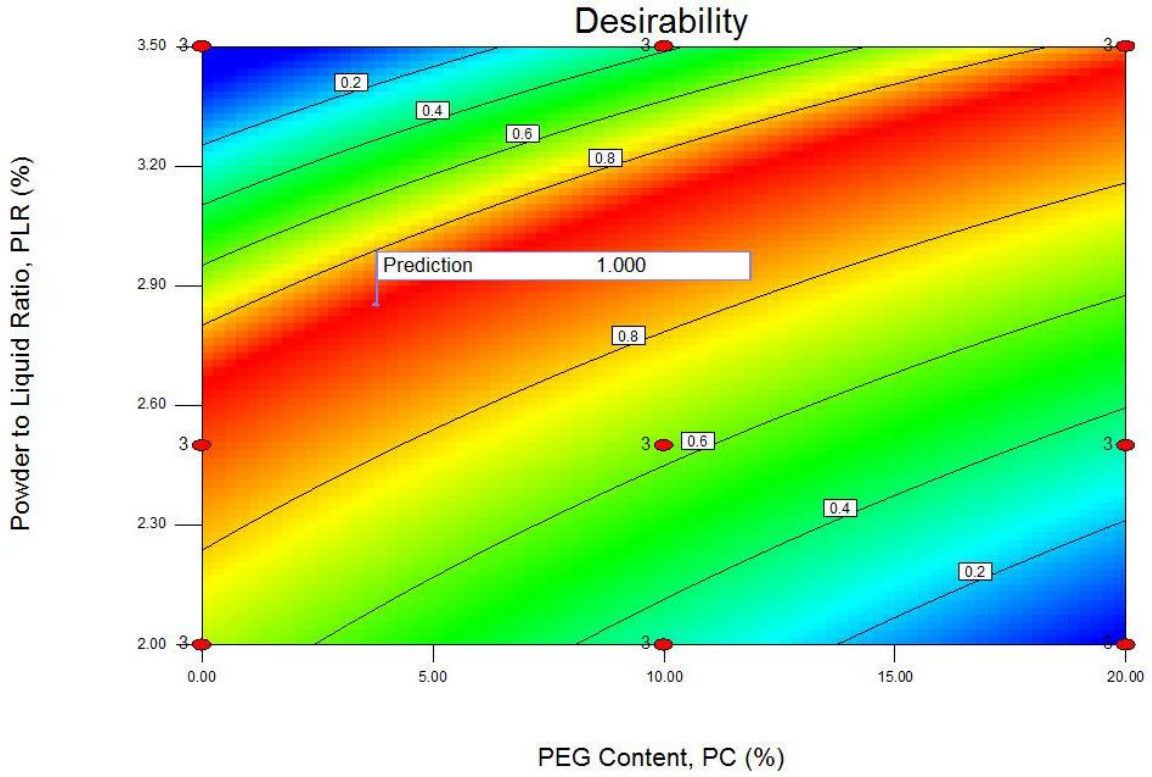

Fig 25. The response surface plot (A), contour plot (B), and desirability plot (C) for the influence of PEG content and PLR on the final setting time of a calcium phosphate cement.

4.6. Case Study #6: Compressive strength of a calcium phosphate cement

4.6.1. Experimental details

The powder constituents of the cement were $CaCO_3$, DCPA, and β–TCP, while the liquid was an aqueous solution of 4 wt/wt% poly(acrylic acid) (PAA) and Na_2HPO_4 (SPC). The powder and liquid were mixed, with a spatula, in a glass dish, until a paste was obtained.

The inside surface of each of the six cells in a cylindrical steel mold, with each cell nominal diameter (D) and height of 6 mm and 12 mm, respectively, was packed with a thin layer of a release agent was spread. The cement powder and liquid were mixed until a paste was obtained, after which it was injected into the cells. To eliminate large air bubbles in the paste, the mold was covered with a solid steel plate and then the whole assembly was put in a mechanical press, under a load of 70 kN, for 1 h. After disassembly, the cement specimens were immersed in a container filled with phosphate buffered saline. A lid was placed on the container and tightened, after which the container was placed in an incubator, set at 37^{o} C. After 1 day, the mold was removed from the container, the specimens punched out of the mold, and then lightly sanded. The specimens were then placed in distilled water for 7 d before being tested. In the test, a specimen was compressed in a servohydraulically-actuated universal materials testing machine, operated at a crosshead displacement rate of 0.5 mm min^{-1}, until its height was reduced to about 10% of its initial value or the specimen fractured, whichever occurred first. From the load-versus-crosshead displacement record, compressive strength (UCS) was calculated thus

$$UCS = (4F_{max})/(\pi D^2), \qquad (31)$$

where F_{max} is the peak load.

Each test was run in triplicate. The results are given in Table 26.

Table 26
Compressive strength (UCS) of a calcium phosphate cement

Na_2HPO_4 content (wt/wt%)	PLR (g mL^{-1})	UCS (MPa)
0	2.5	24 ± 2
0	3.0	31 ± 3
0	3.5	42 ± 5
2	2.5	20 ± 3
2	3.0	27 ± 4
2	3.5	34 ± 6
4	2.5	18 ± 1
4	3.0	24 ± 3
4	3.5	33 ± 4

4.6.2. Design matrix

Two factors (explanatory variables) were considered for their influence on UCS; namely, Na_2HPO_4 content (SPC) and powder-to-liquid ratio (PLR). For each factor, three values were used; thus, there were 27 data points.

For the RSM work (Design Expert®, Version 8), therefore, it was appropriate to use the two-factors, three-levels, central composite design matrix face centered option (CCD option). The values of the factors used and the corresponding level for each factor are given in Table 27 while, in Table 28, the 27 data points are presented both as coded values and as raw values.

Table 27
Factors and their levels: compressive strength of a calcium phosphate cement

Factor	Unit	Coded levels		
		-1	0	+1
Na_2HPO_4 content (SPC)	wt./wt.%	0	2	4
Powder-to-liquid ratio (PLR)	g mL^{-1}	2.5	3.0	3.5

Table 28
Design matrix and experimental results: compressive strength of a calcium phosphate cement

Cement	Coded values		Raw values		UCS (MPa)
	SPC	PLR	SPC (wt/wt%)	PLR ($g\ mL^{-1}$)	
A	-1	-1	0.00	2.50	22
	-1	-1	0.00	2.50	24
	-1	-1	0.00	2.50	26
B	-1	0	0.00	3.00	28
	-1	0	0.00	3.00	31
	-1	0	0.00	3.00	34
C	-1	+1	0.00	3.50	37
	-1	+1	0.00	3.50	42
	-1	+1	0.00	3.50	47
D	0	-1	2.00	2.50	17
	0	-1	2.00	2.50	20
	0	-1	2.00	2.50	23
E	0	0	2.00	3.00	23
	0	0	2.00	3.00	27
	0	0	2.00	3.00	31
F	0	+1	2.00	3.50	28
	0	+1	2.00	3.50	34
	0	+1	2.00	3.50	40
J	+1	-1	4.00	2.50	17
	+1	-1	4.00	2.50	18
	+1	-1	4.00	2.50	19
K	+1	0	4.00	3.00	21
	+1	0	4.00	3.00	24
	+1	0	4.00	3.00	27
L	+1	+1	4.00	3.50	29
	+1	+1	4.00	3.50	33
	+1	+1	4.00	3.50	37

4.6.3. Empirical relationship and regression analysis

The second-order polynomial (regression) equation used to represent the response surface (UCS) is given by

$$UCS = b_o + \sum b_i X_i + \sum b_{ij} X_i X_j + \sum b_{ii} X_i^2, \quad (32)$$

where X_i and X_j are the two factors.

Thus, the selected polynomial could be expressed as

$$UCS = b_o + b_1 (SPC) + b_2 (PLR) + b_{12} (SPC)(PLR) + b_{11} (SPC)^2 + b_{22} (PLR)^2 , \quad (33)$$

where b_o is the average of the responses; b_1 and b_2 are the regression coefficients that characterize the direct effects of the factors; b_{12} is the regression coefficient that characterizes the interaction effect of the factors; and b_{11} and b_{22} are the regression coefficients that characterize the quadratic effects of the factors.

With the computed values of the coefficients, it is found the cubic and above models were aliased. In experimental design, when two interactions, or a main effect and an interaction, share the same column, and so cannot be individually analyzed, then their effects are termed “aliased”. Linear model is suggested to best fit the model. The two factors interaction 2FI model and the quadratic models have non-significant terms and

could not best fit the model. Hence, the linear model is used in RSM and Eq. (33) becomes

$$UCS = -15.22 - 1.83(SPC) + 15.67(PLR) \quad (34)$$

4.6.4. Adequacy of regression model

Analysis of variance (ANOVA) of the regression model was performed and the results (Table 29) were used to examine the adequacy of the model. The desired level of confidence was considered to be adequate provided that 1) the calculated value of the F ratio of the model developed did not exceed the standard tabulated value of the F ratio and 2) the calculated value of the coefficient of determination (R^2) of the developed relationship exceeded the standard tabulated value of the R^2 for a desired level of confidence (in this case study, 0.82).

Table 29
ANOVA results (response parameter: compressive strength (UCS), in MPa, of a calcium phosphate cement

Source	Sum of squares	df	Mean square	F value	p-value Prob>F	
Model	1346.50	2	673.25	55.304	< 0.0001	significant
SPC	242.00	1	242.00	19.879	0.0002	
PLR	1104.50	1	1104.50	90.729	< 0.0001	
Residual	292.17	24	12.17			
Lack of fit	42.17	6	7.03	0.506	0.7958	not significant
Pure error	250.00	18	13.89			
Cor total	1638.67	26				
Std dev	3.49	R^2	0.8217			
Mean	28.11	Adj R^2	0.8068			
COV (%)	12.41	Pred R^2	0.7748			
		Adeq precision	19.776			

The model F-value of 55.304 implies the model is significant because there is only a 0.01% chance that a model F-value this large could occur due to noise. The goodness of fit of the model is indicated by the coefficient of determination (R^2), which was found to be 0.8217, which implies that 82.17% of the experimental data were predicted by the model. The adjusted R^2, 0.8068, was high enough to confirm the high significance of the model. The predicted R^2 is 0.7748, which means that the model could explain 77% of the variability in predicting new UCS observations. The parameter, Adeq precision, is a measure of the signal-to-noise ratio, with a value > 4 considered desirable. In this case

study, the ratio was 19.776, which indicated an adequate signal. The coefficient of variation (COV), 12.41%, is more than 10% but still considered low enough to indicate that the deviations between the experimental and the predicted UCS values are small. All of the aforementioned ANOVA results show that the model (Eq. (34)) was adequate and, thus, may be used to navigate the design space.

For a model term, a value of Prob>F less than 0.0500 indicates that it is significant. Thus, in this case study, SPC and PLR are the only significant model terms and there is no interaction terms or square terms. In this case, the final model Equation is

$$UCS = -15.22 - 1.83(SPC) + 15.67(PLR) \quad (35)$$

For a given response, the contributions of factors can be ranked from their respective F ratio values provided the degrees of freedom are same for all the input parameters. The larger the F ratio the higher is the significance. From the F ratio values (Table 3), it is seen that PLR exerts the greatest influence on UCS.

4.6.5. Residuals and correlation exercises

The normal probability plot of the residuals for UCS is linear (Fig. 26), indicating that the errors are distributed normally. The match between the predicated and the experimental UCS values is very good (Fig. 27).

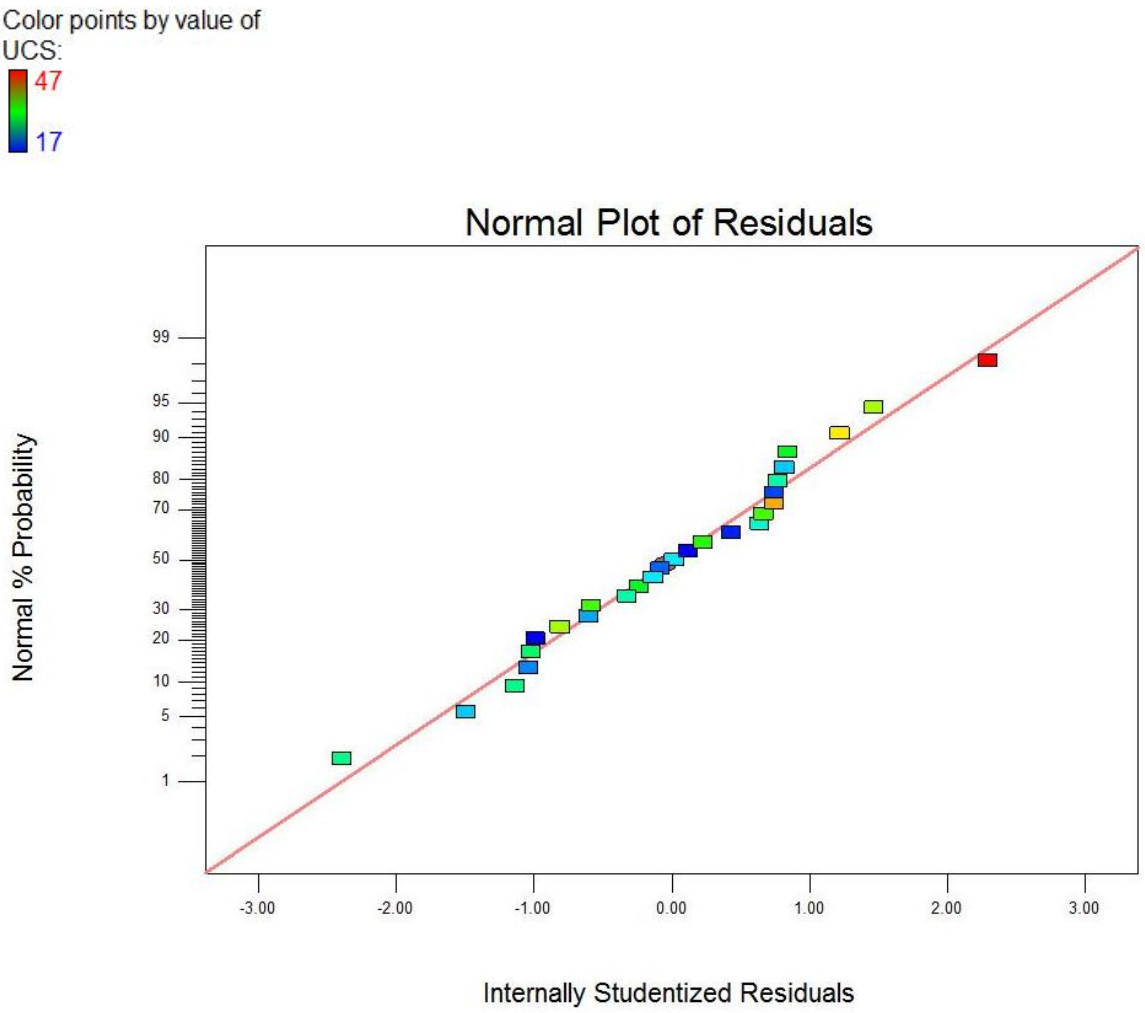

Fig. 26. The normal probability plot of the compressive strength results for a calcium phosphate cement.

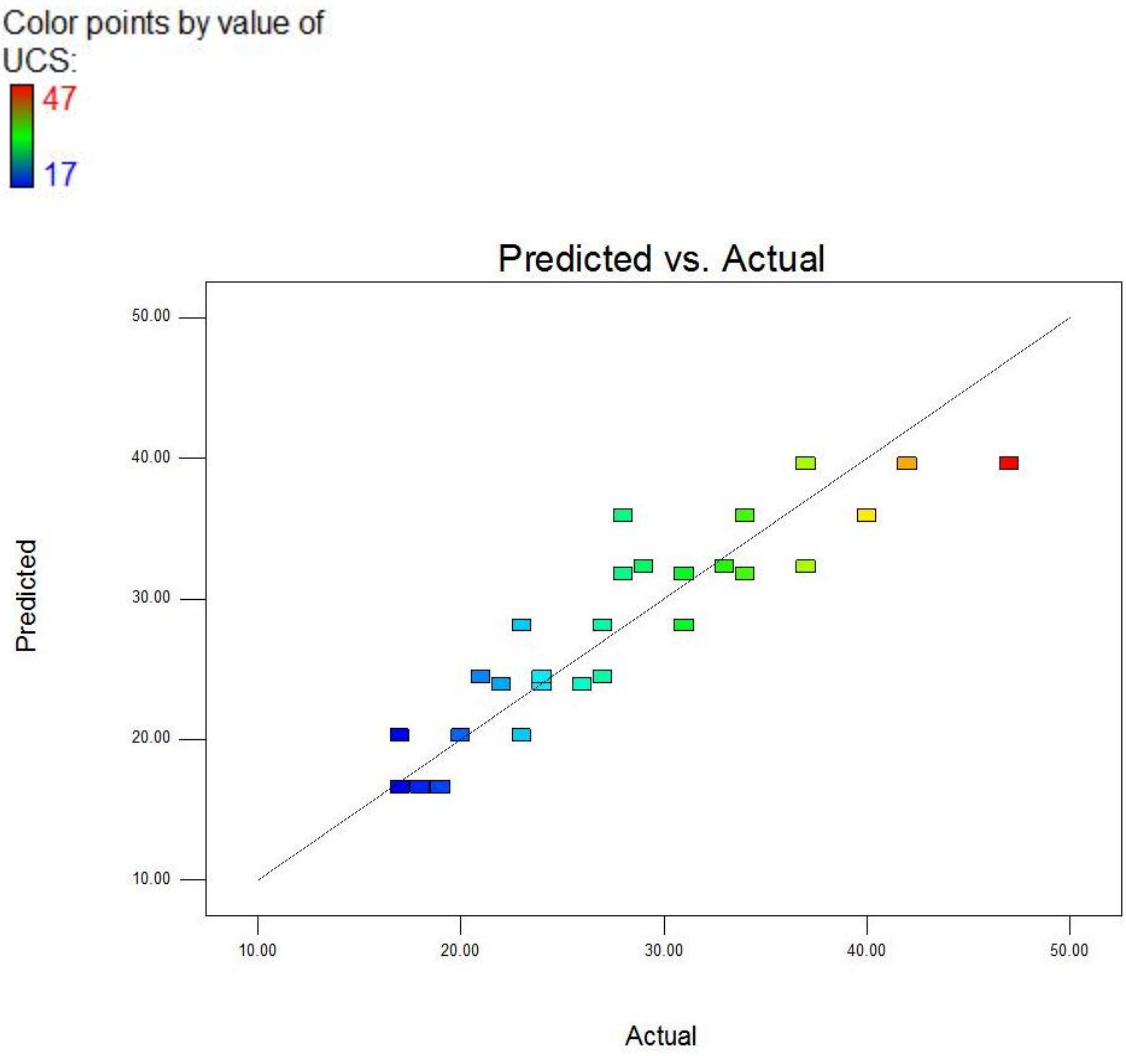

Fig. 27. The correlation plot of the compressive strength results for a calcium phosphate cement.

4.6.6. Optimization exercise

To obtain the optimum combination for maximizing UCS of the cement, response surface, contour, and desirability plots were developed for the proposed model that contained only the significant coefficients (Eq. (35)). A contour plot is produced to display the regions of the optimal factor settings. Either the response surface plot or the contour plot can be used to predict the response (UCS value) for any zone of the experimental domain. The left-hand tip of the response plot (Fig. 28A) shows the maximum achievable UCS. After identifying the stationary point in a contour plot, it has to be determined if it is the maximum, minimum, or saddle point. An analysis of the response surface and contour plots (Figs. 28A and B), the maximum achievable UCS is 39.11 MPa. The corresponding parameters that yielded this maximum value (desirability = 0.754) (Fig. 28C) were Na_2HPO_4 content = 0 and PLR = 3.5 g mL^{-1}.

A

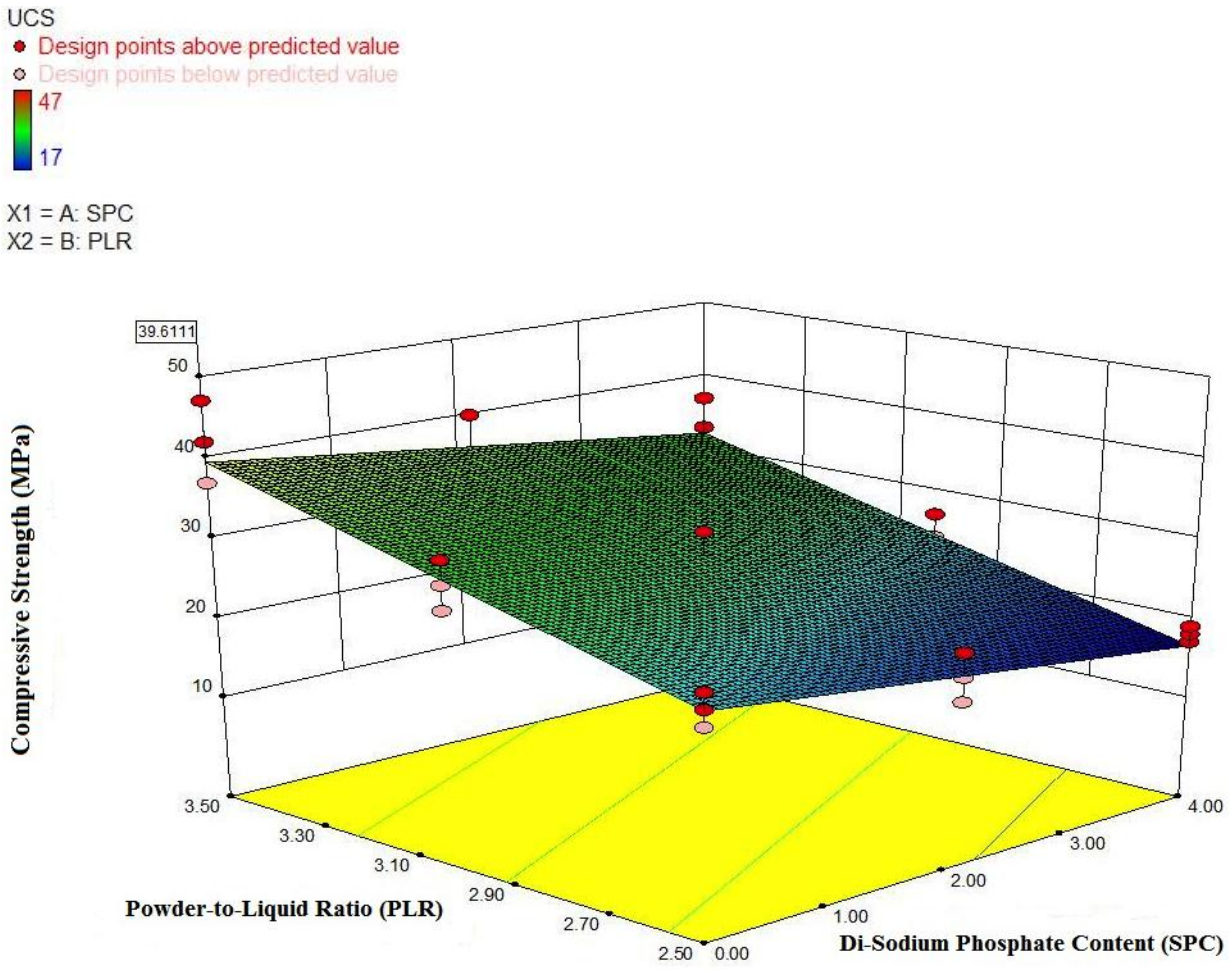
UCS
Design points above predicted value
Design points below predicted value
47
17
X1 = A: SPC
X2 = B: PLR
39.6111
50
40
30
20
10
Compressive Strength (MPa)
3.50
3.30
3.10
2.90
2.70
2.50
Powder-to-Liquid Ratio (PLR)
0.00
1.00
2.00
3.00
4.00
Di-Sodium Phosphate Content (SPC)

B

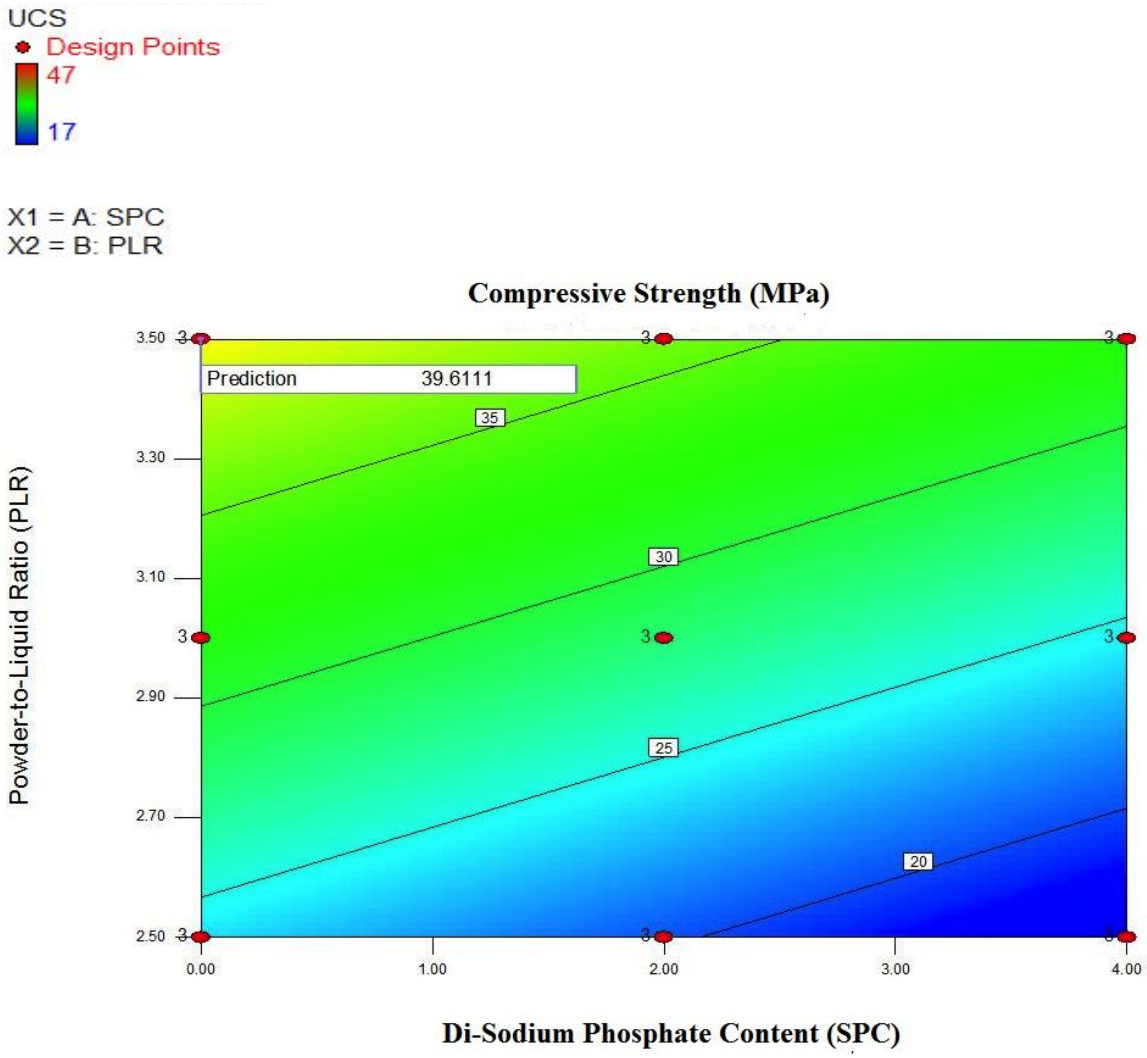
UCS
Design Points
47
17
X1 = A: SPC
X2 = B: PLR
Compressive Strength (MPa)
Prediction 39.6111
35
30
25
20
Powder-to-Liquid Ratio (PLR)
3.50
3.30
3.10
2.90
2.70
2.50
0.00
1.00
2.00
3.00
4.00
Di-Sodium Phosphate Content (SPC)

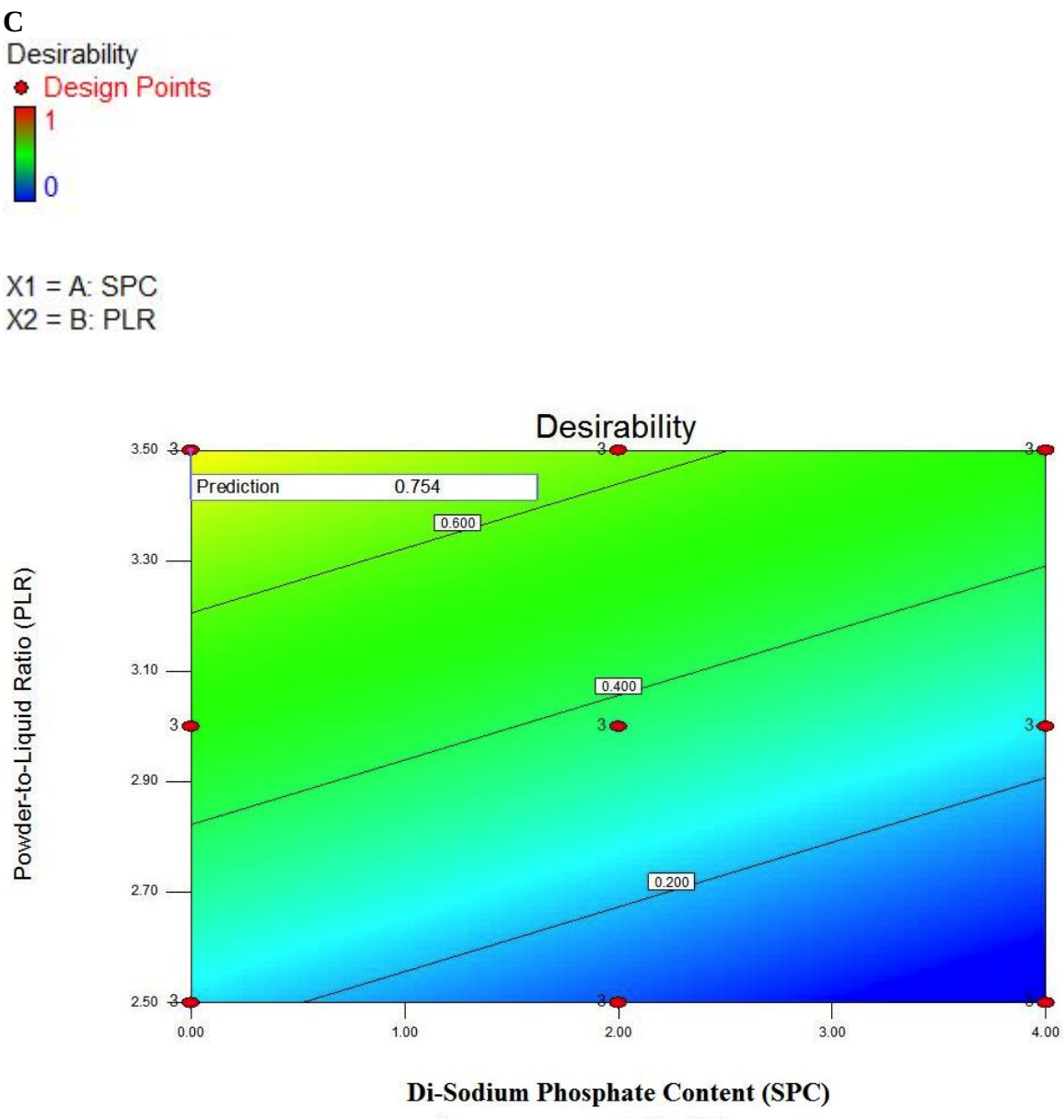

Fig. 28. The response surface plot (A), contour plot (B), and desirability plot (C) for the influence of di-sodium phosphate content and powder-to-liquid ratio on the compressive strength of a calcium phosphate cement.

CHAPTER 5

CONCLUSIONS AND RECOMMENDATIONS

Based on the results obtained in this study, using the response surface methodology (RSM), the following are the main conclusions:

(1) While interaction effects are significant for injectability and final setting time of a calcium phosphate cement, they are not significant for degradability, maximum exotherm temperature, and residual monomer content of a PMMA bone cement, and compressive strength of a calcium phosphate cement.

(2) For a given cement property, its optimum value was obtained together with the values of the experimental variables to produce this result. Thus, in the case of a PMMA bone cement, 1) the minimum exotherm temperature (48^{o} C) could be attained using a cement having barium sulfate and quaternary amine commoner contents of 26.5 wt/wt% and 19.8 wt/wt%, respectively; 2) the minimum residual monomer content 7 days after the cement was cured (1.81%) could be attained using a cement having barium sulfate and quaternary amine commoner contents of 20.3 wt/wt% and 0, respectively; and 3) the optimum degradability (41%) could be attained using a cement having a PMMA bead, bioactive glass particles, and chitosan particles contents of 51, 37, and 12 wt/wt%, respectively. In the case of a calcium phosphate bone cement, 1) the optimum injectability (98%) could be attained using a cement having a polyethylene glycol (PEG) content of 20 wt/wt% and mixed using a powder-to-liquid ratio (PLR) of 2.0 g mL^{-1}; 2) a final mixing time of 15 min could be attained using a cement having a PEG content of 3.96 wt/wt% and mixed using a PLR of 2.86 g mL^{-1}. In addition, multiple numerical solutions exist for this target time; and 3) the optimum 7-day compressive strength

(39 MPa) could be attained by adding no Na_2HPO_4 to the poly(acrylic acid) for the cement liquid and mix the powder and the liquid using PLR of 3.5 g mL^{-1}.

(3) In the case of a calcium phosphate cement (CPC), PLR exerts significant direct effects on each of the three cement properties that were investigated (injectability, final setting time, and 7-day compressive strength). Clinicians should keep this finding mind when preparing a CPC for use in vertebroplasty and balloon kyphoplasty.

The following recommendations are made for future study:

(1) For each property considered in this study, it should be determined experimentally using the computed values of the explanatory variables. For example, determine T_{max} of the PMMA bone cement having barium sulfate and quaternary amine comonomer contents of 26.5 wt/wt% and 19.8 wt/wt%, respectively, and compare the result to that computed using RSM (that is, 48^o C). Another example is final setting time F of the CPC, where multiple numerical solutions found can also be verified experimentally using the computed values of the explanatory variables.

(2) Experimental determinations of the cement properties should be conducted using a host of variables. For example, in the case of the CPC, 7-day compressive strength (UCS) should be determined for a cement in which the variables are PEG content, nanosized titania particles, citric acid content, disodium pamidronate content, and PLR. After that, RSM should be used to analyze the experimental results in order to compute the optimum UCS.

References

[1] Lewiecki EM. Osteoporosis: clinical evaluation. Chapter 12. New Mexico Clinical Research & Osteoporosis Center, University of New Mexico School of Medicine, Albuquerque, NM.; 2010. http://www.endotext.org/parathyroid/ parathyroid12/ parathyroidframe12.htm

[2] Dallessio KM. An introduction to osteoporosis and bone mineral density testing. Continuing Education and Career Development. http://www.eradimaging.com/ site/article.cfm?ID=762.

[3] Youssef JA, Salas VM, Loschiavo RG. Management of painful osteoporotic vertebral compression fractures: vertebroplasty and kyphoplasty. Oper Tech Orthop 2003;13:222-6.

[4] Marucci G, Brandi ML. Kyphoplasty and vertebroplasty in the management of osteoporosis with subsequent vertebral compression fractures. Clin Cas Min Bone Metab 2010;7:51-60.

[5] Heaney RP. Advances in therapy for osteoporosis. Clin Med Res 2003;1:93-9

[6] Lewis G. Percutaneous vertebroplasty and kyphoplasty for the stand-alone augmentation of osteoporosis-induced vertebral compression fractures: present status and future directions. J Biomed Mater Res Part B: Appl Biomater 2007;81B:371-86.

[7] Ma XL, Xing Dan, Ma JX, Xu WG, Wang J, Chen Y. Balloon kyphoplasty versus percutaneous vertebroplasty in treating osteoporotic vertebral compression fracture: grading the evidence through a systematic review and meta-analysis. Eur Spine J 2012;21:1844-59.

[8] Ortiz AO, Zoarski GH, Beckerman M. Kyphoplasty. Tech Vasc Interven Radio 2002;5:239-49.

[9] Turner TM, Urban RM, Singh K, Hall DJ, Renner SM, Lim TH, Tomlinson MJ, An HS. Vertebroplasty comparing injectable calcium phosphate cement compared with polymethylmethacrylate in a unique canine vertebral body large defect model. Spine J 2008;8:482-87.

[10] Zebarjad SM, Sajjadi SA, Sdrabadi TE, Yaghmaei A, Naderi B. A Study on mechanical properties of PMMA/hydroxyapatite Nnnocomposite Sci Res Eng 2011;3:795-801.

[11] Lopez A, Unosson E, Engqvist H, Persson C. Direct and interactive effects of three variables on properties of PMMA bone cement for vertebral body augmentation. J Mater Sci 2011;22:1599-1606.

[12] Anderson MJ, Whitcomb PJ. RSM simplified: optimizing processes using response surface methods. Productivity Press/CRC Press, Boca Raton, FL; 2004.

[13] Website http://www.mayfieldclinic.com/PDF/PE-AnatSpine.pdf. Anatomy of the spine basic level.

[14] Burge R, Dawson-Hughes B, Solomon DH, Wong JB, King A, Tosteson A. Incidence and economic burden of osteoporosis-related fractures in United States, 2005-2025. J Bone Min Res 2007;22:465-75.

[15] Johnell O, Kanis J. Epidemiology of osteoporotic fractures. Osteopor Int 2005;16:S3-S67.

[16] National Institutes of Health (NIH). Consensus development panel conference. Osteoporosis prevention, diagnosis, and therapy. JAMA 2001;285:785-95.

[17] Philips FM, Pfeifer BA, Lieberman IH, Kerr III EJ, Choi IS, Pazianos AG. Minimally invasive treatments of osteoporotic vertebral compression fractures: vertebroplasty and kyphoplasty. AAOS Instr Course Lectures Spine;32:293-301.

[18] Bono CM, Einhorn TA. Overview of osteoporosis: pathophysiology and determinants of bone strength. Eur Spine J 2003;12:S90-6.

[19] Osteoporosis handout on health. Online version updated January 2011. US Department of Health & Human Services.

[20] Kanis KA. Diagnosis of Osteoporosis and assessment of fracture risk. Lancet 2002;359:1929-36.

[21] Lim LS, Hoeksema LJ, Sherin K. Screening for osteoporosis in the adult US population ACPM position statement on preventive practice. Am J Prev Med 2009;36.

[22] Noris CM. Back Stability – Integrating Science and Therapy. 2nd edition; 2007. Publisher - Human Kinetics.

[23] Cloft HJ, Jensen ME. Kyphoplasty: An assessment of a new technology. Am J Neuroradiol 28:200-03.

[24] Ploeg WT, Veldhuizen AG, The B, Sietsma MS. Percutaneous vertebroplasty as a treatment for osteoporotic vertebral compression fractures a systematic review. Eur Spine J 2006;15:1749-58.

[25] Mcgraw JK, Cardella J, Barr JD, Mathis JM, Sanchez O, Schwartzberg MS, Swan TL, Sacks D: Society of interventional radiology quality improvement guidelines for percutaneous vertebroplasty. J Vasc Interv Radiol 2003;14:827-31.

[26] Dion JE. Percutaneous vertebroplasty. Med Mundi 2001;20-8.

[27] Pateder DB, Khanna J, Lieberman IH. Vertebroplasty and kyphoplasty for the management of osteoporotic vertebral compression fractures. Orthoped Clin N Amer 2007;38:409-18

[28] Carrino JA, Chan R, Vaccaro AR. Vertebral augmentation vertebroplasty and kyphoplasty. Sem Roentgen 2004;39: 68-84.

[29] Peh WCG, Munk PL, Rashid F, Gilula LA. Percutaneous vertebral augmentation: vertebroplasty, kyphoplasty and skyphoplasty. Radiol Clin N Amer 2008;46:611-35.

[30] Website reference www.RadiologyInfo.org. Vertebroplasty and kyphoplasty.

[31] Australian Safety and Efficacy Register of New Interventional Procedures. Kyphoplasty and vertebroplasty: new and emerging techniques;2002.

[32] Comparative effectiveness of kyphoplasty for osteoporotic insufficiency fractures. The Orthopaedics One: The Orthopaedic Knowledge Network. http://www.orthopaedicsone.com/.

[33] A patient's guide to vertebroplasty. The Methodist Hosp Sys – Methodist Orthoped 2003.

[34] Gani A, Guth S, Imbert JP, Marin H, Dietemann JL. Percutaneous vertebroplasty: indications, technique, and results. Radio Graphics 2003;23:e10

[35] Barrocas AM, Eskey CJ, Hirsch JA. Vertebral augmentation in osteoporotic fractures. Injury 2007;38S3:S88-S96.

[36] National Health Service (NHS), UK. National Institute for Clinical Excellence. Balloon kyphoplasty for vertebral compression fractures. November, 2003.

[37] Heini PF, Orler R. Kyphoplasty for treatment of osteoporotic vertebral fractures. Eur Spine J 2004;13:184-92.

[38] Shedid D, Togawa D, Lieberman I. Kyphoplasty-vertebral augmentation for compression fractures. Clin Geriatr Med 2006;22:535-44.

[39] Taylor RS, Fritzell P, Taylor RJ. Balloon kyphoplasty in the management of vertebral compression fractures an update systematic review and meta-analysis. Eur Spine J 2007:16:1085-100.

[40] Website www.proteanservices.com/2011/12/balloon-kyphoplasty/ December 26, 2011.

[41] Lavelle W, Carl A, Lavelle ED, Khaleel MA. Vertebroplasty and kyphoplasty. Anesthes Clin 2007;25:913-28.

[42] Togawa D, Kayanja MM, Lieberman IH. Percutaneous vertebral augmentation. Internet J Spine Sur 2005;1:DOI: 10.5580/1454.

[43] Marcucci G, Brandi ML. Kyphoplasty and vertebroplasty in the management of osteoporosis with subsequent vertebral compression fractures. Clin Cases Miner Bone Metab 2010;7: 51-60.

[44] Khanna AJ, Lee S, Villarraga M, Gimbel J, Steffey D, Schwardt J. Biomechanical evaluation of kyphoplasty with calcium phosphate cement in a 2-functional spinal unit vertebral compression fracture model. Spine J 2008;8:770–7.

[45] Kenny SM, Buggy M. Bone cements and fillers: a review. J Mat Sci 2003;14:923-38: 2003.

[46] Preparation and safe use of PMMA bone cements. A continuing education self-study activity. http://www.pfiedler.com/ce/1155/1155.pdf.

[47] Combs SP, Greenwald AS. The effects of barium sulfate on the polymerization temperature and shear strength of Surgical Simplex P. Clin Orthop 1979;145:287–91.

[48] Haas SS, Brauer GM, Dickson G. A characterization of polymethylmethacrylate bone cement. J Bone Joint Surg 1975;57A:380–91.

[49] Kuhn KD. Bone cements up-to-date comparison of physical and chemical properties of commercial materials. Springer-Verlag, Berlin Heidelberg; 2000.

[50] Hosseinzadeh HRS, Emami M, Lahiji F, Shahi AS, Masoudi A, Emami S. The acrylic bone cement in arthroplasty Chapter 5. http://dx.doi.org/10.5772/53252 .

[51] Heini PF, Berlemann U. Bone substitutes in vertebroplasty. Eur Spine J 2001;10: S205-13.

[52] Poitout DG, Kotz R: Biomechanics and biomaterials in orthopedics.2004 edition.

[53] Brown WE, Chow LC. A new calcium phosphate, water-setting cement, in: Cements Research Progress 1986. P.W. Brown, ed. American Ceramic Society, Ohio 1987;352-79.

[54] Dorozhkin SV. Calcium orthophosphate cements and concretes. Materials 2009;2: 221-91.

[55] Lewis G. Injectable bone cements for use in vertebroplasty and kyphoplasty: state-of-the-art review. J Biomed Mater Res Part B: Appl Biomater 2006;76B:456-68.

[56] Website reference http://www.biomaterials.org/week/bio20.cfm.

[57] American Society for Testing and Materials (ASTM). Standard test method for time of setting of hydraulic-cement paste by Gillmore needles. ASTM C266-08e1. In Annual Book of ASTM Standards; vol. 04.01. ASTM, West Conshohocken, PA, USA;2012.

[58] American Society for Testing and Standards (ASTM). Standard test method for time of setting of hydraulic cement paste by Vicat needle. ASTM C191-08. Annual Book of ASTM standards; vol. 04.01. ASTM, West Conshohocken, PA, USA; 2012.

[59] Lui C, Huang Y, Zheng H. Study of the hydration process of calcium phosphate cement by AC impedance spectroscopy. J Am Ceram Soc 1999;82:1052-57.

[60] Baroud G, Bohner M, Heini P, Steffen, T. Injection biomechanics of bone cements used in vertebroplasty. Biomed Mater Eng 2004;14:487-504.

[61] Bohner M, Gbureck U, Barralet JE. Technological issues for the development of more efficient calcium phosphate bone cements: a critical assesment. Biomater 2005;26:6423-9.

[62] Leung KS, Siu WS, Li SF, Qin L, Cheung WH, Tam KF, Po P, Lui Y. An *in vitro* optimized injectable calcium phosphate cement for augmenting screw fixation in osteopenic goats. J Biomed Mater Res Part B: Appl Biomater 2006;78B:153-60.

[63] Baroud G, Matsushita C, Samara M, Beckman L, Steffen T. Influence of oscillatory mixing on the injectability of three acrylic and two calcium phosphate bone cements for vertebroplasty. J Biomed Mater Res Part B: Appl Biomater 2004;68B:105-11.

[64] Bohner M, Baroud B, Gasser B. Snapshot: critical aspects in the use of injectable calcium phosphates in spinal surgery.

[65] Alves HLR, dos Santos LA, Bergmann CP. Injectability evaluation of tricalcium phosphate bone cement. J Mater Sci: Mater Med 2008;19:2241-46.

[66] Khairoun I, Boltong MG, Driessens FCM, Planell JA. Some factors controlling the injectability of calcium phosphate bone cements. J Mater Sci: Mater Med 1998;9:425-28.

[67] Costantino PD, Friedman CD, Jones K, Chow LC, Sisson GA. Experimental hydroxyapatite cement cranioplasty. Plast Reconstr Surg 1992;90:174-85.

[68] Bohner M. Physical and chemical aspects of calcium phosphates used in spinal surgery. Eur Spine J 2001;10:S114-21.

[69] Mickiewicz RA, Mayes AM, Knaack D. Polymer–calcium phosphate cement composites for bone substitutes. J Biomed Mater Res 2002;61:581-92.

[70] Myers RH, Montgomery DC, Anderson-Cook CM. Response surface methodology: process and product optimization using designed experiments 2008. Third edition. Wiley & Sons, New York; 2008.

[71] Engineering statistics handbook. NIST/SEMATECH e-handbook of statistical methods. http://www.itl.nist.gov/div898/handbook/ 2012.

[72] Khuri AI, Mukhopadhyay S. Response surface methodology. Wiley & Sons, Inc., New York;2010.

[73]Boger A, Bohner M, Heini P, Verrier S, Schneider E. Properties of injectable low modulus PMMA bone cement for osteoporotic bone. J of Biomed Mater Res Part B: Appl Biomater 2008;86B:474-82.

[74] Boger A, Bisig A, Bohner M, Heini P, Schneider E. Variation of the mechanical properties of PMMA to suit osteoporotic cancellous bone. J. Biomater Sci Polym Edn 2008;19:1125-42.

[75] Lopez A, Hoess A, Thersleff T, Ott M, Engqvist H, Persson C. Low-modulus PMMA bone cement modified with castor oil. Bio-Med Mat Eng 2011;21:323-32.

[76] Arens D, Rothstock S, Windolf M, Boger A. Bone marrow modified acrylic bone cement for augmentation of osteoporotic cancellous bone. J Mech Behav Biomed Mater 2011;4:2081-89.

[77] Boger A, Wheeler KD, Schenk B, Heini PF. Clinical investigations of polymethylmethacrylate cement viscosity during vertebroplasty and related in vitro measurements. Eur Spine J 2009;18:1272-78.

[78] Lewis G, Koole LH, Hooy-Corstjens CSJ. Influence of powder-to-liquid monomer ratio on properties of an injectable iodine-containing acrylic bone cement for vertebroplasty and balloon kyphoplasty. J Biomed Mater Res Part B: Appl Biomater 2009;91B:537-44.

[79] Hernandez L, Munoz ME, Goni I, Gurruchaga M. New injectable and radiopaque antibiotic loaded acrylic bone cements. J Biomed Mater Res Part B: Appl Biomater 2008;87B:312-20.

[80] Baroud G, Samara M, Steffen T. Influence of mixing method on the cement temperature-mixing time history and doughing time of three acrylic cements for vertebroplasty. J Biomed Mater Res Part B: Appl Biomater 2004;68B:112-16.

[81] Carrodeguas RG, Lasa BV, Barrio JSRd. Injectable acrylic bone cements for vertebroplasty with improved properties. J Biomed Mater Res Part B: Appl Biomater 2004;68B:94-104.

[82] Rodrigues DC, Gilbert JL, Hasenwinkel JM. Two-solution bone cements with cross-linked micro and nano-particles for vertebral fracture applications: effects of zirconium dioxide content on the material and setting properties. J Biomed Mater Res Part B: Appl Biomater 2010;92B:13-23.

[83] Vlad MD, Torres R, Lopez J, Barraco M, Moreno JA, Fernadez E. Does mixing affect the setting of injectable bone cement? An ultrasound study. J Mater Sci 2007;18:347-52.

[84] Weir MD, Xu HHK. High-strength in situ-setting calcium phosphate composite with protein release. J Biomed Mater Res 2008;85A:388-96.

[85] Mickiewicz RA, Mayes AN, Knaack D. Polymer-calcium phosphate cement composites for bone substitutes. J Biomed Mater Res2002;61:581-92.

[86] Khairoun I, Boltong MG, Driessens FCM, Planell JA. Limited compliance of some apatitic calcium phosphate bone cements with clinical requirement. J Mater Sci 1998;9:667-71.

[87] Gbureck U, Spatz K, Thull R, Barralet JE. Rheological enhancement of mechanically activated α-tricalcium phosphate cements. J Biomed Mater Res Part B: Appl Biomater 2005;73B: 1-6.

[88] Takechi M, Miyamoto Y, Ishikawa K, Nagayama M, Kon M, Asaoka K, Suzuki K. Effects of added antibiotics on the basic properties of anti-washout-type fast-setting calcium phosphate cement. J Biomed Mater Res 1998;39:308-16.

[89] Takechi M, Miyamoto Y, Momota Y, Yuasa T, Tatehara S, Nagayama M, Ishikawa K. Effects of various sterilization methods on the setting and mechanical properties of apatite cement. J Biomed Mater Res Part B: Appl Biomater 2004;69B:58-63.

[90] Burguera EF, Xu HHK, Sun L. Injectable calcium phosphate cement. effects of powder-to-liquid ratio and needle size. J Biomed Mater Res Part B: Appl Biomater 2008;84B: 493-502.

[91] Bohner M, Baroud G. Injectabiltiy of calcium phosphate pastes. Biomater 2005:26:1553-63.

[92] Gbureck U, Barralet JE, Spatz K, Grover LM, Thull R. Ionic modification of calcium phosphate cement viscosity. part I: hypodermic injection and strength improvement of apatite cement. Biomater 2004;25: 2187-95.

[93] Barralet JE, Grover LM, Gbureck U. Ionic modification of calcium phosphate cement viscosity. part II: hypodermic injection and strength improvement of brushite cement. Biomater 2004:25:2197-2203.

[94] Nilsson M, Fernandez E, Sarda S, Lidgren L, Planell JA. Characterization of a novel calcium phosphate/sulphate bone cement. J Biomed Mater Res 2002;61:600-07.

[95] Ginebra MP, Rilliard A, Fernandez E, Elvira C, Roman JS, Planell JA. Mechanical and rheological improvement of calcium phosphate cement by the addition of a polymeric drug. J Biomed Mater Res 2001;57:113-18.

[96] Leroux L, Hatim Z, Freche M, Lacout JL. Effects of various adjuvants (lactic acid, glycerol, and chitosan) on the injectability of a calcium phosphate cement. Bone 1999;25:31S-4S.

[97] Hesaraki S, Zamanian A, Moztarzadeh F. The influence of the acidic component of the gas-foaming porogen used in preparing an injectable porous calcium phosphate cement on its properties: acetic acid versus citric acid. J Biomed Mater Res Part B: Appl Biomater 2008;86B:208-216.

[98] Fujishiro Y, Takahashi K, Sato T. Preparation and compressive strength of α-tricalcium phosphate/gelatin gel composite cement. J Biomed Mater Res 2001:54; 525-30.

[99] Burguera EF, Xu HHK, Weir MD. Injectable and rapid-setting calcium phosphate bone cement with dicalcium phosphate dihydrate. J Biomed Mater Res Part B: Appl Biomater 2006;77B:126-34.

[100] Burguera EF, Guitian F, Chow LC. A water setting tetracalcium phosphate-dicalcium phosphate dihydrate cement. J Biomed Mater Res 2004;71A: 275-82.

[101] dos Santos LA, Carrodeguas RG, Boschi AO, de Arruda ACF. Fiber-enriched double-setting calcium phosphate bone cement. J Biomed Mater Res 2003;65A:244-50.

[102] Lin J, Zhang S, Chen T, Liu C, Lin S, Tian X. Calcium phosphate cement reinforced by polypeptide copolymers. J Biomed Mater Res Part B: Appl Biomater 2006;76B:432-39.

[103] Miyamoto Y, Toh T, Ishikawa K, Yuasa T, Nagayama M, Suzuki K. Effect of added $NaHCO_3$ on the basic properties of apatite cement. J Biomed Mater Res 2001;54:311-19.

[104] Burguera EF, Guitian F, Chow LC. Effect of the calcium to phosphate ratio of tetracalcium phosphate on the properties of calcium phosphate bone cement. J Biomed Mater Res 2008;85A:674-83.

[105] Sarda S, Fernandez E, Nilsson M, Balcells M, Planell JA. Kinetic study of citric acid influence on calcium phosphate bone cements as water-reducing agent. J Biomed Mater Res 2002:61:653-59.

[106] Barralet JE, Gaunt T, Wright AJ, Gibson IR, Knowles JC. Effect of Porosity reduction by compaction on compressive strength and microstructure of calcium phosphate cement. J Biomed Mater Res 2002;63:1-9.

[107] Habraken WJEM, de Jonge LT, Wolke JGC, Yubao L, Mikos AJ, Jansen JA. Introduction of gelatin microspheres into an injectable calcium phosphate cement. J of Biomed Mats Res Part A 2008;87A:643-55.

[108] Chow LC, Hirayama S, Takagi S, Parry E. Diametral tensile strength and compressive strength of a calcium phosphate cement: effect of applied pressure. J Biomed Mater Res 2000;53:511-17.

[109] Ito A, Kawamura H, Miyakawa S, Layrolle P, Kanzaki N, Treboux G, Onuma K, Tsutsumi S. Resorbability and solubility of zinc-containing tircalcium phosphate. J Biomed Mater Res 2002;60:224-31.

[110] Hoekstra JWM, van den Beuken JJJP, Leeuwenburgh SCG, Meijer GJ, Jansen JA. Tantalumpentoxide as a radiopacifier in injectable calcium phosphate cements for bone substitution. Tissue Eng Part C 2011;17:907-13.

[111] Gu T, Shi H, Ye J. Reinforcement of calcium phosphate cement by incorporating with high-strength β-tricalcium phosphate aggregates. J Biomed Mater Res Part B: Appl Biomater 2012;100B:350-59.

[112] Alge DL, Goebel WS, Chu TMG. *In vitro* degradation and cytocompatiblity of dicalcium phosphate dehydrate cements prepared using the monocalcium phosphate monohydrate/hydroxyapatite system reveals rapid conversion to HA as a key mechanism. J Biomed Mater Res Part B: Appl Biomater 2012;100B:595-602.

[113] Yin H, Li YG, Si M, Li JM. Simvastatin-loaded macroporous calcium phosphate cement: preparation, *in vitro* characterization, and evaluation of *in vivo* performance. J Biomed Mater Res Part A 2012;100A:2991-3000.

[114] Hesaraki S, Alizadeh M, Borhan S, Pourbaghi-Masouleh M. Polymerization nanoparticulate silica-reinforced calcium phosphate bone cement. J Biomed Mater Res Part B: Appl Biomater 2012;100B:1627-35.

[115] Moreau JL, Weir MD, Xu HHK. Self-setting collagen-calcium phosphate bone cement: mechanical and cellular properties. J Biomed Mater Res 2009; 91A:605-13.

[116] Lopez-Heredia MA, Pattipeilohy J, Hsu S, Grykien M, Weijden BVD, Leeuwenburgh SCG, Salmon P, Wolke JGC, Jansen JA. Bulk physicochemical, interconnectivity, and mechanical properties of calcium phosphate cements-fibrin glue composites for bone substitute applications. J Biomed Mat Res Part A 2013; 101A:478-90.

[117] Thirumalaikumarasamy D, Shanmugam K, Balasubramanian V. Influences of atmospheric plasma spraying parameters on the porosity level of alumina coating on AZ31B magnesium alloy using response surface methodology. Prog Natur Sci Mat Int 2012;22:468-79.

[118] Rajakumar S, Muralidharan C, Balasubramanian. Predicting tensile strength, hardness and corrosion rate of friction stir welded AA6061-T_6 aluminium alloy joints. Mater Design 2011;32:2878-90.

[119] Bhushan RK. Optimization of cutting parameters for minimizing power consumption and maximizing tool life during machining of Al alloy SiC particle composites. J Clnr Prod 2013;39:242-54.

[120] Gil MV, Martinez M, Garcia S, Rubiera F, Pis JJ, Pevida C. Response surface methodology as an efficient tool for optimizing carbon adsorbents for CO_2 capture. Fuel Proc Tech 2013;106:55-61.

[121] Elsayed K, Lacor C. Modeling, analysis and optimization of aircyclones using artificial neural network, response surface methodology and CFD simulation approaches. Powder Tech 2011;212:115-33.

[122] Cisneros-Pindeda OG, Cauich-Rodriguez JV, Cervantes-Uc, JM, Vazquez B, Roman SJ. Combined influence of barium sulfate content and co-monomer concentration on properties of PMMA bone Cements for vertebroplasty. J Biomat Sci 2011;22:1563-80.

[123] O'Hara RM, Dunne NJ, Orr JF, Buchanan FJ, Wilcox RK, Barton DC. Optimization of the mechanical and handling properties of an injectable calcium phosphate cement. J Mater Sci 2010;21:2299-2305.

[124] Low KL, Tan SH, Zein SHS, McPhail DS, Boccaccini AR. Optimization of the mechanical properties of calcium phosphate/multi-walled carbon nanotubes/bovine serum albumin composites using response surface methodology. Mater Design 2011;32:3312-19.

[125] International Standards Organization (ISO). ISO 5833:2002. Implants for surgery—acrylic bone cements. ISO, Geneva, Switzerland; 2011.

[126] Asnis SE, Ernberg JJ, Bostrom MPG, Wright TM, Harrington RM, Tencer A, Peterson M. Cancellous bone screw thread design and holding power. J Orthop Trauma 1996;10:462-9.

[127] Gaitanis IN, Hadijipavlou AG, Katonis PG, Tzermiadiamos MN, Pasku DS, Patwardhan AG. Balloon kyphoplasty for the treatment of pathological vertebral compressive fractures. Eur Spine J 2005;14:250-60.

[128] Kasperk C, Hillmeier J, Noldge G, Grafe IA, Da Fonseca K, Raupp D, Bardenheuer H, Libicher M, Liegibel UM, Sommer U, Hilscher U, Pyerin W, Vetter M, Meinzer H-P, Meeder P-J, Taylor RS, Nawroth P. Treatment of painful vertebral fractures by kyphoplasty in patients with primary osteoporosis; a prospective nonrandomized controlled study. J Bone Miner Res 2005;20:604-12.

[129] Molloy S, Mathis JM, Belkoff SM. The effect of vertebral body percentage fill on mechanical behavior during percutaneous vertebroplasty. Spine 2003;28:1549-54.